

Technical Report

**TR-16-08**

November 2017



# Modelling of the mechanical interaction between the buffer and the backfill in KBS-3V

## Modelling results 2015

Lennart Börgesson

Jan Hernelind

SVENSK KÄRNBRÄNSLEHANTERING AB

SWEDISH NUCLEAR FUEL  
AND WASTE MANAGEMENT CO

Box 3091, SE-169 03 Solna  
Phone +46 8 459 84 00  
skb.se

SVENSK KÄRNBRÄNSLEHANTERING



ISSN 1404-0344

**SKB TR-16-08**

ID 1541999

November 2017

# **Modelling of the mechanical interaction between the buffer and the backfill in KBS-3V**

## **Modelling results 2015**

Lennart Börgesson, Clay Technology AB

Jan Hernelind, 5T Engineering AB

*Keywords:* KBP1018, Bentonite, Swelling, Compression.

This report concerns a study which was conducted for Svensk Kärnbränslehantering AB (SKB). The conclusions and viewpoints presented in the report are those of the authors. SKB may draw modified conclusions, based on additional literature sources and/or expert opinions.

A pdf version of this document can be downloaded from [www.skb.se](http://www.skb.se).

© 2017 Svensk Kärnbränslehantering AB



## Abstract

One important role of the backfill is to restrict upwards swelling of the buffer in deposition holes. If the buffer can swell upwards it will lose density and by that also important properties. A possible but extreme scenario is the so called dry case of buffer/backfill interaction meaning that the water inflow into the deposition tunnel is very low but at the same time there is a fast wetting of a deposition hole.

The report describes the modelling of the mechanical interaction between the buffer and the backfill at a dry backfill that were carried through in 2015. All calculations were done with the finite element code Abaqus. The purpose of the calculations has been to understand and evaluate the influence of different factors of the interaction between the buffer and a dry backfill on the final state of the buffer after swelling and homogenisation of the buffer. The average density of the buffer shall according to a new criterion be such that it corresponds to a swelling pressure of between 3 MPa and 10 MPa below a horizontal plane located 0.5 m above the canister lid.

A full scale test carried through in Äspö HRL was used to check the response of a dry backfill to an upwards swelling of the buffer. In the test a full scale bentonite block in a deposition hole was forced to move upwards by four cylinders and the force and displacement measured. The backfill was designed as the reference backfill in a deposition tunnel. By modelling this test, the modelled response of the backfill could be checked against the measured response and the backfill model could be validated. Comparison between modelled and measured results of the swelling test showed a very good agreement up to 8 cm displacement, after which cracking of the blocks took place and the material model of the blocks was invalid. Sensitivity analyses showed that the stiffness and thickness of the pellet filling in the floor and roof were the factors most sensitive to changes. It was concluded that for further modelling the models and parameters used are adequate to use if cracking of the blocks are avoided.

The base case with an average buffer density at saturation of 2000 kg/m<sup>3</sup> and the swelling pressure 7 MPa with the same backfill as in the field test was modelled as having a completely homogeneous buffer from start. Both the old mechanical material model for saturated buffer materials with Drucker-Prager plasticity model (used in SR-Site) and the new plastic Cap model derived in the TF EBS were used for comparison. The backfill response was modelled by using the extrapolated test results and by including changes in geometry. The same base case was modelled but with the initial density of the buffer in the deposition hole, i.e. buffer blocks, buffer rings and pellets. Also for this case both material models were used for comparison. A comparison between the results when the Drucker-Prager model was used and when the Plastic Cap model was used showed that the difference is small. It seems as the introduction of a cap and a curved failure envelope does not affect the results very much at this type of upwards swelling. The density distribution under and along the canister differed very much for the two initial conditions. The inhomogeneous model had a remaining very strong radial density spreading in comparison with the homogeneous model. Above the canister, where the large swelling takes place, there is also a clear difference with a much stronger swelling for the inhomogeneous model.

A general conclusion is that the inhomogeneous model should be used if possible. Underestimation of the swelling may otherwise be the case.

15 cases with different average density and swelling pressure of the buffer and different geometry of the backfill were modelled with the new material model and initially inhomogeneous buffer. The purpose was to study the sensitivity to changes in geometry and density. The backfill response was modelled with the extrapolated test results and with changes in geometry taken into account. Six cases with wet backfill blocks in the upper part of the deposition hole were modelled with simplified models that took the density loss into the bevel into account. The results showed that the influence of the pellet filling in the floor and the influence of the bevel are rather strong but for most cases not critical. Only four cases resulted in an average stress above the canister that was close to or under 2 MPa.

General conclusions were:

- Pellets filling thickness in the floor influences the results more than the bevel.
- Only low density buffer yields problems with fullfilling requirements.
- Cases with bevel and 10 cm pellet filling thickness fulfilled the requirements.

In order to check that the extrapolation of the stress-strain behaviour of the backfill used in the analyses is a valid model, 3D analyses of two of the cases in the sensitivity analysis were performed. The same backfill block configuration as in the field test and an inhomogeneous buffer were modelled and compared with the simplified 2D calculation. The results show that the agreement was rather poor. The 3D model for both cases yielded less upwards swelling and higher remaining density above the canister than the 2D model. The main reason for this difference is that the 3D calculations were interrupted before equilibrium due to convergence difficulties.

In order to study the influence of the width of the pellet filled slot at the ceiling 3D-models with two different slot widths including a backfilled dry tunnel was simulated. The comparison between the results showed that the influence of the width of the pellet filled slot at the ceiling is rather small due to the lateral stress spreading in the backfill. This is good for the concept since the rock surface at the ceiling can be very irregular. However, the geometry of the masonry is important. If there is no overlapping of the blocks the stress will continue through the block without spreading and with retained stress level.

The backfill blocks in the field test cracked after about 8 cm displacement of the simulated buffer. In order to study the effect of block cracking, one case in the sensitivity analysis was modelled and compared with the results of the field test after 8 cm displacement as backfill response. The calculation showed that the effect on the buffer is rather large. The swelling of the buffer/backfill interface was slightly over 30 cm and the average stress above the canister lid was about 1.5 MPa. However, the density according to the new criterion was 1 966 kg/m<sup>3</sup> and thus acceptable.

In the sensitivity analyses the effect of having the upper part of the deposition hole and the pellet filled bevel wetted was investigated with the pessimistic assumption that the entire backfill part (upper 1.25 m and the bevel) was homogenised, which results in a rather low density in that part of the deposition hole. In order to study the relevance of those models 3D calculations of two of the cases including the bevel were performed. The results showed that the density loss in the buffer above the canister was much lower in the 3D-case. In spite of the large horizontal swelling the density distribution after equilibrium was still very inhomogeneous in the upper part of the deposition hole and the bevel. The assumption of complete homogenization in the sensitivity analyses is thus very pessimistic and the results not reliable. All cases with 10 cm pellet filling in the floor and only pellet filling in the bevel were acceptable.

All modelling results have been evaluated according to the recently proposed buffer density criteria, which says that only the buffer located between the bottom of the deposition hole and the 0.5 m above the canister shall be used for calculating the average density. The results show that the criterion rather well captures the critical cases at upwards swelling scenarios. All cases with a swelling pressure above the canister lid  $\leq 2$  MPa gave average densities according to the new criterion  $\leq 1\,950$  kg/m<sup>3</sup> at water saturation, which corresponds to a swelling pressure of about 3 MPa.

Only in one case the new buffer criterion failed to discover a critical case with swelling pressure above the canister lid less than 2 MPa. This case was the case of backfill block failure.

# Sammanfattning

En viktig roll som återfyllningen har är att begränsa uppåtriktad svällning av bufferten i deponeringshålen. Om bufferten sväller tappar den densitet och därmed också viktiga egenskaper. Ett möjligt men också extremt scenario är det s.k. torra fallet av buffert/återfyllnings-samverkan vilket innebär att vatteninflödet i tunneln är så lågt att återfyllningen förblir torr samtidigt som bevätningen av bufferten är så snabb att full vattenmättnad inträffar tidigt.

Rapporten beskriver de modellberäkningar av den mekaniska samverkan buffert/återfyllning som gjorts under 2015. Finita elementprogrammet Abaqus användes för samtliga beräkningar. Syftet med beräkningarna har varit att förstå och utvärdera inverkan av olika faktorer på interaktionen mellan bufferten och en torr återfyllning på det slutliga tillståndet hos bufferten efter svällning och homogenisering. Medeldensiteten hos bufferten skall enligt de uppdaterade kraven vara så att den motsvarar ett svälltryck på mellan 3 och 10 MPa under ett horisontellt plan beläget 0,5 m över kapselns lock.

Ett fullskaleförsök som genomförts i Äspö HRL under 2015 användes för att kontrollera det mekaniska motståndet av en torr återfyllning mot uppåtsvällning. I försöket användes ett fullstort bentonitblock avsett för deponeringshål som försköts uppåt med hjälp av fyra cylindrar under samtidig mätning av kraft och deformation. Återfyllningen motsvarade referensfallet. Genom att modellera försöket kunde återfyllningens mekaniska mothåll jämföras med det uppmätta och återfyllningsmodellen valideras. Jämförelsen mellan modellerade och uppmätta resultat visade på mycket god överensstämmelse upp till 8 cm förskjutning. Därefter började återfyllningsblocken spricka sönder och materialmodellen gick sedan inte att använda för de fortsatta förskjutningarna. Känslighetsanalyser visade att styvhet och tjocklek på pelletsfyllningen i golvet och i taket var de faktorer som mest påverkade resultaten. Slutsatsen var att de använda modellerna och parametrarna även kan användas i de fortsatta beräkningarna om uppspräckning av återfyllningsblocken kan undvikas.

Basfallet med en medeldensitet vid vattenmättnad hos bufferten av  $2000 \text{ kg/m}^3$  och svälltrycket 7 MPa med samma återfyllning som i fältförsöket, modellerades under antagandet att bufferten var homogen från start. Både den gamla materialmodellen för vattenmättad buffert med Drucker-Prager plasticitetsmodell (som användes i SR-Site) den nya Plastic Cap modellen (som användes och validerades i TF EBS) användes vid beräkningarna för att kunna jämföra resultaten. Återfyllningens mothåll modellerades genom att använda det extrapolerade resultatet från fältförsöket med vederbörliga korrigeringar för andra geometrier. Samma basfall modellerades också men med ursprunglig densitet hos bufferten dvs med block, ringar och pellets samt med båda materialmodellerna. En jämförelse av resultaten för Drucker-Prager modellen och Plastic Cap modellen visade att skillnaden var mycket liten. Det visar att skillnaderna mellan modelleran inte påverkar resultaten särskilt mycket för denna typ av uppåtsvällning. En jämförelse av resultaten för ursprunglig homogen och inhomogen buffert visade att densitetsfördelningen längs kapseln mantelyta skilde sig mycket åt. Den inhomogena modellen hade en kvarstående mycket stor radiell densitetspridning i jämförelse med den homogena modellen. Ovanför kapseln, där den stora svällningen äger rum, fanns också en klar skillnad med en mycket större svällning i det inhomogena fallet.

En generell slutsats var att den inhomogena modellen om möjligt bör användas annars kan svällningen underskattas.

15 fall med olika medeldensitet och svälltryck hos bufferten och olika geometrier hos återfyllningen modellerades med den nya materialmodellen och ursprunglig inhomogen buffert. Syftet var att studera känsligheten för förändringar i geometri och densitet. Återfyllningens respons modellerades genom att använda det extrapolerade resultatet från fältförsöket med vederbörliga korrigeringar för andra geometrier. I sex av fallen inkluderades den övre delen av deponeringshålet med förenklade antaganden att bentoniten i avfasningen och den övre delen av deponeringshålet var fullständigt homogeniserad och vattenmättad från start utan att avfasningen ingick i modellen. Resultaten visade att inverkan av pelletsfyllningen i golvet och inverkan av att ta med avfasningen var ganska stor men inte kritisk. Endast fyra av fallen resulterade i en medelspänning ovanpå kapseln som var nära eller mindre än 2 MPa.

Generella slutsatser var att pellettfyllningens tjocklek i golvet påverkar resultaten mer än avfasningen, att bara låg ursprunglig buffertdensitet innebär problem och att alla fallen med 10 cm tjock pellettfyllning i golvet uppfyller kraven.

För att kontrollera att den extrapolerade responsen hos återfyllningen är korrekt gjordes en 3D-analys av två av fallen i känslighetsanalysen. Samma blockgeometri och egenskaper hos återfyllningen användes som i modelleringen av fältförsöket och jämfördes med de förenklade 2D-beräkningarna. Resultatet visade att överensstämmelsen var dålig. 3D-modellerna gav för båda fallen mindre uppåtsvällning och högre densitet ovanför kapseln än 2D-modellerna. Den huvudsakliga anledningen till skillnaden var att 3D-beräkningarna avbröts innan jämvikt på grund av svårigheter att uppnå konvergens.

För att studera inflytandet av tjockleken hos pelletsfyllningen i taket gjordes två 3D-simuleringar med torr tunnel och olika spalttjocklek. Jämförelsen visade att inverkan var ganska liten på grund av spänningsspridningen i återfyllningen, vilket är bra eftersom taket kan vara mycket oregelbundet. Men geometrin hos blockmurverket är viktig. Om det inte finns någon överlappning mellan blockraderna kommer spänningen att fortplanta sig genom återfyllningen med bibehållen spänning utan spridning.

Återfyllningsblocken i fältförsöket började spricka efter c:a 8 cm förskjutning av den simulerade uppåtsvällande bufferten. För att studera effekten av blockkupsprickning modellerades ett fall i känslighetsanalysen genom att använda resultaten i fältförsöket efter 8 cm förskjutning som återfyllningsmodell. Beräkningarna visade att påverkan på bufferten är ganska stor. Svällningen hos buffert/återfyllningsranden blev drygt 30 cm och medelspänningen alldeles över kapseln c:a 1,5 MPa. Emellertid, blev densiteten enligt det nya kriteriet  $1966 \text{ kg/m}^3$  och alltså acceptabel.

I känslighetsanalysen undersöktes inverkan av att ha en vattenmättad bentonit även i överdelen av deponeringshålet och i avfasningen med det pessimistiska antagandet att hela återfyllningsdelen (övre 1,25 m och avfasningen) var helt homogeniserad, vilket resulterar i en ganska låg densitet i deponeringshålet. För att studera relevansen hos detta antagandet gjordes 3D-beräkningar av två av fallen i känslighetsanalysen. Resultaten visade att densitetsförlusten i bufferten ovanför kapseln var mycket lägre i 3D-modellen. Trots stor horisontell svällning var densitetsfördelningen i avfasningen mycket ojämn med ganska hög kvarstående densitet i deponeringshålet. Antagandet av fullständig homogenisering i känslighetsanalysen är alltså mycket pessimistisk. Alla fall med 10 cm tjock pellettfyllning i golvet och enbart pellets i avfasningen var acceptabla.

Alla modelleringsresultat utvärderades enligt det uppdaterade buffertkriteriet, som säger att bara bufferten som ligger mellan botten av deponeringshålet och 0,5 m ovanför kapseltoppen skall inkluderas i medelvärdesberäkningen av densiteten. Resultaten visar att kriteriet ganska väl fångar de kritiska fallen vid uppåtsvällningsscenarierna. Alla fall med ett svälltryck ovanför kapsellocket  $\leq 2 \text{ MPa}$  gav densiteter enligt det nya kriteriet  $\leq 1950 \text{ kg/m}^3$  vid vattenmättnad, vilket motsvarar ett svälltryck på c:a 3 MPa.

I endast ett fall avslöjade inte det nya buffertkriteriet att svälltrycket ovanför kapsellocket var mindre än 2 MPa nämligen fallet med blockkupsprickning.



# Contents

<b>1</b>	<b>Introduction</b>	9
<b>2</b>	<b>Modelling program 2015</b>	11
2.1	General	11
2.2	Modelled cases	11
2.3	Comments	12
<b>3</b>	<b>Modelling of the Buffer swelling test in Äspö HRL</b>	13
3.1	General	13
3.2	Test description	13
3.3	Modelling	14
3.3.1	General	14
3.3.2	Material models	14
3.3.3	Element mesh	16
3.3.4	Boundary conditions	17
3.3.5	Contact surfaces	17
3.4	Calculations	17
3.5	Modelling results and comparison with measurements	17
3.6	Sensitivity analysis	20
3.6.1	General	20
3.6.2	Case R1: Influence of the gap width at the roof	20
3.6.3	Case J2: Influence of the stiffness of the joints	23
3.6.4	Compilation of results from the sensitivity analysis	24
3.7	Comment and conclusions	25
<b>4</b>	<b>Modelling of the buffer and backfill mechanical interaction with different initial conditions and different material models of the buffer</b>	27
4.1	General	27
4.2	Material models	27
4.2.1	General	27
4.2.2	Hydraulic model	27
4.2.3	Mechanical models	28
4.2.4	Contact properties	30
4.2.5	Other materials	30
4.3	Initially homogeneous buffer	30
4.3.1	Finite element model	30
4.3.2	Results	32
4.4	Initially inhomogeneous buffer	32
4.4.1	Finite element model	32
4.4.2	Results	36
4.5	Calculation of average density up to 0.5 m above the canister lid	39
4.6	Comments and conclusions	42
<b>5</b>	<b>Influence of buffer density and backfill geometry</b>	45
5.1	General	45
5.2	Model	45
5.2.1	Geometry	45
5.2.2	Initial conditions	46
5.2.3	Material models	49
5.2.4	Boundary conditions	50
5.3	Results	50
5.4	Conclusions	53
<b>6</b>	<b>3D model for checking the 2D models</b>	55
6.1	General	55
6.2	Case 3e (10 MPa swelling pressure and 50 cm pellet filling)	56
6.3	Case 3a (10 MPa swelling pressure and 10 cm pellet filling)	60
6.4	Comments and conclusions	65

<b>7</b>	<b>3D model for studying the influence of the width of the pellet filled slot at the ceiling</b>	67
7.1	General	67
7.2	60 cm slot at the ceiling ( <i>Tunnel_swelling2b</i> )	67
7.3	Base case with 45 cm slot at the ceiling ( <i>Tunnel_swelling2b_standard</i> )	72
7.4	Comments and conclusions	75
<b>8</b>	<b>Modelling of the case with backfill block failure</b>	77
8.1	General	77
8.2	Model	77
8.3	Results	77
<b>9</b>	<b>3D model with bevel of wet upper part of deposition hole</b>	81
9.1	General	81
9.2	Case 2c (swelling pressure 7 MPa)	82
9.3	Case 3c (swelling pressure 10 MPa)	87
9.4	Comments and conclusions	92
<b>10</b>	<b>Summary and conclusions</b>	93
10.1	General	93
10.2	Modelled cases	93
10.3	New buffer criterion	95
	<b>References</b>	97
	<b>Appendix 1</b> Results of the sensitivity analyses	99

# 1 Introduction

One important task for the backfill is to restrict upwards swelling of the buffer in deposition holes. If the buffer can swell upwards it will lose density and by that also important properties. A possible scenario is the so called dry case of buffer/backfill interaction meaning that the water inflow into the deposition tunnel is very low but at the same time there is a fast wetting of a deposition hole. This means that the buffer in the deposition hole will swell and there will be a pressure build up pushing the dry backfill upwards. The backfill blocks will be piled according to a certain pattern with overlapping. The slots between the backfill blocks and the rock will be filled with bentonite pellets and the compression properties of this filling will also influence the ability of the backfill to prevent heaving of the buffer.

The most uncertain properties of the dry block backfill are the compression properties of the joints between the backfill blocks. Since the blocks are piled in an overlapping pattern (like masonry), the gap thickness and compressibility of these joints are unknown. A full scale test has been performed at Äspö HRL where a backfill exercise filling a tunnel with blocks in the reference pattern has been used to test the deformation properties of the masonry at upwards movement of a steel plate simulating the buffer (Buffer swelling test). The results of this test have been used to check and calibrate the model of the dry backfill and the response has been used as input for the backfill stress-strain properties in a number of modelling cases.

All modelling results were evaluated according to the recently proposed buffer density criteria, which says that only the buffer located between the bottom of the deposition hole and 0.5 m above the canister shall be used for calculating the average density (Posiva SKB 2017). The average density of the buffer shall according to this criterion be such that it corresponds to a swelling pressure of between 3 MPa and 10 MPa.

The report describes the efforts 2015 to model the mechanical interaction between the buffer and the backfill at a dry backfill. The purpose of the calculations has been to understand and evaluate the influence of different factors on the interaction between the buffer and a dry backfill and the influence on the final state of the buffer after swelling and finalized homogenisation of the buffer.



## 2 Modelling program 2015

### 2.1 General

A large number of cases have been modelled. All of them refer to the so called dry backfill case, which means the extreme case that the backfill is assumed to be completely dry and the buffer is assumed to be wetted to full water saturation. Most cases have not included the geometry of the bevel. The buffer has in all cases been assumed to be completely water saturated from start but with different initial density distributions.

### 2.2 Modelled cases

The following cases have been modelled:

#### ***The buffer swelling test in Äspö HRL.***

This full scale test was used to check the response of a dry backfill to an upwards swelling of the buffer. Instead of buffer a bentonite block in a deposition hole was forced to move upwards by three cylinders and the force and displacement measured. The backfill was designed as the base backfill in a deposition tunnel. By modelling this test the modelled response of the backfill could be checked against the measured response and the backfill model could be validated. A sensitivity analysis was also made.

#### ***Modelling of the buffer and backfill mechanical interaction with different initial conditions and different material models of the buffer.***

The base case of a buffer of MX-80 with a density at saturation of  $2\,000\text{ kg/m}^3$  and the swelling pressure 7 MPa with the same backfill as in the field test has been modelled as having a completely homogeneous buffer from start. Both the old mechanical material model for saturated buffer materials (used in SR-Site in Åkesson et al. 2010a, b) and the new material model derived in the TF EBS (international Task Force for modelling Engineered Barrier Systems organised by SKB), have been used for comparison. The backfill response was modelled with the extrapolated test results and with changes in geometry taken into account.

The same base case corresponding to an average density at saturation of  $2\,000\text{ kg/m}^3$  and the average swelling pressure 7 MPa with the same backfill as in the field test has been modelled with the initial density of the buffer in the deposition hole, i.e. buffer blocks, buffer rings and pellets. Also for this case both the old mechanical material model for saturated buffer material and the new material model derived in the TF EBS have been used for comparison. The backfill response was modelled with the extrapolated test results and with changes in geometry taken into account.

#### ***Influence of buffer density and backfill geometry***

15 cases with different average density and swelling pressure of the buffer and different geometry of the backfill have been modelled with the new material model and initially inhomogeneous buffer. The purpose has been to study the sensitivity to changes in geometry and density. The backfill response was modelled with the extrapolated test results and with changes in geometry taken into account. In six cases the backfill blocks in the upper part of the deposition hole was modelled with simplified models that takes the density loss into the bevel into account.

#### ***3D model for checking the backfill compression model***

In order to check that the extrapolation of the stress-strain behaviour of the backfill used in the analyses is a valid model, 3D analyses of two of the cases in the sensitivity analysis was performed. The same backfill block configuration as in the field test and an inhomogeneous buffer were modelled and compared with the simplified 2D calculation.

### ***3D model for studying the influence of the width of the pellet filled slot at the ceiling***

The sensitivity analysis was done with the same backfill geometry as in the field test. In order to study the influence of the width of the pellet filled slot at the ceiling 3D-models with two different slot widths including a backfilled dry tunnel was simulated.

### ***Modelling of the case with backfill block failure***

The backfill blocks in the field test cracked after about 8 cm displacement of the simulated buffer. In order to study the effect of block cracking one of the cases in the sensitivity analysis was modelled with the results of the field test after 8 cm displacement as backfill response.

### ***3D model with bevel of wet upper part of the deposition hole***

Some attempts were also made to model the case that also the backfill in the upper part of the deposition hole was wetted. These models were 3D-models and included also the bevel. Two cases were successfully simulated after great efforts.

## **2.3 Comments**

All calculations have been done with the finite element code Abaqus.

All modelling results have been evaluated according to the recently proposed buffer density criteria which says that only the buffer located between the bottom of the deposition hole and the 0.5 m above the canister (Posiva SKB 2017) shall be used for calculating the average density, which will be used for calculating the swelling pressure (average stress).

The acceptable average stress in the bentonite is according to this criterion 3.0–10.0 MPa. The lower limit, which is critical for the buffer swelling cases is thus 3.0 MPa, which corresponds to a density at saturation for the bentonite MX-80 of about  $\rho_m=1\,950\text{ kg/m}^3$ . This value has been used in the evaluations in the report.

The acceptable value of the average stress above the canister lid has been set to 2 MPa, since this was used in earlier evaluations.

Values below  $\rho_m=1\,950\text{ kg/m}^3$  (density criterion) and 2.0 MPa (on canister lid) have been stated to be critical.

### 3 Modelling of the Buffer swelling test in Äspö HRL

#### 3.1 General

The modelling of the reference case of this test has been reported in a separate report (Martino et al. 2016) and will only be briefly treated here. However, the sensitivity analyses done are reported in Section 3.5. The results of the field test have also been reported separately (Sandén et al. 2015).

#### 3.2 Test description

A drawing showing the principle test design is provided in Figure 3-1. An “artificial deposition hole” with a depth of about 1.5 meter was drilled in the tunnel floor. A concrete tube with an inner diameter of 1600 mm was placed in the hole and the slot between the tube and the rock was filled with concrete. Four hydraulic jacks were installed on the bottom of the hole. Above the hydraulic jacks a steel plate with an outer diameter of 1.75 m was placed. In order to better simulate the dry upper bentonite block in a deposition hole a bentonite block with correct dimensions was placed on top of the steel plate. The buffer block was pushed upwards by the hydraulic jacks during the test, simulating the swelling bentonite from a deposition hole. A detailed drawing showing all main components is provided in Figure 3-2.

The test was performed in the TASS tunnel at Äspö HRL at a depth of about 420 m below ground. The installation of the backfill blocks had a length of 12 meters and the artificial deposition hole was placed in the centre of the block masonry i.e. 6 meters from the tunnel end.

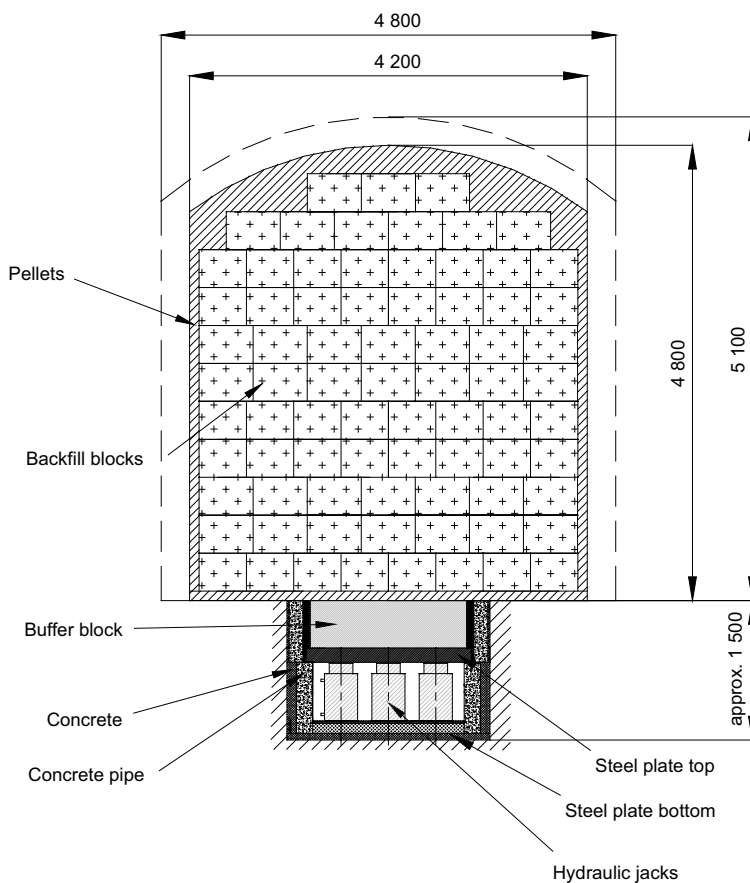
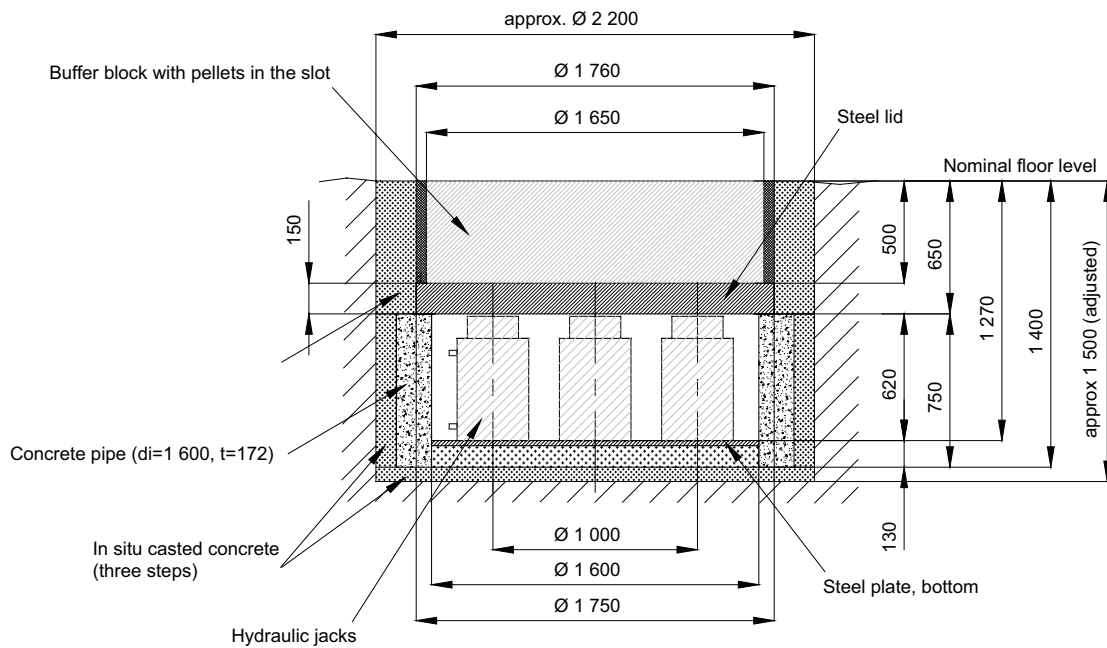


Figure 3-1. Schematic drawing showing the principle test design.



**Figure 3-2.** Detailed description showing the main components of the test design.

A number of measurements were done before, during and after the test.

- The force on the steel plate was applied and measured by 4 hydraulic jacks.
- The displacement of the steel plate was measured by 4 displacement transducers placed under the steel plate.
- The maximum vertical pressure was measured in 41 points on the blocks.
- The positions of 28 blocks were measured before and after the test.
- The total stress on the rock surface was measured in 5 points in the ceiling and the rock wall.
- The rock contour and the distance between the rock surface and the blocks were measured.

### 3.3 Modelling

#### 3.3.1 General

The results showed that failure with cracking of many blocks have occurred, but this process is not possible to model with currently used models so only the results up to 8 cm displacements have been used for evaluation and comparison with measurements. The calculations were only run to 10 cm displacement.

#### 3.3.2 Material models

There were three different parts included in the dry backfill, namely the blocks, the joints between the blocks and the pellet filling. In addition one buffer block with the same dimensions and properties as the buffer blocks in a deposition hole was included.

##### **Block section of masonry**

The backfill blocks were modelled as a linear elastic material with the following properties (Johannesson 2008):

$$E = 245 \text{ MPa}$$

$$\nu = 0.17$$

$$\text{Initial average stress } p_0 = 0 \text{ MPa}$$



Although the blocks used in the test differed somewhat from the reference blocks (mainly by having a lower dry density) the properties of the reference blocks were used as the base case. Each block was modelled with one element.

### **Buffer block**

The buffer block that was displaced upwards was allotted the same elastic properties as the backfill blocks.

### **Pellet section**

The parts filled with pellets were modelled with linear elasticity and Drucker-Prager plasticity. The plastic behaviour was modelled with Drucker-Prager plasticity.

#### *Drucker-Prager plasticity*

$\beta$  = friction angle in the  $p$ - $q$  plane

$\delta$  = cohesion in the  $p$ - $q$  plane

$\psi$  = dilation angle

$q = f(\varepsilon_{pl}^d) =$  yield function

$\beta = 55^\circ$  (corresponds to a Mohr-Coulomb friction angle of  $\phi=30^\circ$ )

$\delta = 52$  kPa (intercept on  $q$ -axis ( $p=0$ ))

$\psi = 0^\circ$  dilatancy

#### **Yield function (ideally plastic at the yield surface)**

$q$ (kPa)	$\varepsilon_{pl}$
100	0

#### *Elastic properties*

$E = 3.9$  MPa (base case)

$\nu = 0.3$

Initial average stress  $p_0 = 0$  MPa

The base case corresponds to the stiffness of a pellet filling that has not been compacted.

The compressibility of different pellet fillings has been tested (Andersson and Sandén 2012). The E-modules used are evaluated from those measurements for an increase in stress from 0 to 2 MPa.

### **Joints between blocks**

Since the bottom bed on which the blocks rest cannot be made as a completely plane or horizontal surface the backfill blocks will be placed slightly uneven in relation to each other. This means that there will be joints that are not even due to slightly inclined blocks that also have slightly different heights. The properties of these joints between the blocks are not known but they will have compression and friction properties that deviate significantly from the properties of the blocks.

The following properties were applied to the joints (both horizontal and vertical):

- Average joint thickness: 4 mm (fictive).
- Compression properties: the joints are closed at an external pressure of 10 MPa.
- Friction angle  $f = 20^\circ$ .

Figure 3-3 shows the stress-compression relation that has been used for the joints.

The joint is a contact surface property where the contact pressure is defined versus the normal vertical displacement. The joint is seemingly closed at 4 mm displacement corresponding to the normal pressure 10 MPa but if the pressure exceeds 10 MPa the compression will continue. However, the actual pressure will never be near such a high value.

**Rock**

The rock was modelled as an elastic material with high stiffness, which means that it only works as a boundary.

$E=1.85 \cdot 10^8 \text{ kPa}$

$\nu=0.3$

**3.3.3 Element mesh**

The backfill block masonry was placed with the pattern that is referred to as the reference backfill design and used in earlier calculations.

Figure 3-4 shows the geometry and the mesh of the block masonry.

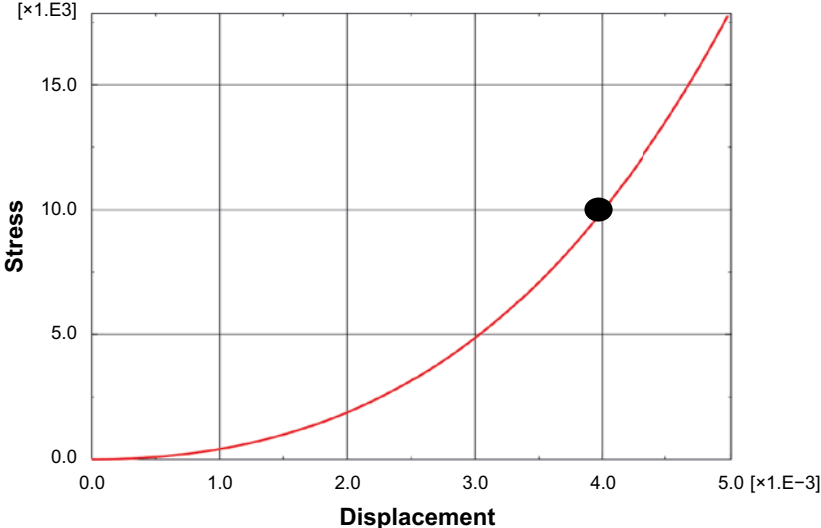


*Figure 3-3. Mechanical model of the joints between blocks. The displacement or compression (m) of the joint is plotted as a function of the total stress (kPa) perpendicular to the joint. After 4 mm compression the 4 mm joint is closed.*

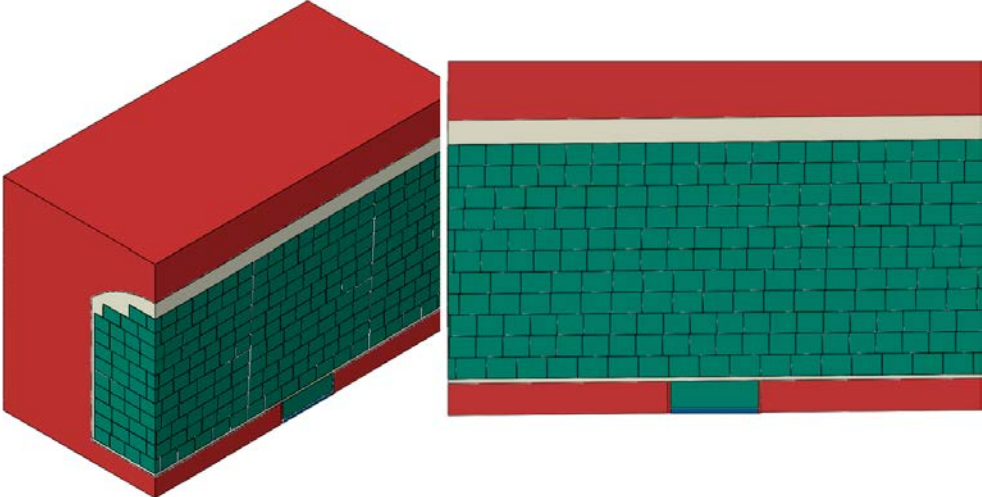


*Figure 3-4. Geometry used for the calculation. Each block is one element. The mesh of the other materials is not shown.*

The thickness of the pellet filling has been set as follows:

- At the crown of the ceiling: 46 cm.
- At the walls: 10 cm.
- At the floor: 8 cm.

The element size of the pellet fillings was about  $4 \times 10 \times 10 \text{ cm}^3$ .

### 3.3.4 Boundary conditions

The following boundary conditions were applied:

#### ***Mechanical***

The vertical boundary planes are symmetry planes and free to move parallel with the plane and fixed perpendicular to the plane.

The horizontal boundaries are fixed.

### 3.3.5 Contact surfaces

The contact between the pellets filling and the rock was not tied in order to allow slip. Instead interface properties with a specified friction were applied between the different materials. The friction was modelled with Mohr Coulomb's parameter friction angle  $\phi$  and without cohesion  $c$ .

$$\phi = 30^\circ$$

$$c=0$$

This friction angle corresponds to the friction angle of the pellets filling  $\beta = 55^\circ$  in the Drucker-Prager model, which means that the contact surfaces are considered rough.

The contact surfaces were made not to withstand tensile stress, which means that the contact may be lost and a gap formed between the surfaces.

## 3.4 Calculations

The calculations are purely mechanical. The steel plate has been displaced vertically until the total displacement 10 cm. The calculations included a technique for facilitating the convergence conditions by introducing damping forces.

Gravity has not been included in the calculations so an extra pressure corresponding to the own weight of the block masonry should be added in final the evaluation. With the total height of 4.4 m and the density of the blocks  $\rho=1989 \text{ kg/m}^3$  the additional pressure is  $\Delta\sigma=87.5 \text{ kPa}$ .

Except for the reference calculation with the parameter setting shown in Section 3.3 a sensitivity analysis has been done with a number of parameters successively varied. The stiffness of the different pellet fillings was varied. A change in stiffness corresponds to a change in thickness, since the pellet filling is modelled as linear elastic. The sensitivity analysis can thus also be considered an analysis of the influence of a change in gap width of the pellet fillings.

## 3.5 Modelling results and comparison with measurements

The modelling results are described in more detail in Martino et al. (2016). Figure 3-5 shows the modelled deformed block structure and the vertical stresses in the blocks in the centre after 10 cm displacement of the buffer block. A picture taken during excavation is also shown.

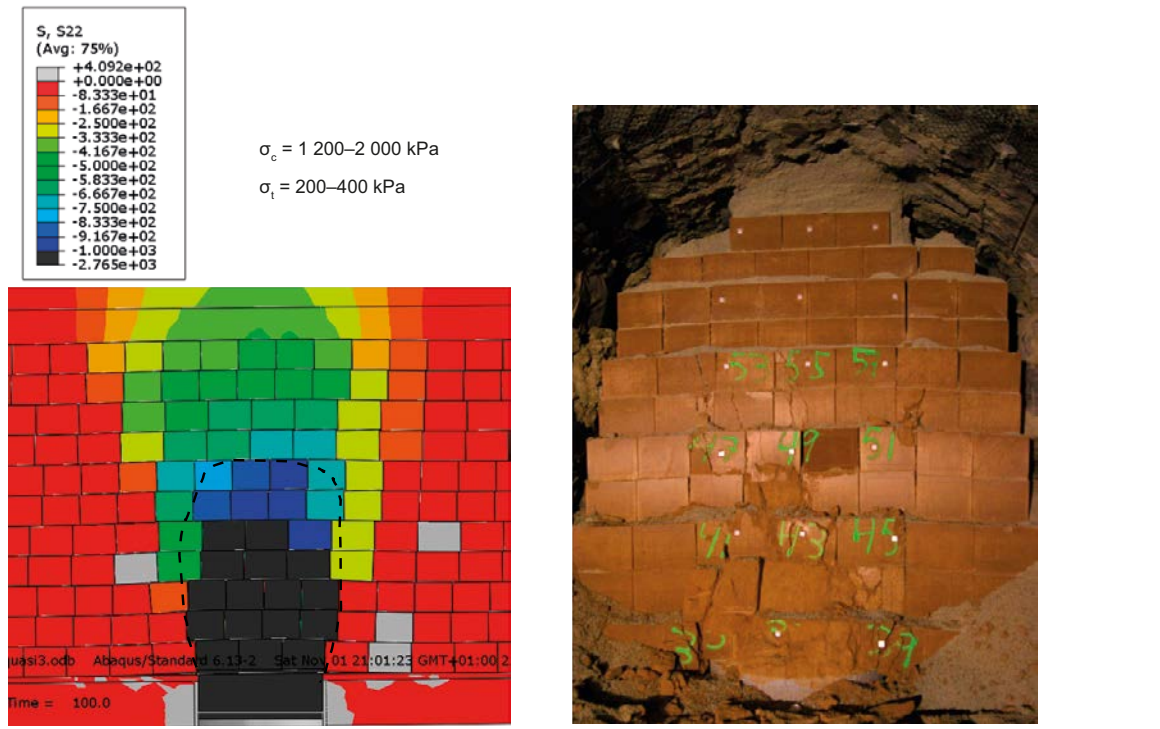


**Figure 3-5.** Modelled vertical stress in the backfill blocks after 10 cm displacement and picture taken at the central part after excavation of half the test.  $\sigma_c$ =compression strength and  $\sigma_t$ = tension strength of the blocks measured in laboratory.

At excavation it was seen that many blocks above the simulated deposition hole were cracked.

The modelled evolution of stresses on the steel plate and in the measuring points on the rock surface is shown in Figure 3-6.

The modelled evolution of stresses on the steel plate and in the ceiling is compared with the measured in Figures 3-7 and 3-8.

The modelled total stress evolution on the steel plate shows very good agreement with the measured stress up to about 8 cm displacement. The measurements show stress relaxation that originates from the loading sequence that was done stepwise with 15 minutes rest between the load steps.

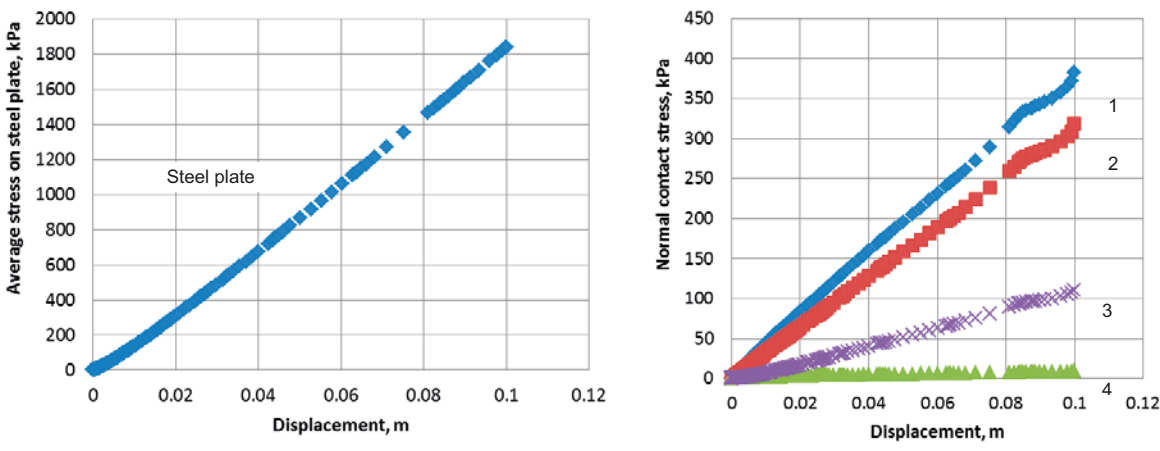


**Figure 3-6.** Modelled normal stress distribution as function of the displacement of the steel plate. The average normal stress on the steel plate is shown in the left figure and the stresses on the rock surface in the left figure. See Martino et al. (2016) for the location of the stress gauges.

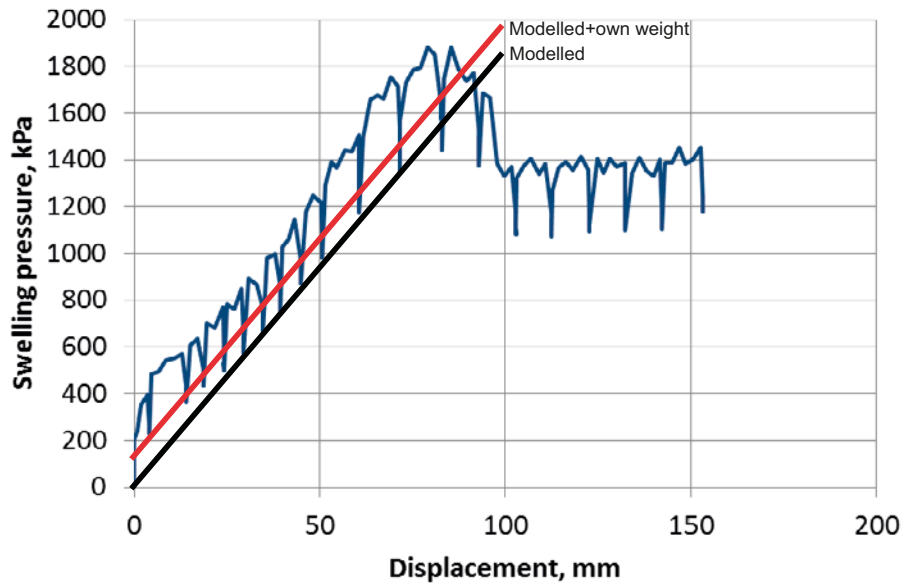


*Figure 3-7. Modelled and measured evolution of total vertical average stress on the steel plate. The own weight of the backfill block is also added in the figure.*

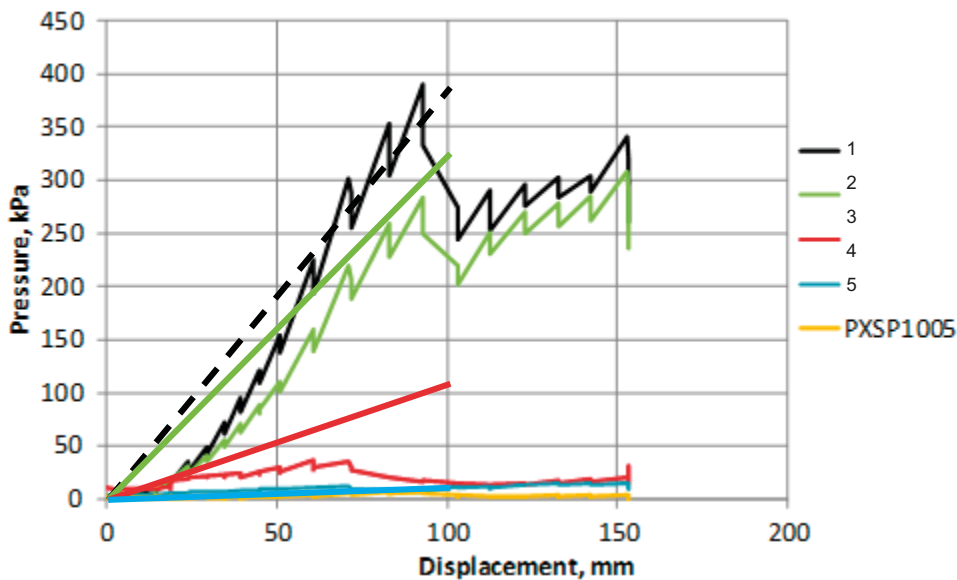


*Figure 3-8. Modelled and measured evolution of total stress perpendicular to the rock surface in the central cross section. Sensor 5 is located in the crown 2 m away from the central section.*

After 8 cm there is a peak value and a decrease until a constant residual stress is reached. The reason for this is judged to be failure of some of the backfill blocks, which is confirmed by other measurements and observations after the test. This failure is not modelled since it is not included in the material model so what happened after 8 cm displacement cannot be used for evaluation of the modelling.

The modelled and measured stresses in the ceiling and in the wall also agree very well while the modelled stress at the corner between the wall and the ceiling is higher than measured.

## 3.6 Sensitivity analysis

### 3.6.1 General

In spite of the good agreement between modelled and measured results up to 8 cm displacement there is a need for a sensitivity analysis in order to see how sensitive the solution is to changes in different properties and geometries. A good agreement between modelling and measurement is not a guarantee that the properties are correct. It may well be that several sets of parameters yield the same results. However, the fact that the original parameters have been used without adaptation of parameters in order to yield good results is a strong indicator that the models are correct.

The following variations have been tested:

- Stiffness of the three different pellets parts (roof, wall and floor).
- Width of the three different pellets parts (roof, wall and floor).
- Stiffness (or widths) of the gaps between the backfill blocks.

Table 3-1 shows a table of the variations.

**Table 3-1. Reference calculation and variations for the sensitivity analyses. Cells marked in yellow show the deviations from the reference case.**

Material/ /Case	Pellet filling in			Joints Compression at 10 MPa (mm)	Remarks Corresponding pellets thickness
	Roof E (MPa)	Walls E (MPa)	Floor E (MPa)		
Reference	3.9	3.9	3.9	4	Initial calculation 46/10/8 cm
R1 (Roof)	1.95	3.9	3.9	4	92 cm
R2	7.8	3.9	3.9	4	23 cm
W1 (Wall)	3.9	1.95	3.9	4	20 cm
W2	3.9	7.8	3.9	4	5 cm
F1 (Floor)	3.9	3.9	1.95	4	16 cm
F2	3.9	3.9	7.8	4	4 cm
J1	3.9	3.9	3.9	2	
J2 (Joints)	3.9	3.9	3.9	8	

The geometry of the model has not been changed but the change in E-modules of the pellet fillings is assumed to correspond to a proportional change in width since the compressibility is linear elastic.

Only some examples of results will be shown and finally a summarizing table that compares end evaluates the results will be given.

### 3.6.2 Case R1: Influence of the gap width at the roof

For this case the stiffness of the pellet filling in the roof has been reduced from  $E=3.9$  MPa to  $E=1.95$  MPa, which corresponds to an increase in gap width at roof from 46 cm to 92 cm. Figure 3-9 shows the modelled evolution of vertical stress on the steel plate and stresses perpendicular to the rock surface in the measuring points.

The modelled stress on the steel plate after 8 cm displacement is  $\sigma=1\,210$  kPa, which can be compared to the reference case  $\sigma=1\,550$  kPa and the measured stress  $\sigma=1\,625$  kPa. The modelled stress on the crown of the roof after 8 cm displacement is  $\sigma=210$  kPa, which can be compared to the reference case  $\sigma=310$  kPa and the measured stress  $\sigma=325$  kPa. The decreased stiffness of the backfill system caused by the increased gap is clearly reflected by the lower stresses.

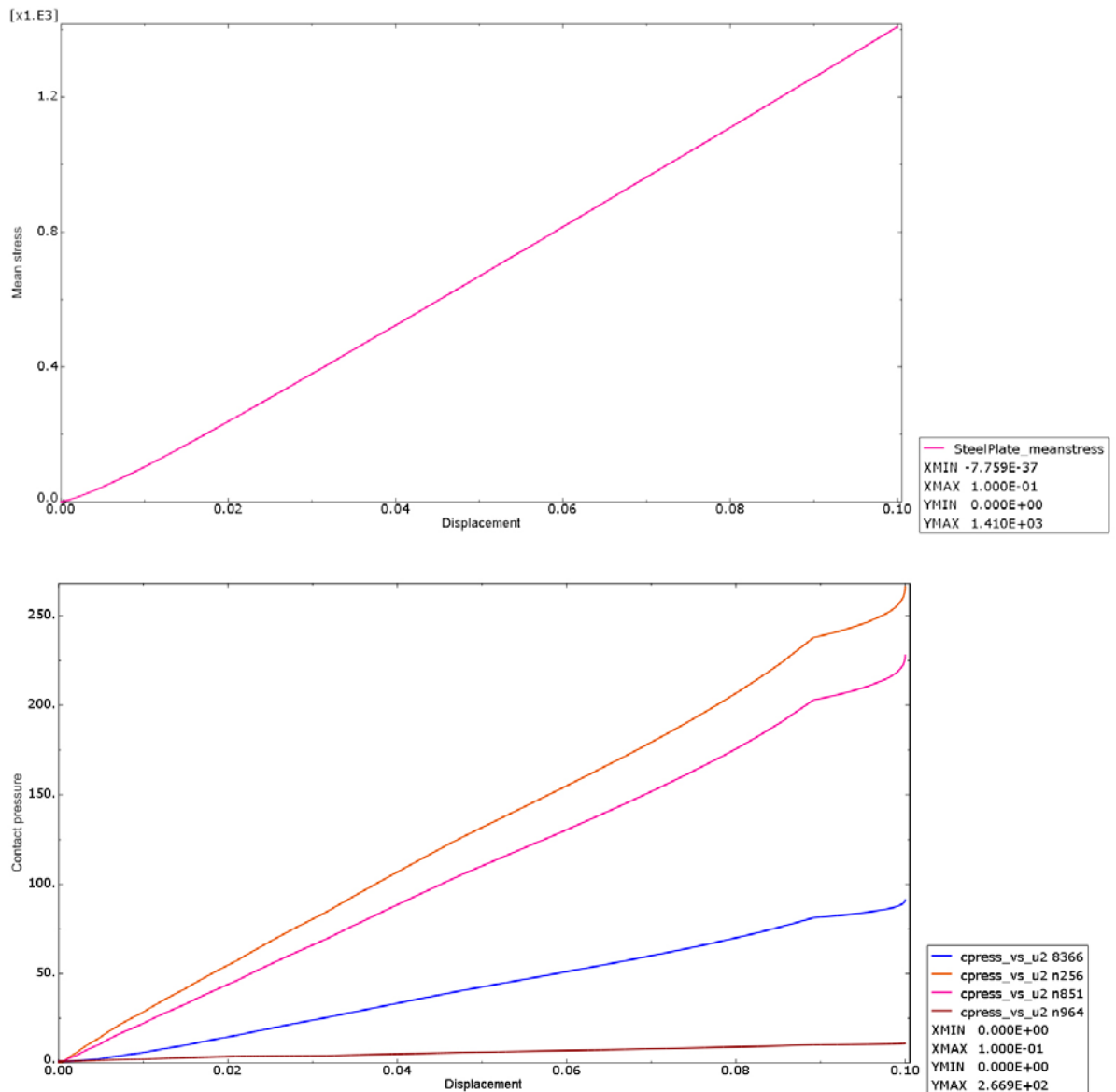


**Figure 3-9.** Case R1. Modelled stress (kPa) on the steel plate (upper) and on the rock surface in the measuring points as function of displacement of the steel plate (m)

Comparison between case R1 and the reference case for vertical stresses, the stresses on the roof and the displacements are shown in Figures 3-10 to 3-13.

These figures also show that the stresses in the backfill and on the rock surface are lower when the slot to the roof is larger (or more compressible) than in the reference case. The influence on the displacements is naturally rather small since the test is displacement controlled but the displacements have an obvious larger lateral spreading.

Comparison with reference case

Vertical stress (kPa)

Case R1:  $E=0.5E_{reference}$

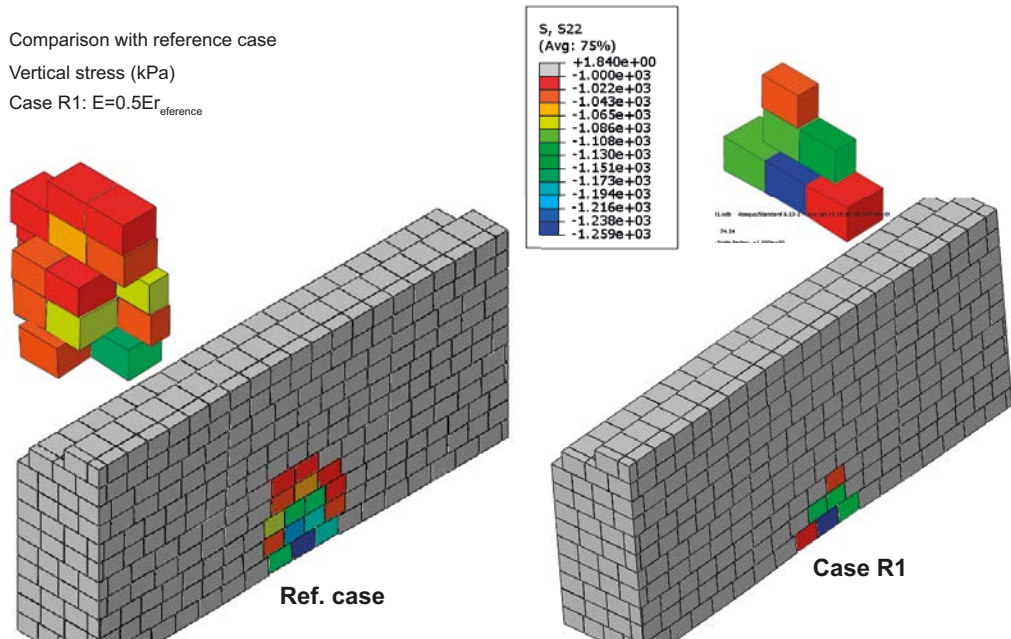


Figure 3-10. Vertical stresses (kPa) higher than 1000 kPa in the backfill blocks. Comparison case R1 and the reference case.

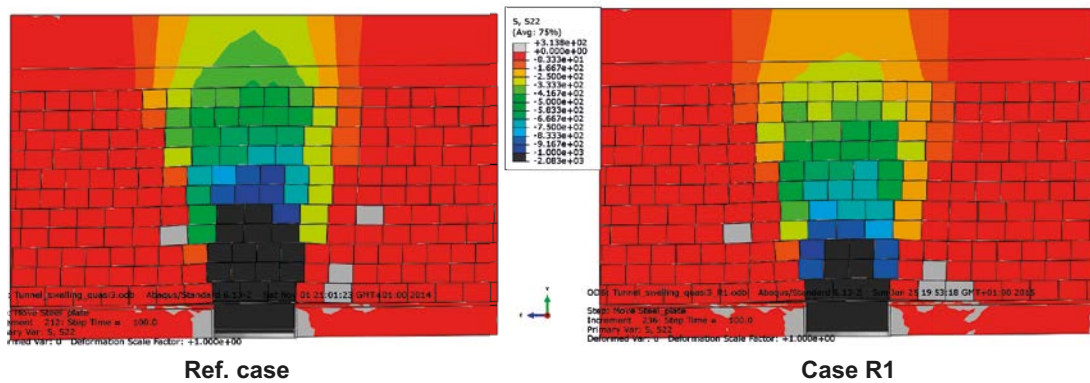


Figure 3-11. Vertical stresses (kPa) lower than 1000 kPa in the backfill blocks. Comparison case R1 and the reference case.

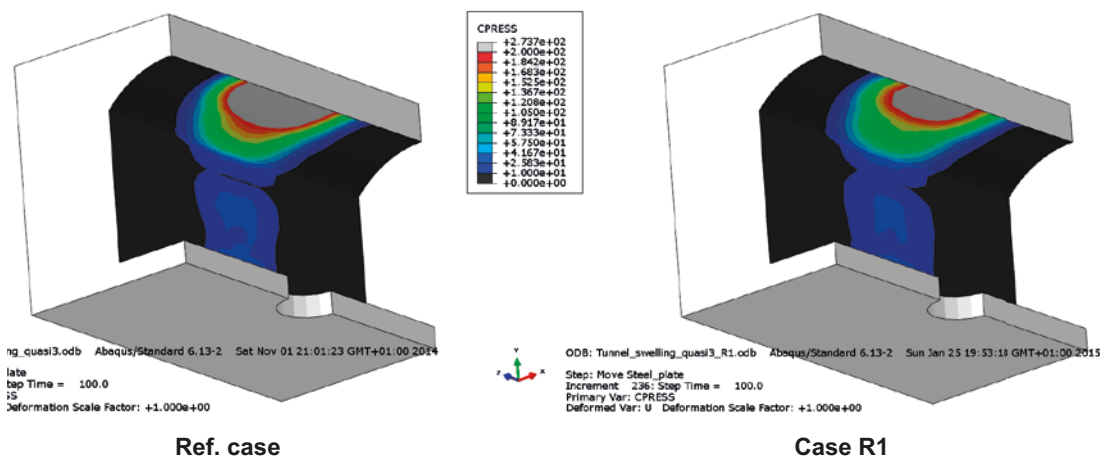


Figure 3-12. Stresses (kPa) on the rock surface. Comparison case R1 and the reference case.



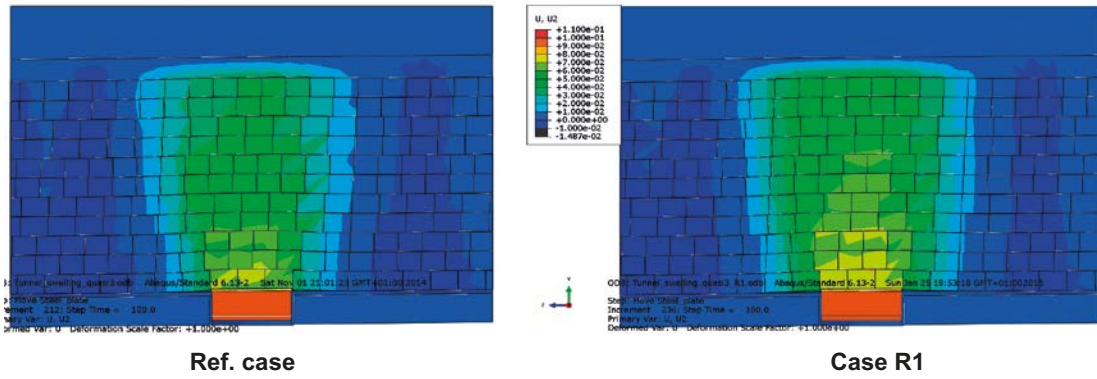


Figure 3-13. Vertical displacements (m). Comparison case R1 and the reference case.

### 3.6.3 Case J2: Influence of the stiffness of the joints

For this case the stiffness of the joints between the backfill blocks has been reduced by increasing the displacement to reach 10 MPa pressure from 4 to 8 mm.

The modelled stress on the steel plate after 8 cm displacement is for this case  $\sigma=1\,440$  kPa, which can be compared to the reference case  $\sigma=1\,550$  kPa and the measured stress  $\sigma=1\,625$  kPa. The modelled stress on the crown of the roof after 8 cm displacement is  $\sigma=285$  kPa, which can be compared to the reference case  $\sigma=310$  kPa and the measured stress  $\sigma=325$  kPa. The decreased stiffness of the backfill system caused by the reduced stiffness of the joints is clearly reflected by the lower stresses.

Comparison between case J2 and the reference case for vertical stresses, the stresses on the roof and the displacements are shown in Figures 3-14 to 3-17.

These figures show in agreement with the pellet filled slot at the roof in case R1 that the stresses in the backfill and on the rock are lower when the joints are more compressible than in the reference case. However, the influence is smaller than for case R1 and the larger lateral spreading of the displacements is not seen for case J2.

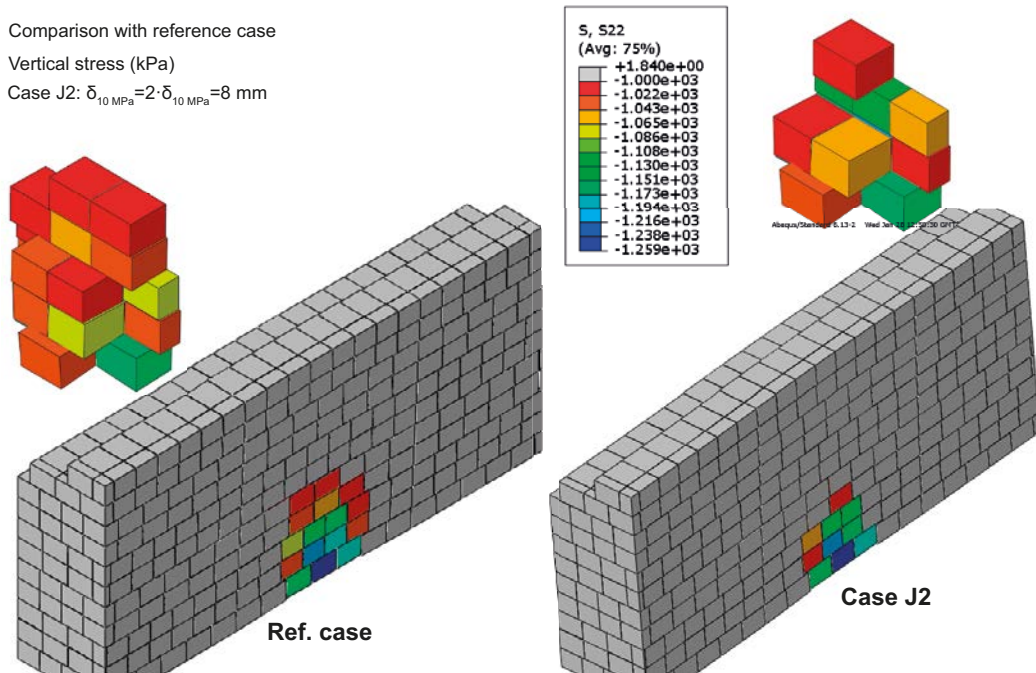


Figure 3-14. Vertical stresses (kPa) higher than 1000 kPa in the backfill blocks. Comparison case J2 and the reference case.

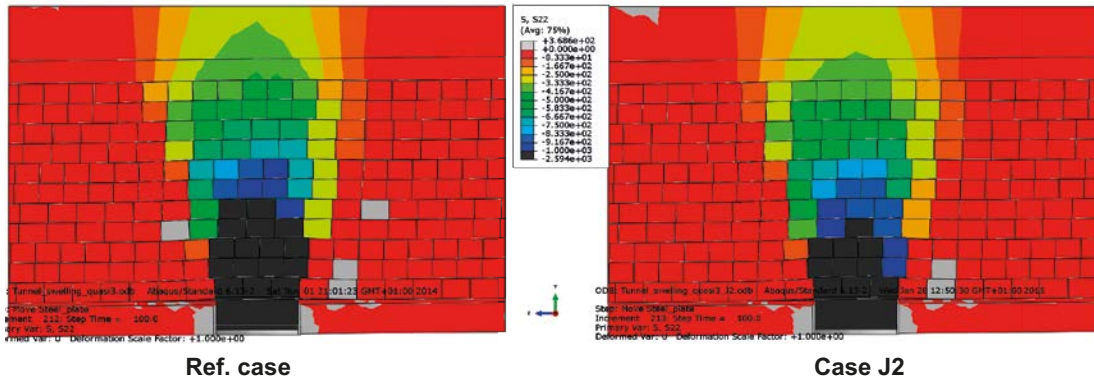


Figure 3-15. Vertical stresses (kPa) lower than 1 000 kPa in the backfill blocks. Comparison case J2 and the reference case.

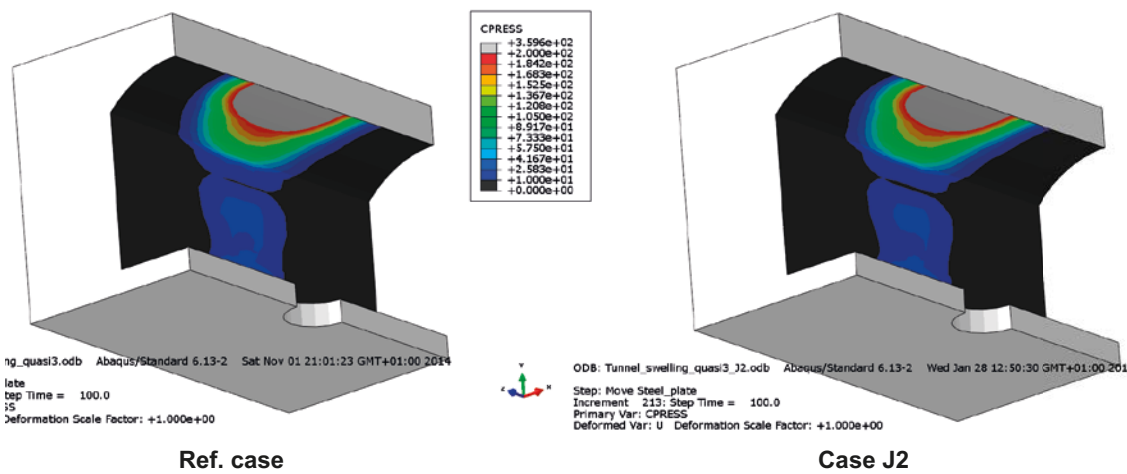


Figure 3-16. Stresses (kPa) on the rock surface. Comparison case J2 and the reference case.

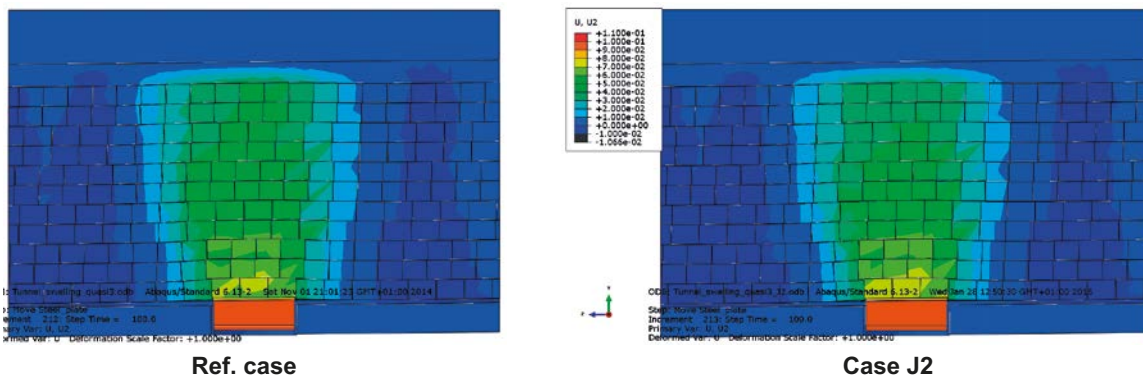


Figure 3-17. Vertical displacements (m). Comparison case J2 and the reference case.

### 3.6.4 Compilation of results from the sensitivity analysis

The other cases not described show similar results as cases R1 and J2. A decreased stiffness of some part of the backfill decreases the stresses on the rock, in the backfill and on the steel plate, while an increased stiffness increases corresponding stresses. The results are summarized in Table 3-2.

Table 3-2 shows that the largest influence, when reducing or increasing the stiffness (or thickness) with a factor 2, is achieved from the pellet filling in the roof and the floor and the lowest from the pellet filling in the walls.

**Table 3-2. Compilation of results of the sensitivity analysis. The modelled and measured pressure on the steel plate and on the rock surface at the displacement 8 cm are shown and compared. Changed parameters in yellow squares**

Material/ /Case	Pellet filling in			Joints, 10 MPa comp (mm)	Buffer pressure at 8 cm displ. (kPa) mod+100	Pressure at the roof at 8 cm displ. (kPa)
	Roof E (MPa)	Walls E (MPa)	Floor E (MPa)			
Measured					1625	325
Reference	3.9	3.9	3.9	4	1550	310
R1 (Roof)	1.95	3.9	3.9	4	1210	210
R2	7.8	3.9	3.9	4	1850	400
W1 (Wall)	3.9	1.95	3.9	4	1520	290
W2	3.9	7.8	3.9	4	1550	310
F1 (Floor)	3.9	3.9	1.95	4	1230	235
F2	3.9	3.9	7.8	4	1700	370
J1	3.9	3.9	3.9	2	1650	330
J2 (Joints)	3.9	3.9	3.9	8	1440	285

When the stiffness is reduced with a factor 2 (or the slot width increased with a factor 2) *in the roof*, the stresses are reduced on the steel plate with 28 % and in the roof with 47 %, while when the stiffness is increased with a factor 2 (or the slot width decreased with a factor 2) the stresses are increased on the steel plate with 19 % and in the roof with 29 %.

When the stiffness is reduced with a factor 2 (or the slot width increased with a factor 2) *in the floor*, the stresses are reduced on the steel plate with 26 % and in the roof with 32 %, while when the stiffness is increased with a factor 2 (or the slot width decreased with a factor 2) the stresses are increased on the steel plate with 10 % and in the roof with 19 %.

When the stiffness is reduced with a factor 2 (or the slot width increased with a factor 2) *in the joints*, the stresses are reduced on the steel plate with 8 % and in the roof with 9 %, while when the stiffness is increased with a factor 2 (or the slot width decreased with a factor 2) the stresses are increased on the steel plate with 6 % and in the roof with 6 %.

The influence of the stiffness or slot width *in the walls* is almost negligible.

Since the test was run to almost double displacement after start cracking of the blocks it is difficult to evaluate what combination of parameters are the correct ones. However, since the properties of pellet filling is known from previous investigations and since the only property that is not known beforehand is the compressibility of the joints it is plausible to assume that this is the property that should be calibrated. In addition it turned out that the prediction of the test resulted in stresses that are very close to the measured ones so the stiffness used of these joints seems to correspond fairly well to the actual stiffness. Even better agreement would have been reached if the closing of the joints at 10 MPa pressure was changed from 4 mm to 2.5 mm but the results are not very sensitive to that value.

### 3.7 Comment and conclusions

Comparison between modelled and measured results of the swelling test showed a very good agreement up to 8 cm displacement, after which cracking of the blocks took place and the model was invalid. Sensitivity analyses showed that the stiffness and thickness of the pellet filling in the floor were the factors most sensitive to changes. For further modelling the models and parameters used are adequate to use. For 2D axial symmetry models the test results can be used as a simplified model of the dry backfill if proper account is taken to changes in slot width and pellet stiffness in the ceiling and floor. The models require of course that improved quality of the backfill blocks can be made so that cracking will not take place.



## 4 Modelling of the buffer and backfill mechanical interaction with different initial conditions and different material models of the buffer

### 4.1 General

Modelling of upwards swelling of a base case was done with two purposes:

- To study the difference of the results when a completely homogenised buffer is assumed as initial conditions, which was the case for the homogenisation calculations in SR-Site, and when the actual densities of the blocks, rings and pellets filling are assumed as initial conditions.
- To see the difference of the results when the old mechanical buffer material model, which was used for the homogenisation calculations in SR-Site, was used and when the new material model, which was developed and checked as a modelling case in the TF EBS, was used.

It is interesting to see how a more realistic assumption of initially inhomogeneous buffer and how the more developed material model affect the results of the upwards swelling modelling.

### 4.2 Material models

#### 4.2.1 General

The test is modelled with the finite element code Abaqus. The code and the material model used for SR-Site are described by Åkesson et al. (2010a, b). The material models used for the present tests are described in detail by Børgesson et al. (1995).

The material models of the buffer materials are coupled hydro-mechanical with the effective stress theory as base. Full water saturation is assumed for these models. The hydraulic model use Darcy's law with hydraulic conductivity modelled as a function of the void ratio

Two mechanical material models have been used. Both models are elastic-plastic models and use porous elasticity for the elastic model. One of the plastic models uses Drucker-Prager plasticity (the old model) while the other one is a plastic cap model derived by Børgesson et al. (1995) (the new model). The models are described in Børgesson et al. (1995, 2015).

The plastic cap model was calibrated and verified in the Task 1 of the homogenisation assignment of TF EBS (Børgesson et al. 2015). The parameter values will be given in this chapter.

#### 4.2.2 Hydraulic model

The applied hydraulic conductivity relation is shown in Table 4-1 (Børgesson et al. 2015).

**Table 4-1. Hydraulic conductivity as a function of void ratio.**

e	k (m/s)
0.45	$0.5 \times 10^{-14}$
0.70	$4.0 \times 10^{-14}$
1.00	$2.0 \times 10^{-13}$
1.5	$1.0 \times 10^{-12}$
2.00	$0.5 \times 10^{-11}$
3.00	$1.0 \times 10^{-11}$
5.00	$3.5 \times 10^{-11}$
10.00	$1.5 \times 10^{-10}$
20.00	$0.75 \times 10^{-9}$

### 4.2.3 Mechanical models

#### **Porous elastic**

*Porous Elastic* implies a logarithmic relation between the void ratio  $e$  and the average effective stress (also called pressure)  $p$  according to Equations 4-1 and 4-2.

$$\Delta e = -\kappa \cdot \Delta \ln p \quad (4-1)$$

$$p = (\sigma_1 + \sigma_2 + \sigma_3) / 3 - u \quad (4-2)$$

where  $\kappa$  = porous bulk modulus

$\sigma_1, \sigma_2, \sigma_3$  = principle stresses

$u$  = pore water pressure

Poisson's ratio  $\nu$  is also required.

$\kappa = 0.175$  (Börgesson et al. 2015)

$\nu = 0.3$

This relation is not valid for low densities (see Börgesson et al. 1995) but only in the interval  $0.7 < e < 1.5$ , which correspond to  $1110 \text{ kg/m}^3 < \rho_d < 1635 \text{ kg/m}^3$ . At lower densities the porous bulk modulus is much larger ( $\kappa \approx 1.37$ ) but this change in modulus is not included in the model. If swelling causes a lower density the swelling will not be correctly modelled for that part.

#### **Drucker-Prager Plasticity model**

This model is the old model used in SR-Site (Åkesson et al. 2010a).

*Drucker-Prager Plasticity contains the following parameters:*

$\beta$  = friction angle in the  $p$ - $q$  plane

$\delta$  = cohesion in the  $p$ - $q$  plane

$\psi$  = dilation angle

$q = f(\epsilon_{pl}^d)$  = yield function

The parameter values in this model are as follows:

$\beta = 17^\circ$

$\delta = 100 \text{ kPa}$

$\psi = 2^\circ$

$q = f(\epsilon_{pl})$  according to Table 4-2.

**Table 4-2. Yield function.**

q (kPa)	$\epsilon_{pl}$
112	0
138	0.005
163	0.02
188	0.04
213	0.1

Figure 4-1 illustrates the Drucker-Prager model.

#### **Claytech plastic cap model**

This model and its background are described in detail in Börgesson et al. (1995, 2015). The model is illustrated in Figure 4-2.

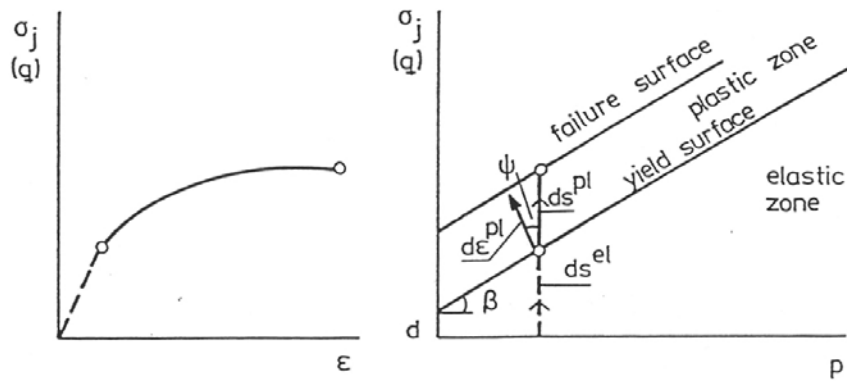


Figure 4-1. Illustration of the Drucker-Prager model.

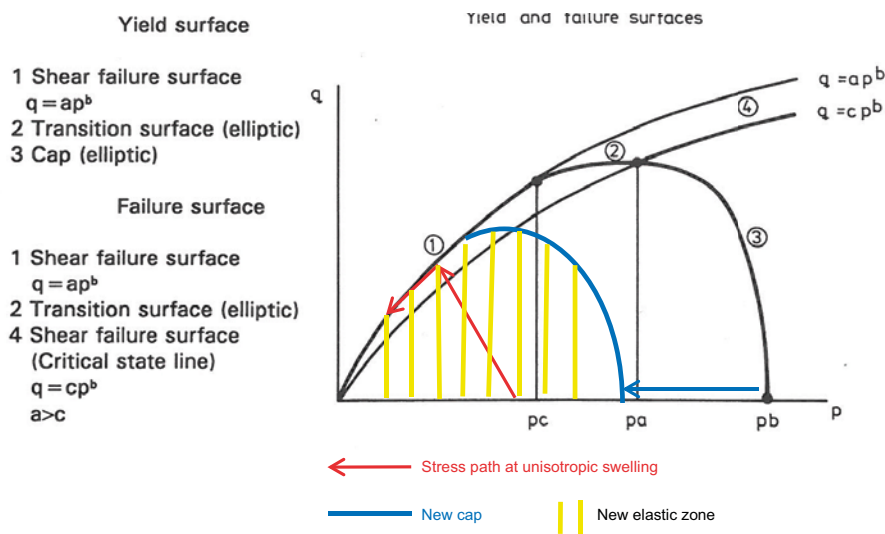


Figure 4-2. Illustration of the plastic cap model and the consequence of unisotropic swelling.

The calibrated parameters of the model (Börgesson et al. 2015) are

*Claytech plastic cap model*

$$a = 2.45$$

$$c = 2.20$$

$$b = 0.77$$

$$K = 1.0$$

$$\gamma = 0.2$$

$$R = 0.1$$

$$p_b = 30\,000 \text{ kPa}$$

$$p_f = -25\,000 \text{ kPa}$$

Cap hardening = see Table 4-3

**Table 4-3. Cap hardening function.**

$p$ kPa	$e^{\log(1+\epsilon^V p)}$
100	0
331	0.1133
934	0.2112
2160	0.2904
3247	0.3289
4294	0.3553
8240	0.4169
10044	0.4356
12530	0.4565
13299	0.4621
17562	0.4884
30000	0.5390

#### 4.2.4 Contact properties

The contacts between the buffer materials and the rock or canister have been modelled with contact surfaces with a friction angle acting between the materials. The shear resistance between the bentonite and steel has been investigated with a large number of friction tests (see e.g. Börgesson et al. 2015). The friction angle varies with the swelling pressure and the smoothness of the surface.

The friction angle of bentonite varies between 9 and 15 degrees at swelling pressures below 5 MPa. Between bentonite and a smooth surface of steel it is about half the inner friction of bentonite while it is equal to the inner friction of the bentonite if the surface is very raw. The friction angle can thus vary between 4.5 and 15 degrees depending on the swelling pressure and surface properties.

For the calculations of the buffer/backfill interaction the following friction angle  $\phi_c$  has been used:

$$\phi_c = 8.69^\circ$$

The friction angle  $8.69^\circ$  corresponds to an average between bentonite and raw and smooth surfaces at the actual swelling pressures 0.5–5 MPa.

#### 4.2.5 Other materials

The canister is modelled as a hydraulically impermeable very stiff elastic monoete that is free to move axially.

The rock is modelled as a hydraulically impermeable very stiff elastic material that is fixed.

The steel plate simulating the boundary between the buffer and the backfill block is modelled as a hydraulically impermeable very stiff elastic monoete that is free to move axially.

### 4.3 Initially homogeneous buffer

#### 4.3.1 Finite element model

The base case with initially homogeneous buffer has been modelled with both material models. The geometry is shown in Figure 4-3.

The initial conditions of the buffer correspond to the swelling pressure 7 MPa at the density at saturation  $2000 \text{ kg/m}^3$ :

$e=0.77$	void ratio
$u=-7000 \text{ kPa}$	pore water pressure
$\sigma=7000 \text{ kPa}$	average effective stress



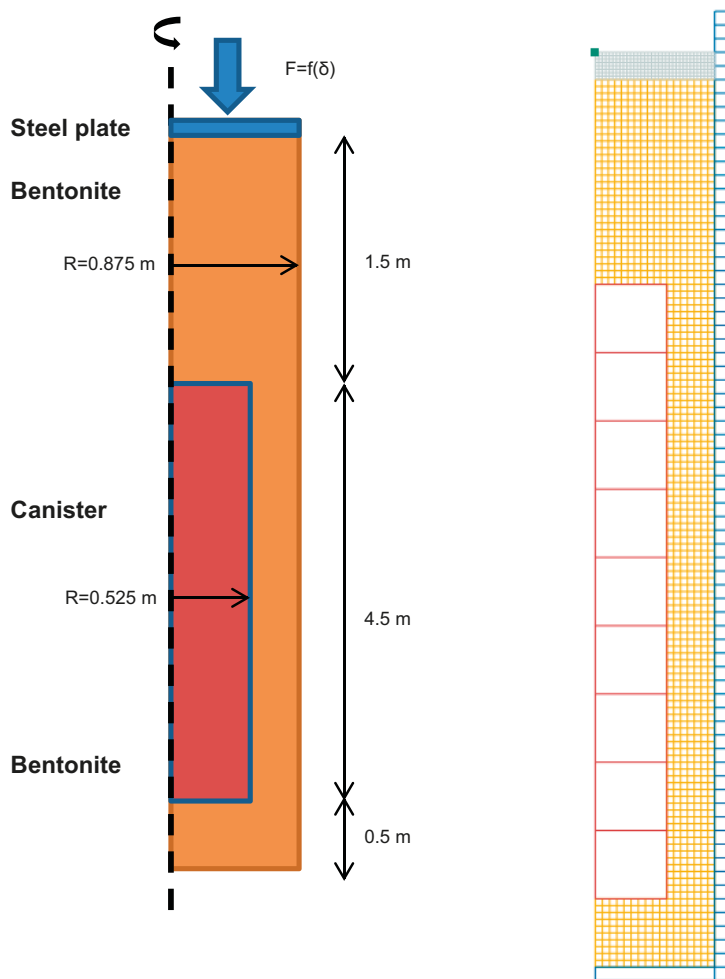


**Figure 4-3.** Schematic drawing of the geometry of the homogeneous model (left) and the element model. The model is axial symmetric around the left boundary.

The boundary conditions are the following:

#### **Hydraulic boundary**

The interface between the buffer and the rock is modelled with a constant pore water pressure that is ramped from  $u=-7$  MPa to  $u=0$  MPa in a couple of days. The reason for using 0 MPa instead of the final hydrostatic water pressure is that it simplifies the calculation and does not affect the result.

#### **Mechanical boundary**

The rock is mechanically fixed to the surroundings. The interfaces of the buffer are modelled with contact surfaces as described earlier.

#### **Resistance of the dry backfill**

The dry backfill in the upper part of the deposition hole and the deposition tunnel is not explicitly modelled. Instead the measured and also modelled stress-deformation relation, as described in Chapter 3, has been used in order to simplify the calculation. The red hatched line in Figure 3-7 was used for simulating the backfill.

### 4.3.2 Results

The calculations were run to  $10^{12}$  seconds or 32 000 years, which was much more than required for equilibrium. Figure 4-4 shows the upwards displacement of the boundary between the buffer and the backfill for both material models.

The results show that equilibrium is reached after about  $2 \times 10^9$  seconds or about 60 years. The displacement curves differ very little. The total displacement with the D-P model is about 12.7 cm while is about 13.0 with the Cap Model.

Figures 4-5, 4-6 and 4-7 show the vertical displacements, the average stress and the void ratio at the end of the calculations for both models.

A comparison shows that the difference between the results of the calculations with the two models is very small. Figure 4-8 shows the final dry density and vertical stress for only the Cap Model.

The upwards swelling creates friction forces on the canister. Figure 4-9 shows the axial shear stress between the buffer and the canister surface. The maximum shear stress is about 0.5 MPa on the canister surface.

## 4.4 Initially inhomogeneous buffer

### 4.4.1 Finite element model

The case corresponding to the initial conditions in the Canister Retrieval Test (CRT) with initially inhomogeneous buffer has been modelled with both material models. The modelling of CRT is described in Börjesson et al. (2016). The geometry is shown in Figure 4-10.

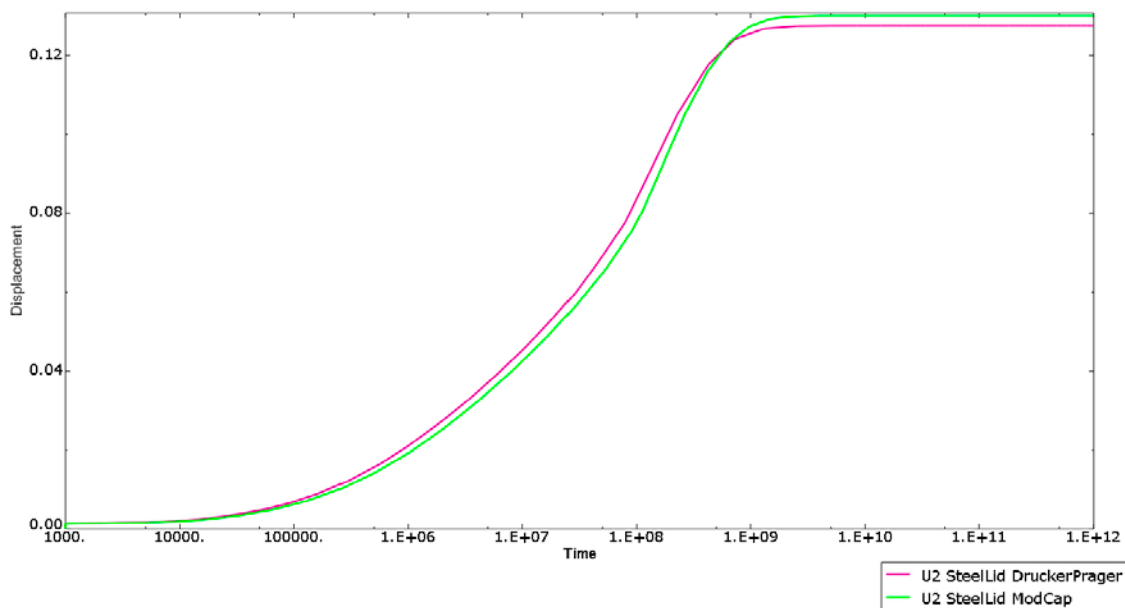


**Figure 4-4.** Modelled displacement (m) of the buffer-backfill interface as function of time for the two models with initially homogeneous buffer.

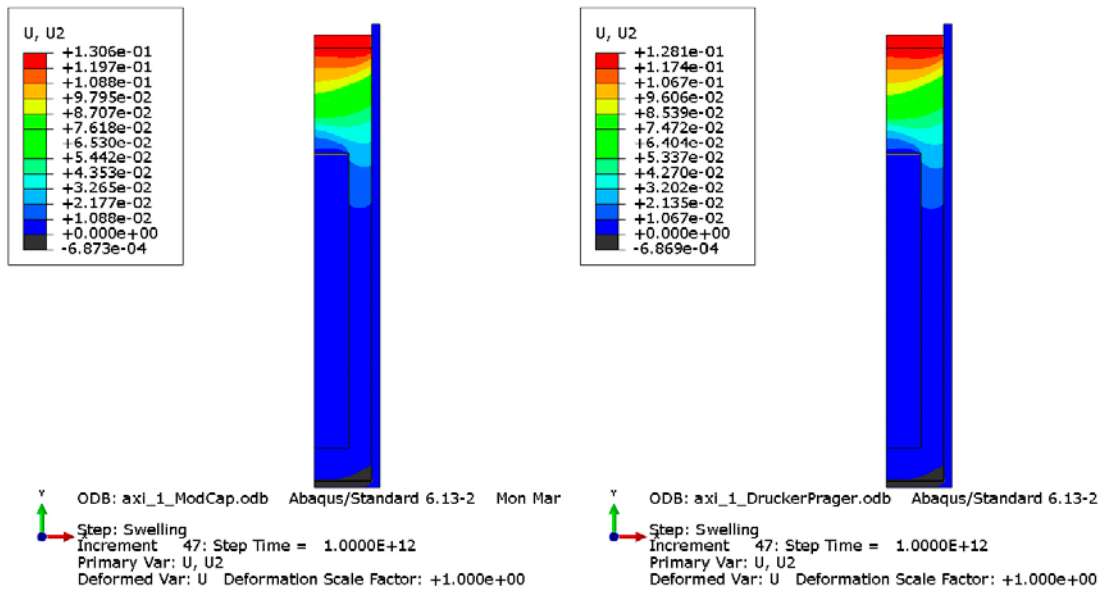


**Figure 4-5.** Modelled final vertical displacements (m) for the two models with initially homogeneous buffer. The Cap Model to the left and the D-P model to the right.

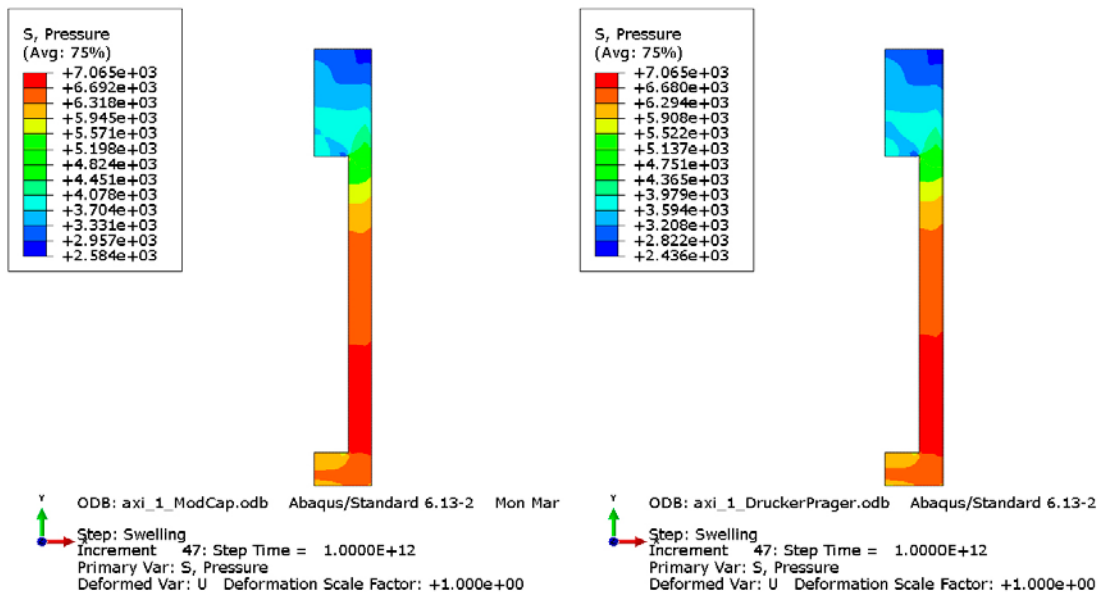


**Figure 4-6.** Modelled final average stress (kPa) for the two models with initially homogeneous buffer. The Cap Model to the left and the D-P model to the right.

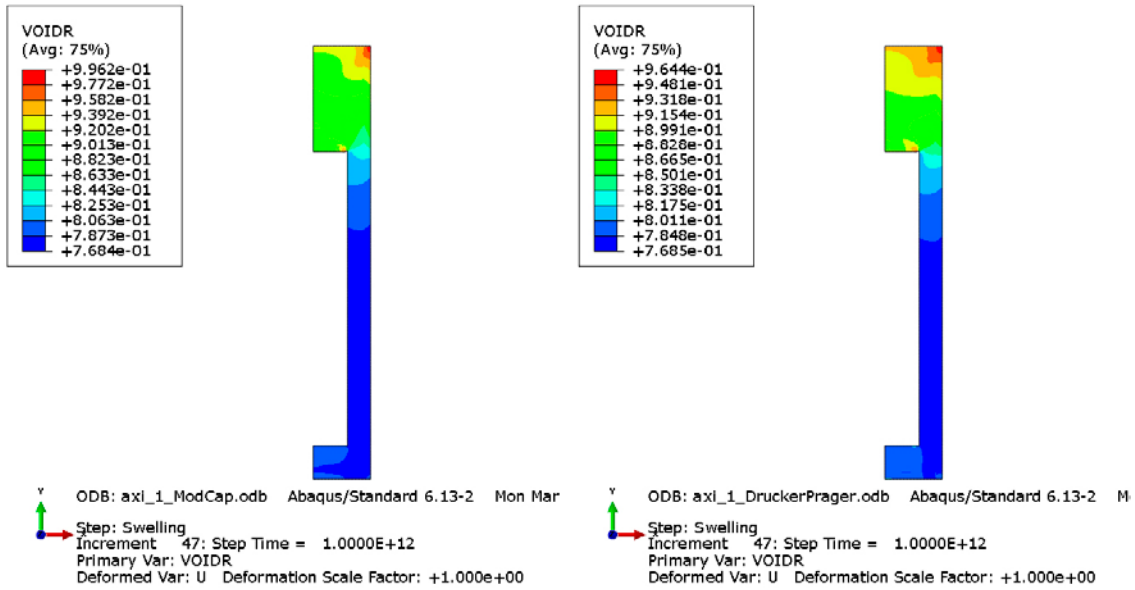


Figure 4-7. Modelled final void ratio for the two models with initially homogeneous buffer. The Cap Model to the left and the D-P model to the right.

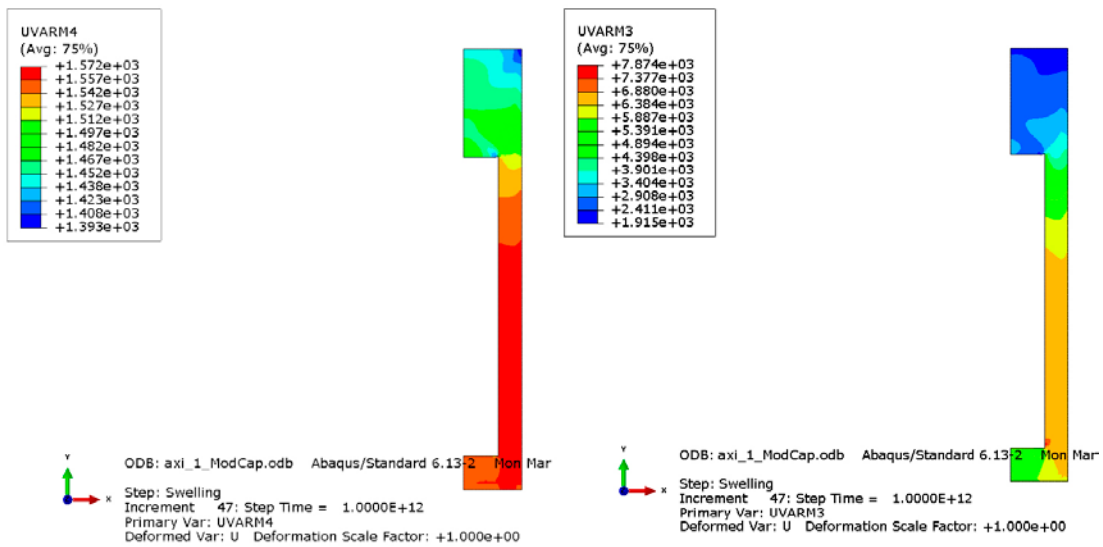
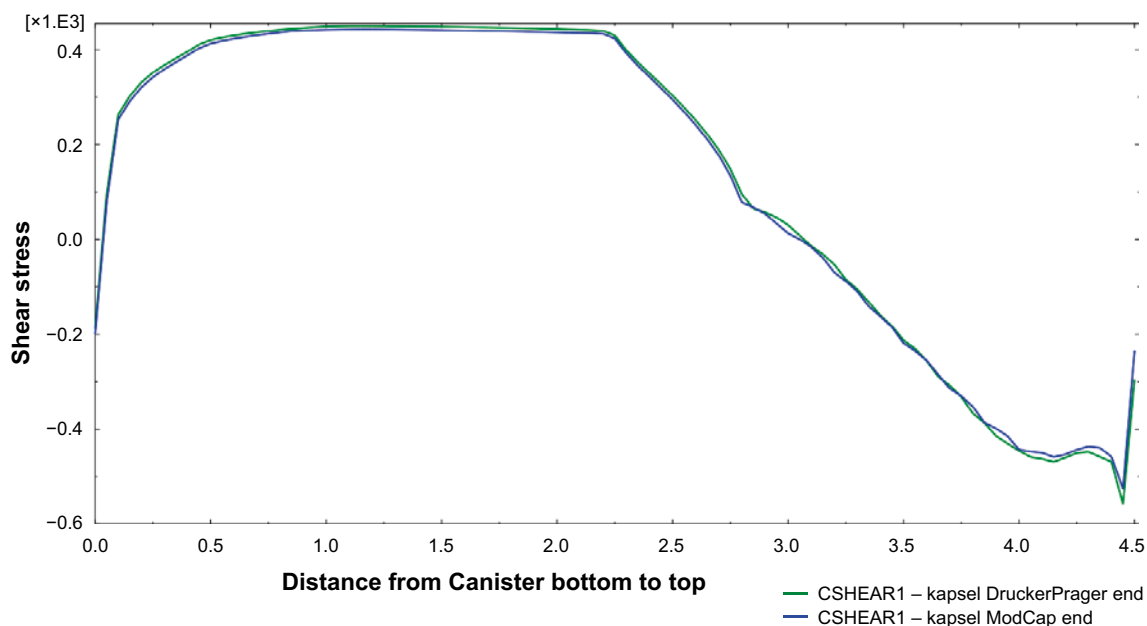


Figure 4-8. Modelled final dry density ( $\text{kg/m}^3$ ) (left) and vertical stress (kPa) for the Cap Model with initially homogeneous buffer.



**Figure 4-9.** Shear stress (kPa) on the canister surface as function of the distance from the canister bottom for the two material models.

The initial conditions of the buffer are thus the same as for the CRT but with full saturation from start:

*Blocks:*

$e=0.636$  void ratio  
 $u=-15\,050$  kPa pore water pressure  
 $\sigma=15\,050$  kPa average effective stress

*Rings:*

$e=0.56$  void ratio  
 $u=-23\,240$  kPa pore water pressure  
 $\sigma=23\,240$  kPa average effective stress

*Pellets:*

$e=1.78$  void ratio  
 $u=-22$  kPa pore water pressure  
 $\sigma=22$  kPa average effective stress

The average density at saturation in CRT is a little higher than  $2\,000\text{ kg/m}^3$ , so a comparison with the homogenised buffer can be a little misleading. In addition the void ratios of the buffer parts are outside the range where the Porous Elastic model is valid ( $0.7 < e < 1.5$ ) according to Börgesson et al. (1995). This has been taken into account in the calculations described later in the report.

The boundary conditions are the following:

### **Hydraulic boundary**

The interface between the buffer and the rock is modelled with a constant pore water pressure that is ramped from  $u=7$  MPa to  $u=0$  MPa in a couple of days.

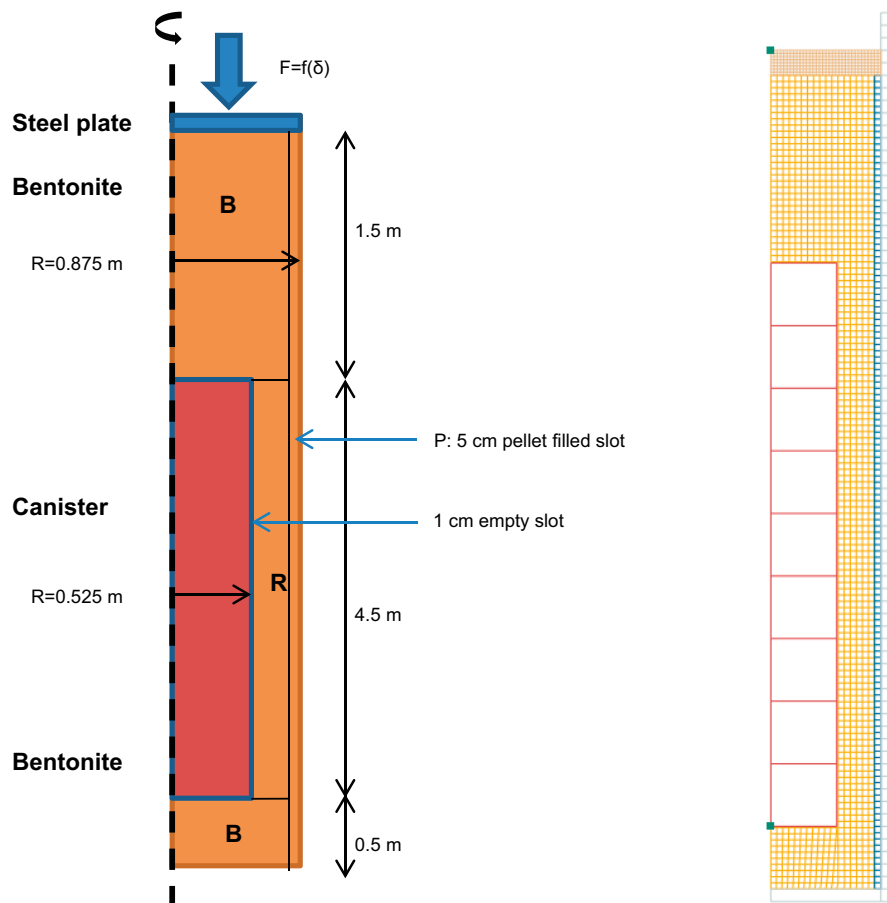


**Figure 4-10.** Schematic drawing of the geometry of the inhomogeneous model (left) and the element model. The model is axial symmetric around the left boundary. The abbreviations of the buffer parts mean: B=blocks, R=rings and P=pellets.

### **Mechanical boundary**

The rock is mechanically fixed to the surroundings. The interfaces of the buffer are modelled with contact surfaces as described earlier.

### **Resistance of the dry backfill**

The dry backfill in the upper part of the deposition hole and the deposition tunnel is not explicitly modelled. Instead the measured and also modelled stress-deformation relation, as described in Chapter 3, has been used in order to simplify the calculation. The red hatched line in Figure 3-7 was used for simulating the backfill.

## **4.4.2 Results**

Also these calculations were run to  $10^{12}$  seconds or 32 000 years, which was much more than required for equilibrium. Figure 4-11 shows the upwards displacement of the boundary between the buffer and the backfill for both material models.

The results show that equilibrium is reached after about  $2 \times 10^9$  seconds or about 60 years. The displacement curves differ very little. The total displacement with the D-P model is about 17 cm while it is about 18 with the Cap Model.

Figures 4-12, 4-13 and 4-14 show the vertical displacements, the average stress and the void ratio at the end of the calculations for both models.

A comparison shows that the difference between the results of the calculations with the two models is very small. Figure 4-15 shows the final dry density and vertical stress for only the Cap Model.

The upwards swelling creates friction forces on the canister. Figure 4-16 shows the axial shear stress between the buffer and the canister surface. The maximum shear stress is about 0.5 MPa on the canister surface with exception of a peak close to the canister lid.

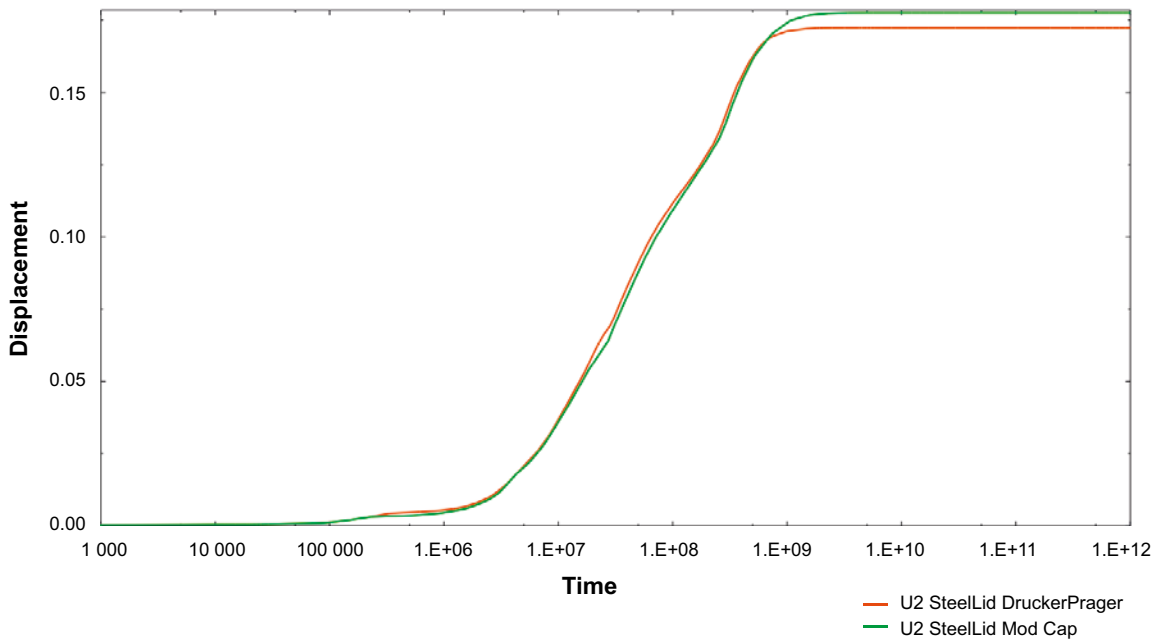


**Figure 4-11.** Modelled displacement (m) of the buffer-backfill interface as function of time for the two models with initially inhomogeneous buffer.

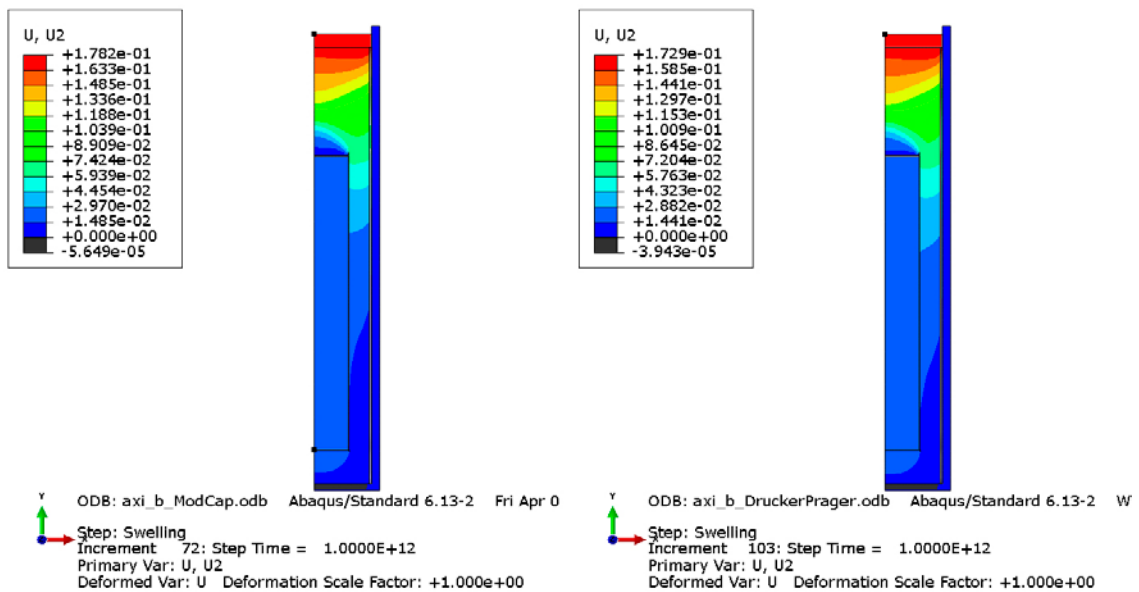


**Figure 4-12.** Modelled final vertical displacements (m) for the two models with initially inhomogeneous buffer. The Cap Model to the left and the D-P model to the right.

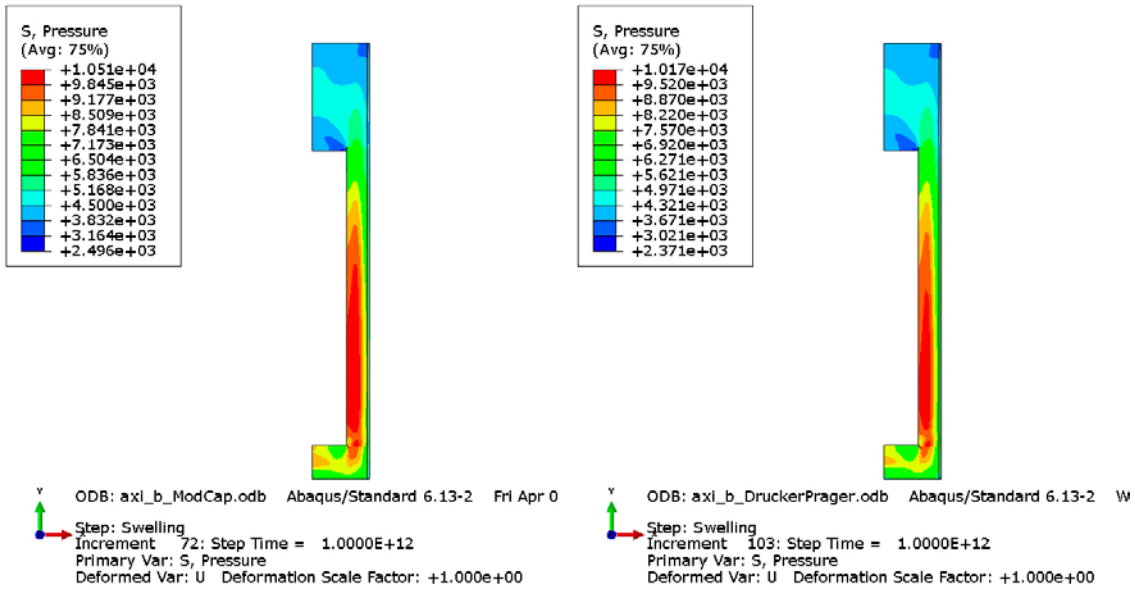


**Figure 4-13.** Modelled final average stress (kPa) for the two models with initially inhomogeneous buffer. The Cap Model to the left and the D-P model to the right.

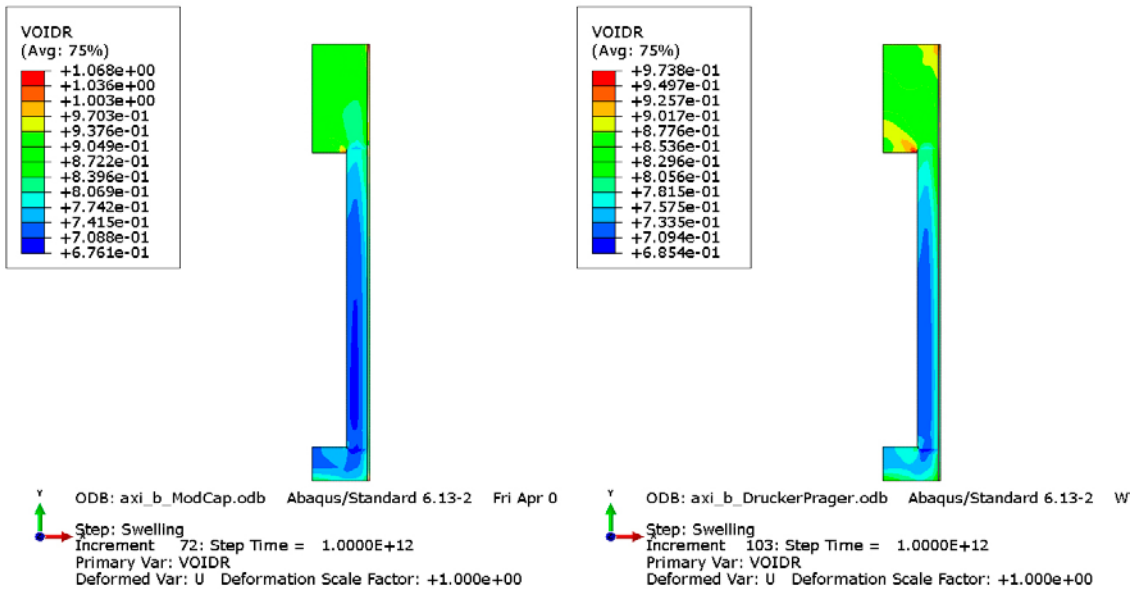


**Figure 4-14.** Modelled final void ratio for the two models with initially inhomogeneous buffer. The Cap Model to the left and the D-P model to the right.



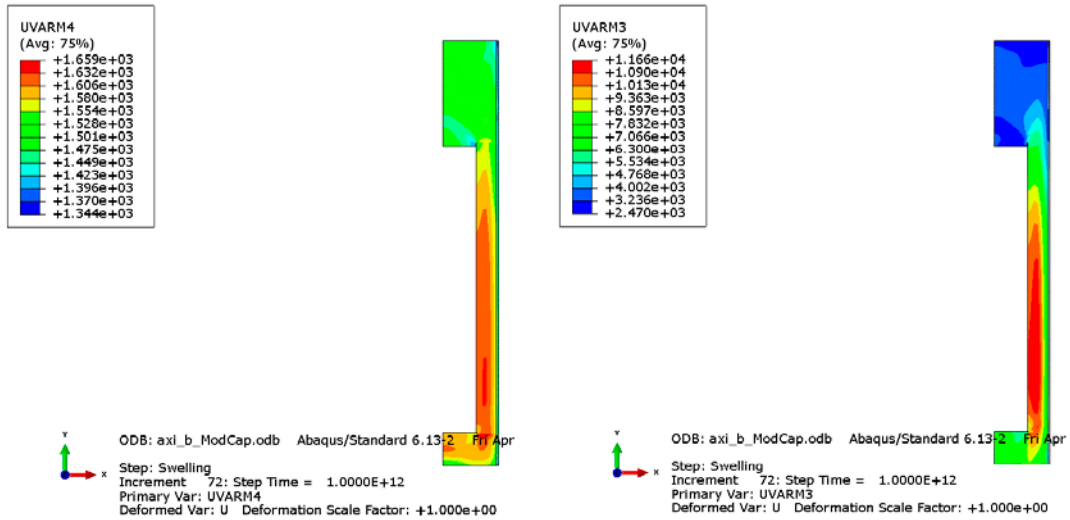


Figure 4-15. Modelled final dry density ( $\text{kg/m}^3$ ) (left) and vertical stress ( $\text{kPa}$ ) for the Cap Model with initially inhomogeneous buffer.

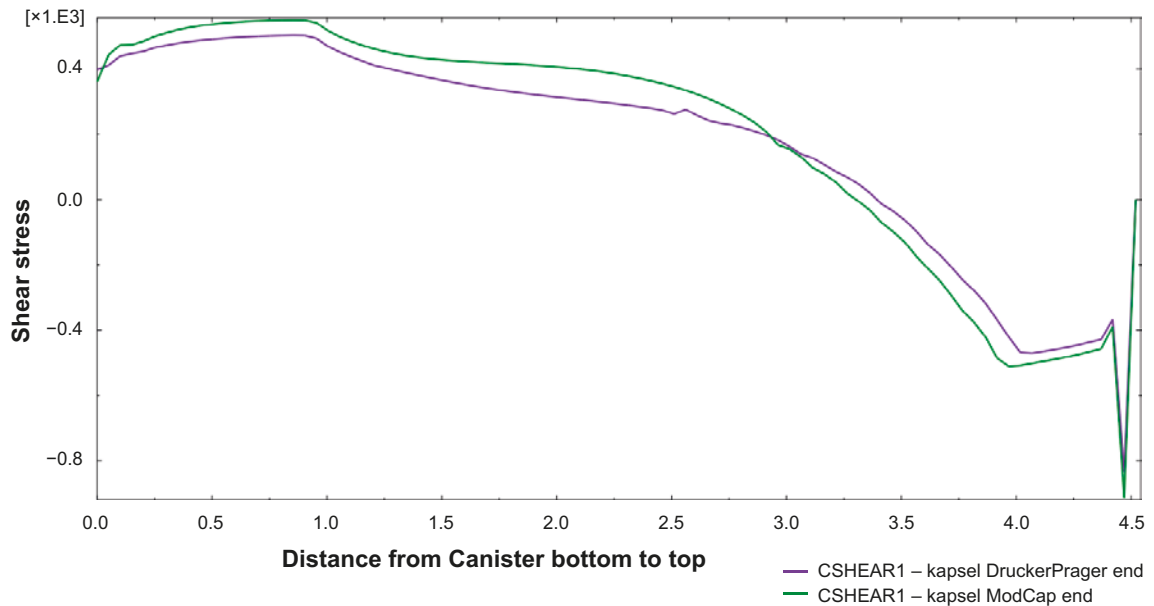


Figure 4-16. Shear stress ( $\text{kPa}$ ) on the canister surface as function of the distance from the canister bottom for the two material models.

#### 4.5 Calculation of average density up to 0.5 m above the canister lid

As mentioned in section 2–3 the newly proposed criteria of buffer density shall be calculated up to 0.5 m above the canister lid. Since Abaqus uses void ratio instead of density the evaluation of the average void ratio will at first be done. Figure 4-17 shows the void ratio distribution for two of the four models.

The average void ratio is calculated from the vertical displacement of the horizontal element plane located initially 0.5 m above the canister top during the swelling process. By integrating the volume of the displacement, the increase in total volume of the buffer up to 0.5 m above the canister top can be calculated. The final average void ratio can then be calculated according to Equation 4-2.

$$e_f = e_i + (e_i + 1) \cdot \Delta V_f / V_i \quad (4-2)$$

where

$e_f$  = final void ratio

$e_i$  = initial void ratio

$\Delta V$  = volume increase

$V_i$  = initial volume

Figure 4-18 shows the vertical displacement of the surface at 0.5 m above the canister for the same models as in Figure 4-17.

Figure 4-18 shows that the appearance and magnitude of the displacements differ significantly. The inhomogeneous case yields larger displacements (almost double) and a maximum at half the hole radius.

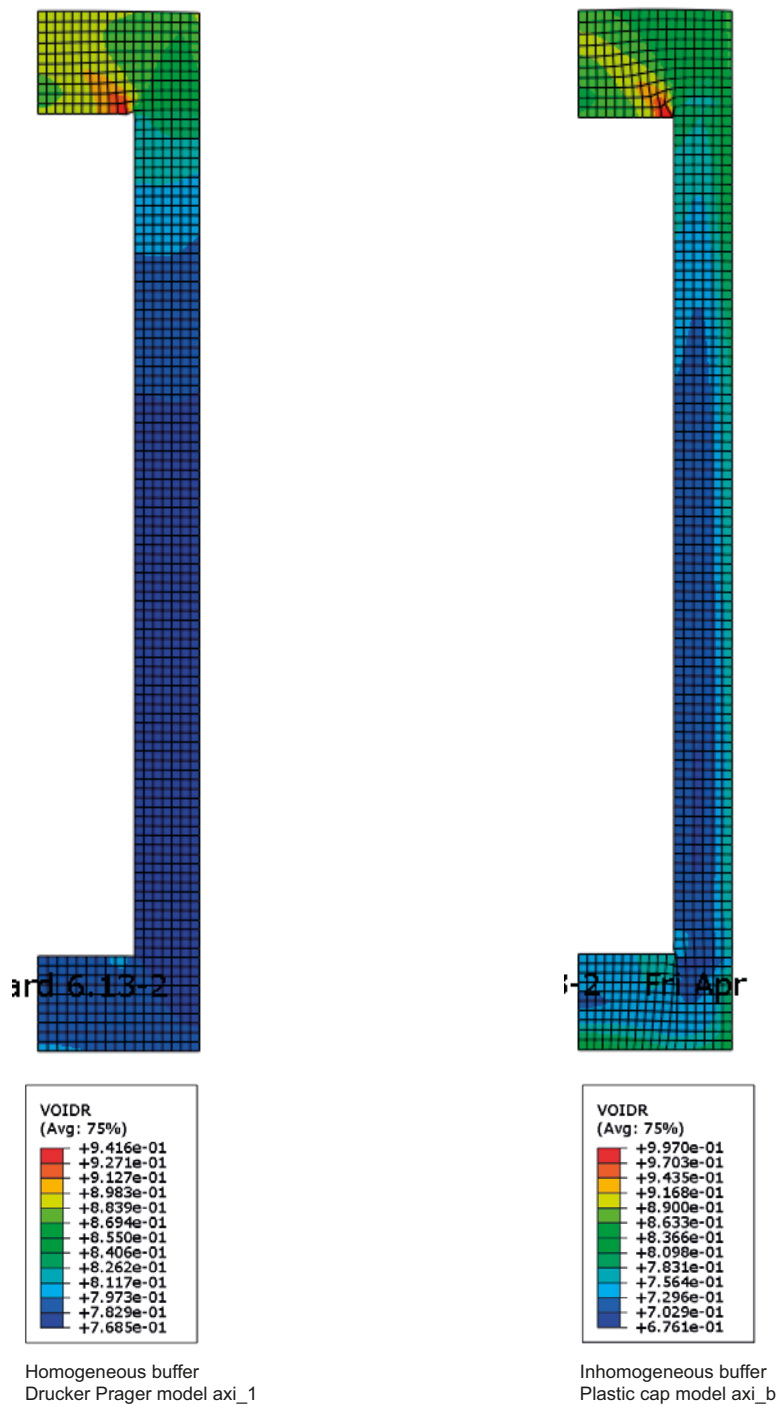
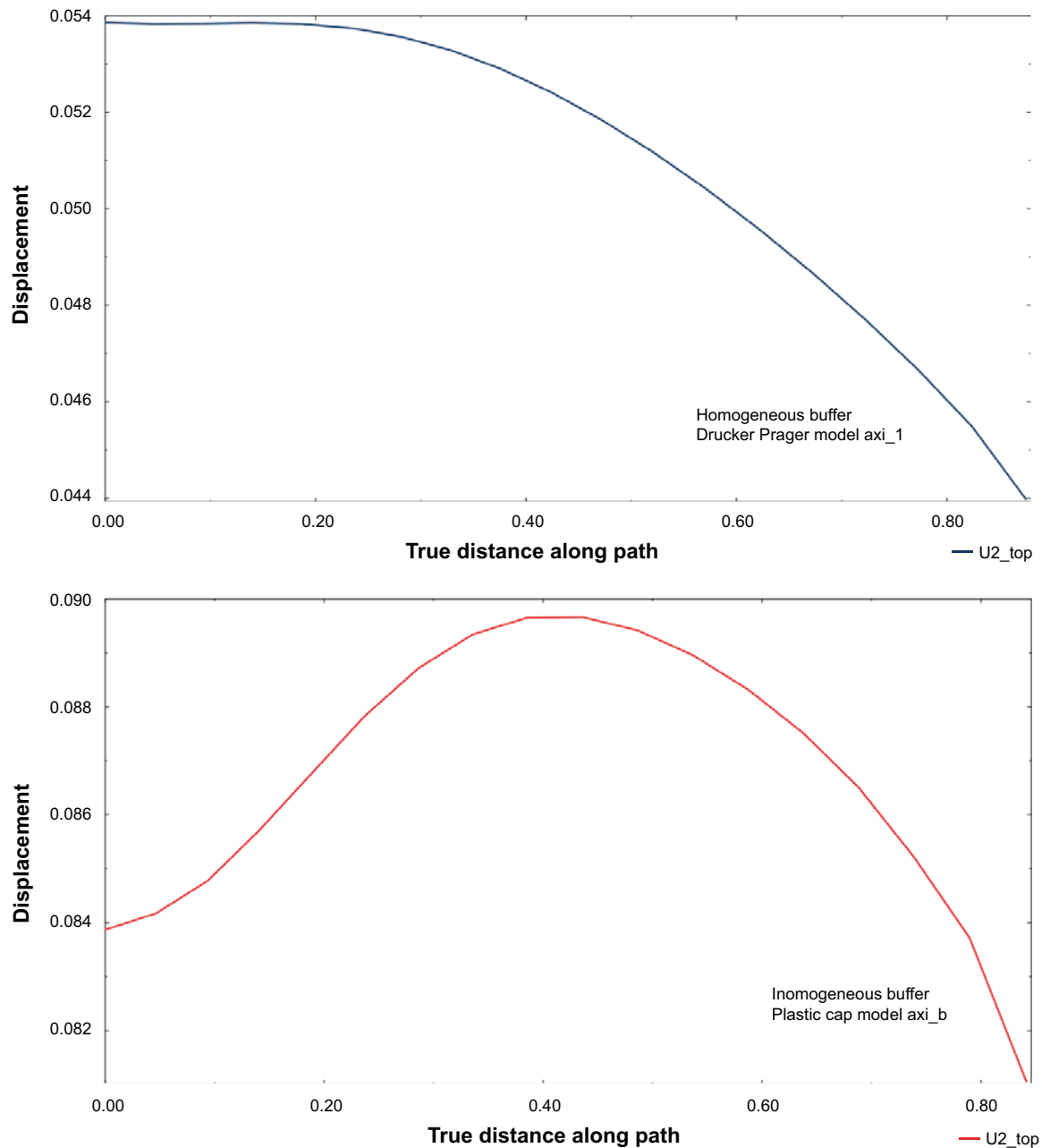


Figure 4-17. Void ratio distribution up to 0.5 m from the canister lid for two of the four models



**Figure 4-18.** Displacement (m) of the surface located 0.5 m above the canister top. The x-axis is plotted as the distance (m) from the centre axis.

The density at saturation can be calculated from the void ratio according to Equation 4-3.

$$\rho_m = (\rho_s + e \cdot \rho_w) / (e + 1) \quad (4-3)$$

where

$\rho_m$  = density at saturation (kg/m<sup>3</sup>)

$\rho_s$  = density of solids (= 2 780 kg/m<sup>3</sup>)

$\rho_w$  = density of water (= 1 000 kg/m<sup>3</sup>)

$e$  = void ratio

Table 4-4 shows the calculated average void ratio and density at saturation for the four cases.

**Table 4-4. Calculated average void ratio and density at saturation up to 0.5 m from the canister top for the four cases. The density change is also included**

Case	Material model	Final void ratio	Density at saturation before and after swelling kg/m <sup>3</sup>	Density change $\Delta\rho$ kg/m <sup>3</sup>
Homogeneous buffer	Drucker-Prager	0.792	2006@1993	13
Homogeneous buffer	Plastic cap	0.793	2006@1993	13
Inhomogeneous buffer	Drucker-Prager	0.810	2032@1983	49
Inhomogeneous buffer	Plastic cap	0.810	2032@1983	49

The table shows that there is small difference after swelling between the two material models. This is a coincidence. The table also shows that the density change is much larger for the inhomogeneous buffer case.

## 4.6 Comments and conclusions

### *Comparison of material models*

A comparison between the results when the D-P model was used and when the Cap Model was used show that the difference is small. It seems as the introduction of a cap and a curved failure envelope does not affect the results very much at the type of swelling that takes place in these models.

The stress paths in a  $p$ - $q$  diagram of some elements are shown in Figure 4-19 in order to illustrate the swelling process. The stresses go with fairly constant average stress up to the failure line and then follow the failure line during decreasing stresses. In spite of that the failure lines are slightly different and the dilatancy at the failure line also differ the difference is obviously not large enough in order to lead to very different results for the two models.

Results from other analyses have shown that the Plastic Cap model yields better agreement with measurements than the Drucker-Prager model (Börgesson et al. 2015). They also show that it sometimes is more difficult to get convergence with the more complicated Plastic Cap models. In the following calculations the plastic Cap model has mainly been used.

### *Comparison of initial conditions*

Comparisons of some results when the actual initial densities of blocks, rings and pellets were used and when the average initial density of the entire buffer was used are shown in Figures 4-18 and 4-19. In spite of that the results are not fully comparable since the initial average density of the inhomogeneous model is a little higher than in the homogeneous model some observations can be done.

The final vertical displacements are compared in Figure 4-20. The figures show that the upwards swelling of the interface is about 18 cm in the inhomogeneous model and 13 cm in the homogeneous model. Even larger differences are seen in the buffer between the canister and rock in level with the top of the canister, where the displacement is 2–3 cm in the homogeneous case and 5–6 cm in the inhomogeneous case. Also the upwards displacement of the canister differ. It is less than 1 cm in the homogeneous case and about 2 cm in the inhomogeneous case.

The final dry density of the buffer for the two models are compared in Figure 4-21.

The density distribution under and along the canister differ very much for the two cases. The inhomogeneous model has a remaining very strong density spreading in comparison with the homogeneous model. However, above the canister, where the large swelling takes place, the difference is not very large.

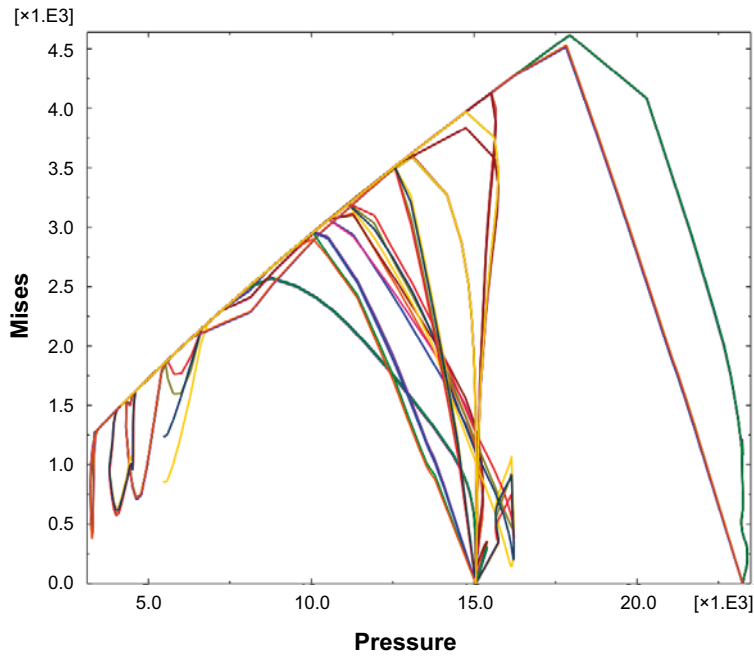


**Figure 4-19.** Stress paths (Mises stress  $q$ , kPa vs. average stress  $p$ , kPa) for some elements in the model with initially inhomogeneous buffer and the Cap Model.

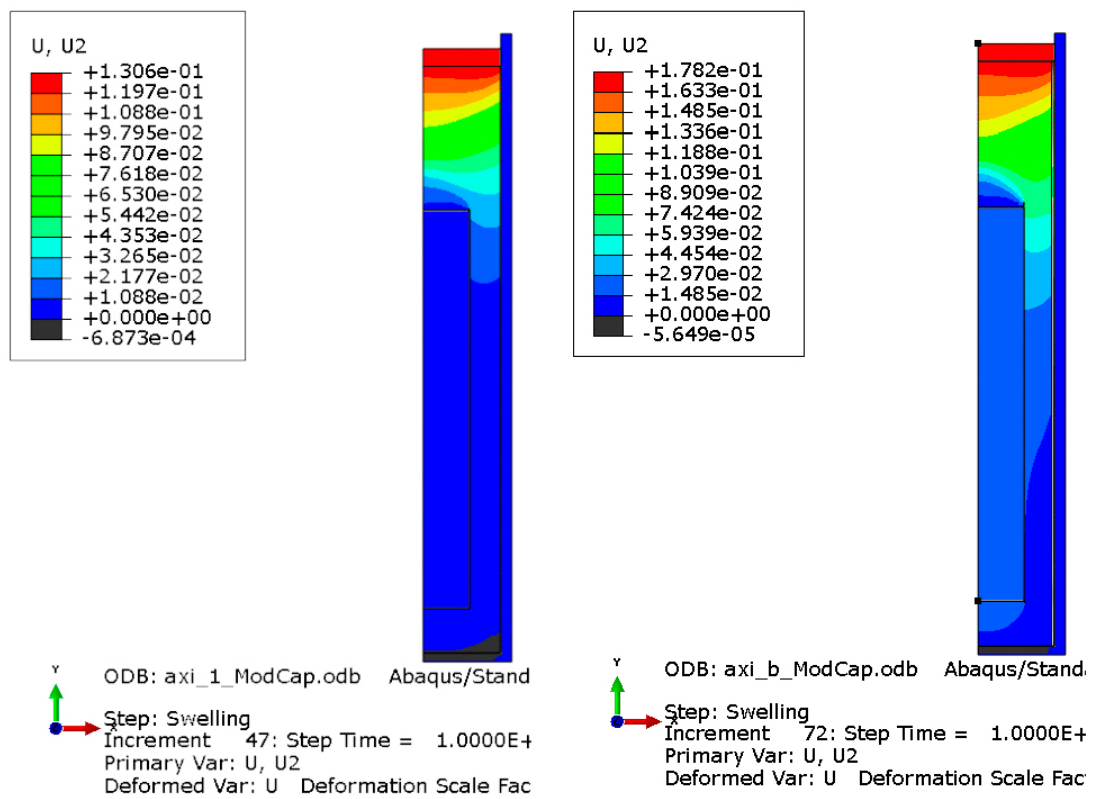


**Figure 4-20.** Comparison between the final vertical displacements (m) in the buffer at initially homogenised buffer (left) and at initially inhomogeneous buffer (right).

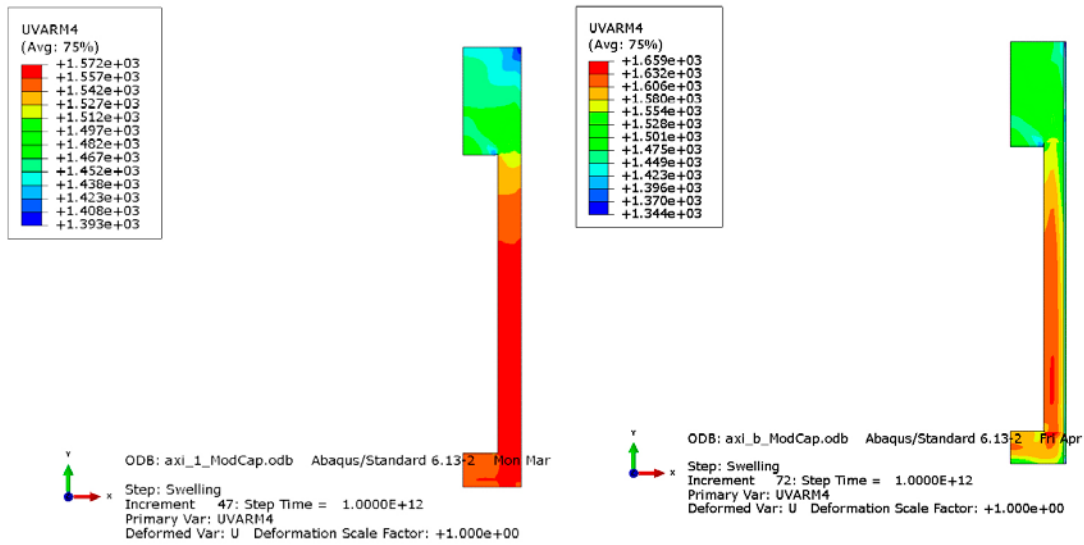


**Figure 4-21.** Comparison between the final dry density ( $\text{kg/m}^3$ ) distribution in the buffer at initially homogenised buffer (left) and at initially inhomogeneous buffer (right).

The average density of the buffer calculated up to 0.5 m from the canister top according to the suggested new criterion yields similar density after swelling but this is caused by the higher initial density of the buffer in the inhomogeneous cases. The density loss is much larger in the inhomogeneous case.

A conclusion is that the inhomogeneous buffer model should be used if possible. Underestimation of the swelling may otherwise be the case.

## 5 Influence of buffer density and backfill geometry

### 5.1 General

15 cases with different average density and swelling pressure of the buffer and different geometry of the backfill have been modelled with the new material model and initially inhomogeneous buffer. The purpose has been to study the sensitivity to changes in geometry and density. The backfill response was modelled with the extrapolated test results and with changes in geometry taken into account. In six cases the backfill blocks in the upper part of the deposition hole was modelled with simplified models that takes the density loss into the bevel into account.

Table 5-1 summarizes the modelled cases.

**Table 5-1. Modelled cases. X denotes dry backfill and Y denotes wet backfill in the upper part of the deposition hole.**

Thickness of bottom layer $t_p$ (a–e) / Swelling pressure $\sigma$ (1–3) and density at saturation $\rho_m$	(a) $t_p=10$ cm	(b) $t_p=25$ cm	(c) $t_p=10$ cm + bevel	(d) $t_p=10$ cm + bevel + blocks	(e) $t_p=50$ cm
(1) $s=4$ MPa, 1965 kg/m <sup>3</sup>	X	X	Y	Y	X
(2) $s=7$ MPa, 2011 kg/m <sup>3</sup>	X	X	Y	Y	X
(3) $s=10$ MPa, 2041 kg/m <sup>3</sup>	X	X	Y	Y	X

Three different average swelling pressures were thus modelled with the swelling pressure 4 MPa, 7 MPa and 10 MPa (cases 1–3). Five different geometries were modelled. Cases *a*, *b* and *e* had the thickness of the bottom layer 10 cm, 25 cm and 50 cm and no bevel. Cases *c* and *d* had the bottom layer thickness 10 cm a simulated bevel.

The bevel in cases *c* and *d* was not included geometrically. Instead it was pessimistically simulated as having a completely homogenised bentonite backfill meaning that the density in the upper part of the deposition hole (the 2.5 upper blocks) had a density equal to the average density of that part and the bevel, i.e. complete homogenisation. These cases also differed from the other cases so that all bentonite in the deposition hole was modelled as completely water saturated while the backfill in the tunnel was still dry.

Initially inhomogeneous buffer with blocks, rings and pellets is used in these calculations according to the conclusions in Section 4.6. The density of the blocks and rings was chosen so that the average density of the buffer would yield the desired swelling pressure of cases 1–3.

The models were made axially symmetric which means that the bevel and the backfill in the tunnel could not be geometrically included. Instead the response from the blocks in the tunnel was modelled with the same stress-strain relation as measured and modelled for the field test described in Chapter 3. The difference in thickness of the pellet filled floor was taken into account by adding calculated additional deformation as described in Section 5.2.3.

### 5.2 Model

#### 5.2.1 Geometry

Figure 5-1 shows the geometry and the element mesh of the model.

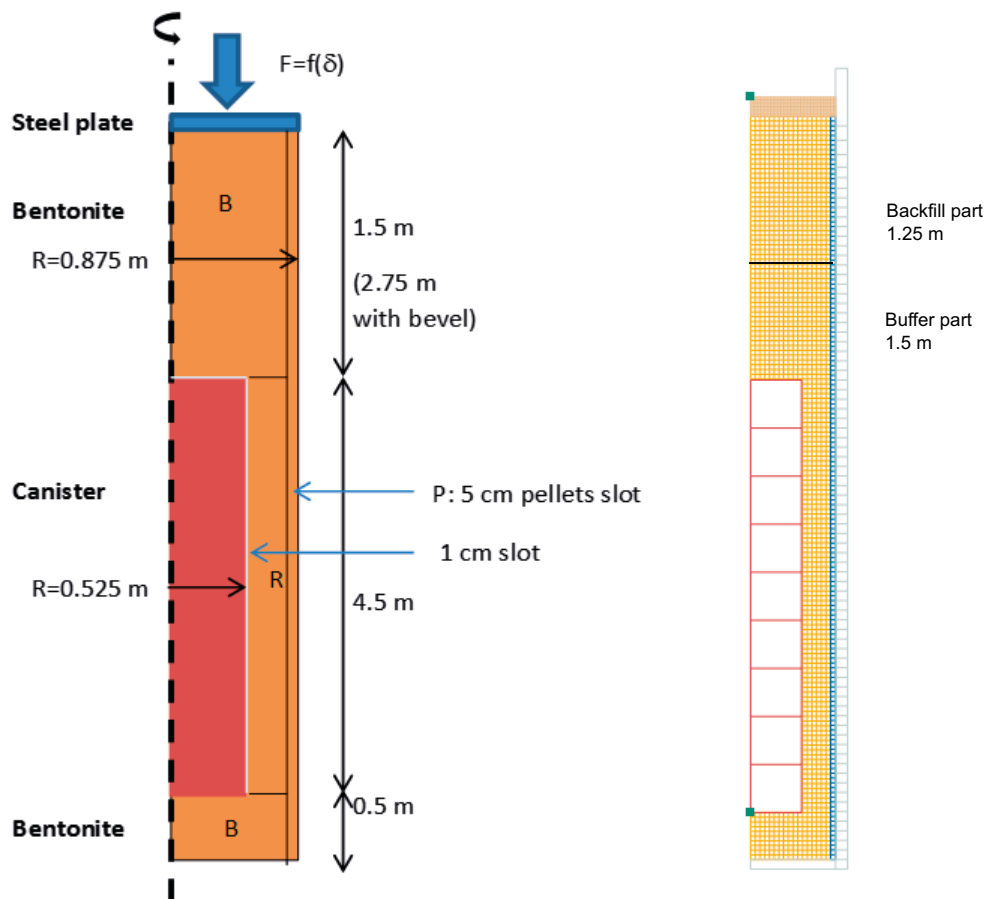


**Figure 5-1.** Schematic drawing of the geometry of the 15 modelled cases. The element mesh of cases c and d is shown to left.

1 cm slot between the rings and the canister and on top of the canister is included.

- Rings (R):  $r_i=0.535$  m,  $r_o=0.825$  m.
- Blocks (B):  $r_i=0$  m,  $r_o=0.825$  m.
- Pellets:  $r_i=0.825$  m,  $r_o=0.875$  m.
- Slot:  $r_i=0.525$  m,  $r_o=0.535$  m.
- 1 cm slot above the canister but not below.

## 5.2.2 Initial conditions

### The buffer

The initial densities of the blocks and rings that would yield the requested average swelling pressure need to be calculated. The relation between void ratio  $e$  and the swelling pressure  $p$  is described by Equation 5-1 for MX-80 bentonite according to Børgesson et al. (1995).

$$e = e_0 \left( \frac{p}{p_0} \right)^\beta \quad (5-1)$$

where

$e$ =void ratio at  $p$

$e_0=1.1$

$p_0=1\ 000$  kPa

$\beta=-0.19$



Average calculated void ratios according to Equation 5-1 and resulting dry densities  $\rho_d$  are shown in Table 5-1. The density of solids  $\rho_s=2\,780\text{ kg/m}^3$  and the density of water  $\rho_w=1\,000\text{ kg/m}^3$  have been used in the calculation.

**Table 5-1. Average void ratio and dry density of the buffer used in the modelling.**

Case	$p$ (kPa)	$e$	$r_d$ (kg/m <sup>3</sup> )
1	4000	0.845	1507
2	7000	0.760	1580
3	10000	0.710	1626

Observe that the average density at saturation at the swelling pressure 10 MPa is  $\rho_m=2\,041\text{ kg/m}^3$ , which is higher than  $\rho_m=2\,022\text{ kg/m}^3$ , since the material model of MX-80 has been used. For  $\rho_m=2\,022\text{ kg/m}^3$  the swelling pressure of MX-80 according to Equation 5-1 is only 7960 kPa, while it is 10 MPa for Ca-bentonite Deponit CaN according to Børgesson et al. (2010).

With the geometries shown in Figure 5-1 the void ratio of the blocks and rings that yield the average void ratios in Table 5-1 will be according to Table 5-2. The corresponding initial conditions regarding pressure and suction are also shown.

For Table 5-2 the void ratio of the pellet filled slot has been set to  $e=1.78$ , which corresponds to the dry density  $\rho_d=1\,000\text{ kg/m}^3$ . Based on this, the geometry and the average void ratio for cases 1–3 the void ratio of the blocks and rings have been calculated. A problem with the Porous Elastic model is that it is only fully valid for void ratios  $0.7 < e < 1.5$ , which is outside the actual values for most blocks and rings. In order to adjust this drawback and ensure that the swelling pressure after swelling is correct the initial conditions of the pressure and pore pressure had to be adjusted. The reason for the problem is that the Porous Elastic model, which is used by Abaqus, is single logarithmic while the relation as described by Equation 5-1 is double logarithmic. This correction is done by adding or subtracting the difference between the swelling pressure according to Equation 5-1 and the swelling pressure calculated according the Porous Elastic model at the initial void ratios.

**Table 5-2. Initial conditions of the buffer components used in the model.**

Case	Void ratio $e_0$	Pressure $p_0$ and Pore pressure $-u_0$ (MPa)	Remarks
<b>Blocks</b>			
(1) 4 MPa	0.771	6.49	
(2) 7 MPa	0.683	10.9	Recalculated <sup>1</sup>
(3) 10 MPa	0.632	14.5	Recalculated <sup>1</sup>
<b>Rings</b>			
(1) 4 MPa	0.679	11.1	Recalculated <sup>1</sup>
(2) 7 MPa	0.591	18.4	Recalculated <sup>1</sup>
(3) 10 MPa	0.541	24.5	Recalculated <sup>1</sup>
<b>Pellet filling</b>			
1–3	1.78	0.022	Recalculated <sup>1</sup>

<sup>1</sup> Recalculated means that the pressure  $p_0$  has been adapted to yield the correct swelling pressure at the desired average density. This must be done for most blocks and the pellets since the validity of the Porous Elastic model is limited to  $0.7 < e < 1.5$ .

### **The backfill in the bevel**

The properties of the “bevel” for cases c and d are calculated with the following assumptions:

- Length of backfilled part of the deposition hole:  $\Delta L=1.25\text{ m}$ .
- Total volume of only bevel:  $2.16\text{ m}^3$ .

- Volume of “backfill blocks”: 2.67 m<sup>3</sup>.
- Volume of pellets in backfilled part of the deposition hole: 0.33 m<sup>3</sup>.
- Dry density of backfill blocks in backfilled part of the deposition hole and in the bevel:  $\rho_d=1\ 704\ \text{kg/m}^3$ .

This data yields the following average initial conditions of void ratio, pressure and pore pressure of the upper part of the deposition hole assuming a completely homogenised bentonite backfill:

*Case c (only pellets in the bevel):*

- Average dry density  $\rho_d=1\ 364\ \text{kg/m}^3$ .
- Average void ratio:  $e=1.04$ .
- Pressure  $p_0=1.34\ \text{MPa}$ .
- Pore pressure  $u_0=-1.34\ \text{MPa}$ .

*Case d (pellets and blocks in the bevel):*

For case d eight bentonite blocks with the dimensions  $0.5 \times 0.4 \times 0.571\ \text{m}^3$  have been placed in the bevel according to Figure 5-2.

This yields an increased average density:

- Average dry density  $\rho_d=1\ 488\ \text{kg/m}^3$ .
- Average void ratio:  $e=0.868$ .
- Pressure  $p_0=3.58\ \text{MPa}$ .
- Pore pressure  $u_0=-3.58\ \text{MPa}$ .

The initial conditions are thus according to Table 5-3.

**Table 5-3. Initial conditions of the upper backfilled part of the deposition hole.**

Bevel + upper 1.25 m deposition hole			
Case	Average void ratio $e_0$	Pressure $p_0$ and Pore pressure $-u_0$ (MPa)	Remarks
c	1.04	1.34	Only pellets
d	0.868	3.58	Pellets and blocks

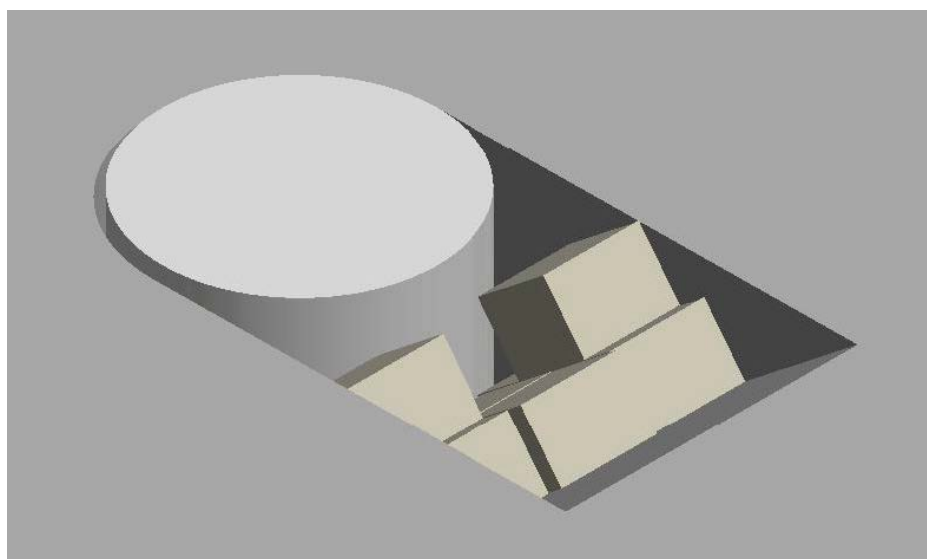


**Figure 5-2.** Placement of 8 blocks in the bevel.

### 5.2.3 Material models

The *hydraulic model* is identical to the model shown in 4.2.2.

The *mechanical models* are identical to the Porous Elastic Model and the Cap Model presented in Section 4.2.3.

The models of the *other materials* are identical to the models presented in Section 4.2.6.

The model of the *backfill in the deposition tunnel* is modelled in the same way as described by the red hatched line in Figure 3-7. This response is valid for the thickness 8 cm of the pellet filling in the floor. However, cases a, b and c refer to other thicknesses and this has to be adjusted for. The compression properties of pellet fillings have been investigated by several tests as shown in Andersson and Sandén (2012). As an average relation the compression test on IBECO extruded pellets has been used. The stress-strain relation is shown in Figure 5-3.

By adding the influence of an increased pellet filling thickness according to Figure 5-3 the response of the dry backfills can be derived. Figure 5-4 shows these relations.

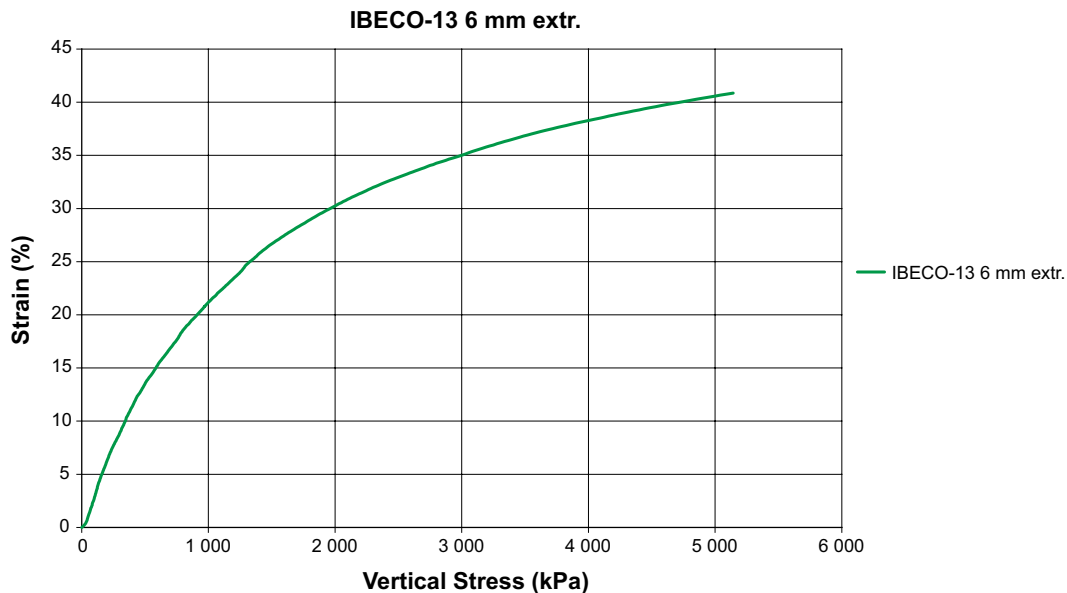


Figure 5-3. Stress-strain relation used for the modelling of the pellet filling.

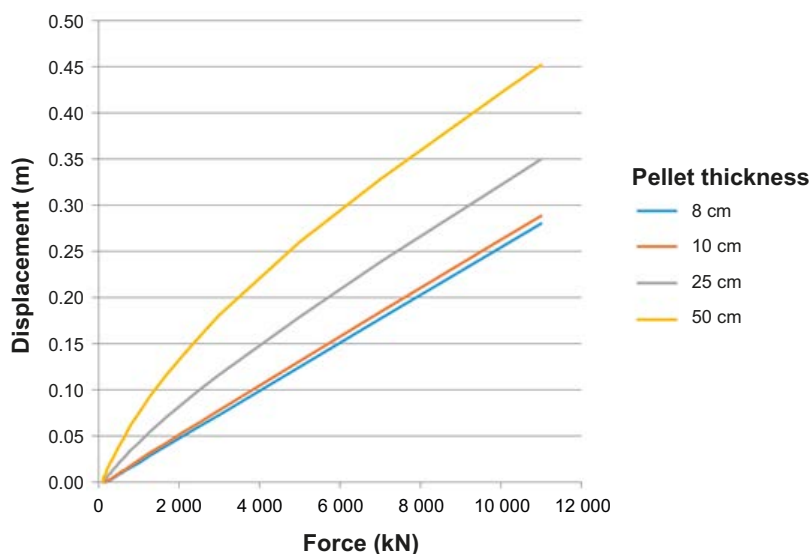


Figure 5-4. Force-displacement relation used for modelling the response of the dry backfill.

Since the response is modelled as a spring acting against the interface between the buffer and the backfill (or for cases c and d the interface at the top of the deposition hole) the force is used instead of the stress.

## 5.2.4 Boundary conditions

### Hydraulic boundary

The interface between the buffer and the rock is modelled with a constant pore water pressure that is ramped to  $u=0$  MPa in a couple of days.

### Mechanical boundary

The rock is mechanically fixed to the surroundings. The interfaces of the buffer are modelled with contact surfaces as described earlier.

## 5.3 Results

The results from all 15 models are shown in Appendix 1. Only the final conditions are plotted since the intermediate results are not very relevant and not very interesting. The following results are plotted as contour plots:

- Dry density.
- Void ratio.
- Radial stresses.
- Axial stresses.
- Average stresses.
- Axial displacements.

The axial displacements and the average stress of case 2a ( $\sigma=7$  MPa,  $t_p=10$  cm), which can be considered a base case, are shown in Figure 5-5.

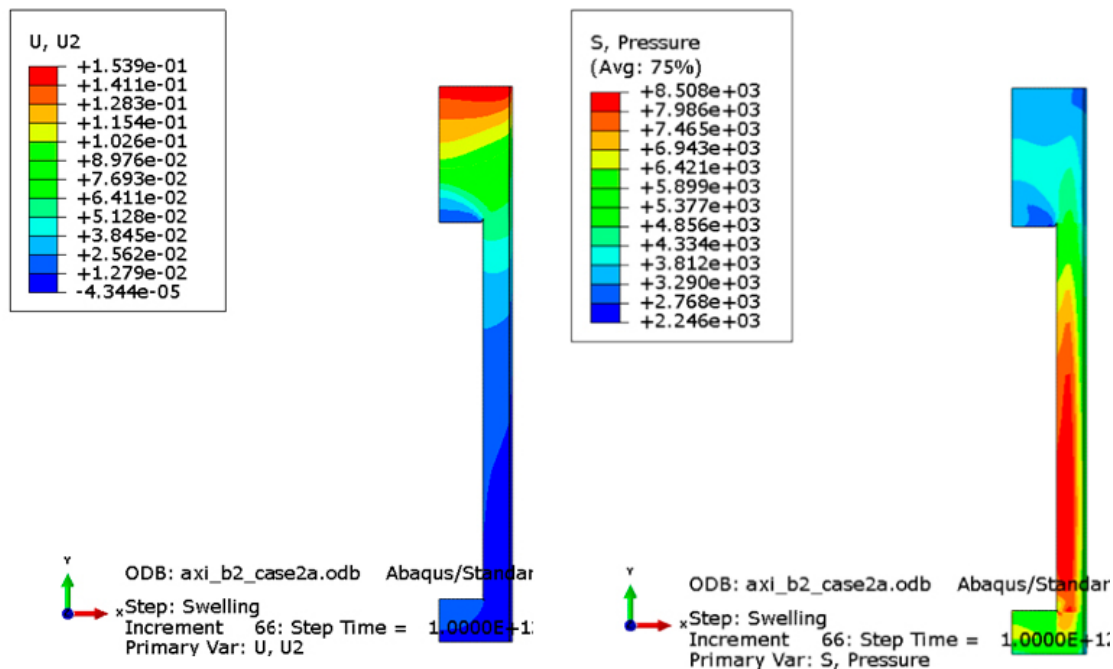


Figure 5-5. Axial displacements (m) (left) and average stress (kPa) of case 2a ( $\sigma=7$  MPa,  $t_p=10$  cm).

Figure 5-5 shows that the upwards swelling of the interface between the buffer and the backfill block in the deposition hole is quite large (15 cm) but also that in spite of this the lowest average stress above the canister is about 3 MPa.

The upwards swelling of all 15 cases are shown in Table 5-4. The table shows the total upwards displacement of the interface between the buffer block and the backfill block for all cases.

**Table 5-4. Total upwards displacement  $\delta$  of the top of the bentonite buffer (1.5 m above the canister).**

Swelling pressure $\sigma$ (1-3)/thickness of bottom layer $t_p$ (a-e)	(a) $t_p=10$ cm	(b) $t_p=25$ cm	(c) $t_p=10$ cm + bevel	(d) $t_p=10$ cm + bevel + blocks	(e) $t_p=50$ cm
(1) $\sigma=4$ MPa	$\delta=11$ cm	$\delta=14$ cm	$\delta=11$ cm	$\delta=7$ cm	$\delta=19$ cm
(2) $\sigma=7$ MPa	$\delta=15$ cm	$\delta=19$ cm	$\delta=16$ cm	$\delta=12$ cm	$\delta=24$ cm
(3) $\sigma=10$ MPa	$\delta=10$ cm	$\delta=22$ cm	$\delta=19$ cm	$\delta=16$ cm	$\delta=27$ cm

The most critical cases for the density of the buffer above the canister are cases *1b* and *1e*, which have an average stress after swelling lower than 2 MPa above the canister lid. Cases *1c* and *2e* have the corresponding stress about 2 MPa. The reason is mainly that cases 1 have the lowest initial density of the buffer.

Figure 5-6 shows the final average stress of cases *1c* and *1e*.

The average void ratio and density of the buffer calculated up to 0.5 m from the canister top according to the suggested new criterion (see Section 4.5) are shown for all 15 cases in Table 5-5 together with the loss in density caused by the swelling.

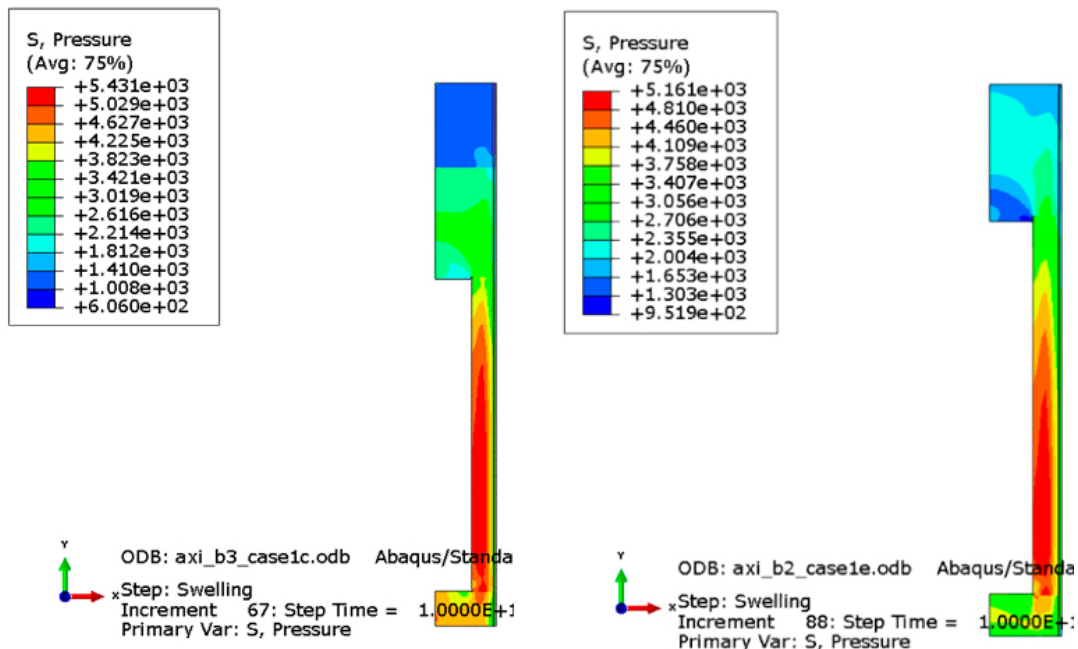


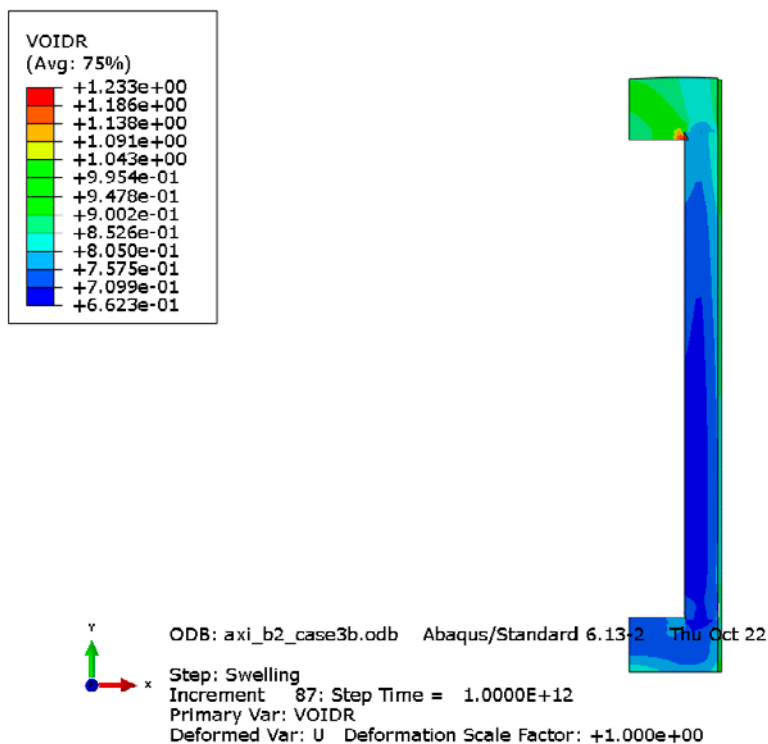
**Figure 5-6. Final average stresses (kPa) for case 1c ( $\sigma=4$  MPa, bevel with pellets) and case 1e ( $\sigma=4$  MPa,  $t_p=50$  cm).**

**Table 5-5. Calculated final average void ratio and density at saturation up to 0.5 m from the canister top for the 15 cases. The decrease in density is caused by the swelling is also shown. The critical and close to critical cases with swelling pressure of 2 MPa or lower above the canister lid are coloured yellow.**

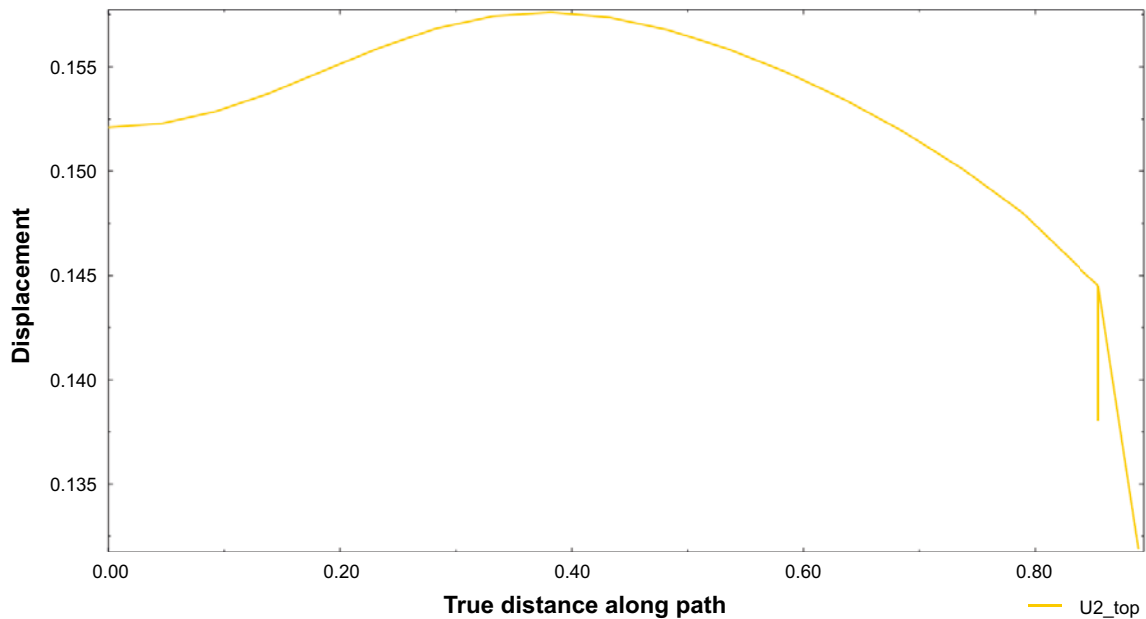
Case	Void ratio	Density at saturation kg/m <sup>3</sup>	Decrease in density kg/m <sup>3</sup>
1a	0.873	1951	14
1b	0.882	1946	19
1c	0.871	1951	14
1d	0.862	1956	9
1e	0.936	1920	45
2a	0.797	1991	20
2b	0.806	1985	26
2c	0.798	1990	21
2d	0.788	1995	16
2e	0.821	1978	31
3a	0.753	2016	25
3b	0.762	2010	31
3c	0.755	2014	29
3d	0.745	2020	21
3e	0.779	2000	41

Table 5-5 shows that three of the four close to critical cases regarding the buffer density (or average stress) above the canister lid also yield the lowest density according to the new criterion, but the fourth one (2e) has higher density than the other non-critical cases 1. Only case 1e has a clearly lower average stress according to the new criterion than acceptable. The reason is the low initial density in combination with the thick pellet layer. The bevel seems to manage all cases. Only case 1c (bevel filled with pellets) is close to critical but has still an average density higher than 1950 kg/m<sup>3</sup>.

As example the void ratio and upwards displacement of the surface 0.5 m above the canister are shown in Figures 5-7 and 5-8 for case 3e.



**Figure 5-7. Void ratio distribution of the buffer up to 0.5 m above the canister top for case 3e.**



**Figure 5-8.** Displacement (m) of the surface located 0.5 m above the canister top for case 2e. The x-axis is plotted as the distance (m) from the centre axis.

## 5.4 Conclusions

The following conclusions can be drawn from the results of the calculations regarding the influence of buffer density and backfill geometry.

The influence of the initial density of the buffer is large on the upwards swelling and the swelling pressure above the canister lid:

- High density yields high upwards swelling but still high swelling pressure.
- Low density yields small upwards swelling but still low swelling pressure.

The influence of the thickness of the pellet filling in the floor and the bevel are strong, but only two cases (1b and 1e) yield average stress  $p < 2$  MPa above the canister top. These cases also yield too low density  $\rho_m < 1\,950$  kg/m<sup>3</sup> according to the new criterion.

All simplified pessimistic cases with the bevel (c and d) fulfilled the requirement with  $p > 2$  MPa above the canister lid and  $\rho_m \geq 1\,950$  kg/m<sup>3</sup>.

The new buffer criterion seems to capture the low density at the top of the canister quite well.

General conclusions are that:

- Pellets filling thickness in the floor influences the results more than the bevel.
- Only low density buffer yields problems.
- Cases with bevel and 10 cm pellet filling thickness fulfilled the requirements.





## 6 3D model for checking the 2D models

### 6.1 General

In order to see how well the 2D models with simplified backfill response described in Chapter 5 agree with a modelling of the entire 3D case with a block filled tunnel two of the modelling cases in Chapter 5 have been simulated.

Modelling of cases 3e and 3a have been done. Case 3e yields the largest total swelling of the buffer, while 3a yields the largest upwards displacement of the backfill blocks in the tunnel.

Identical properties of the buffer blocks and the pellet fillings have been used as described in Chapter 3 and the same geometry and properties backfill blocks in the tunnel as described in Chapter 5. The backfill blocks in the deposition hole were omitted since they are expected to only function as a stiff cylinder due to that they are not wetted. Table 6-1 shows the initial conditions.

**Table 6-1. Initial conditions of the buffer.**

Case	Void ratio $e_0$	Pressure $p_0$ and Pore pressure $-u_0$ (MPa)	Remarks
<b>Blocks</b>			
(3) 10 MPa	0.632	14.5	Recalculated <sup>1</sup>
<b>Rings</b>			
(3) 10 MPa	0.541	24.5	Recalculated <sup>1</sup>
<b>Pellet filling</b>			
1-3	1.78	0.022	Recalculated <sup>1</sup>

<sup>1</sup> Recalculated means that the pressure  $p_0$  has been adapted to yield the correct swelling pressure at the desired average density. This must be done since the validity of the Porous Elastic model is limited to  $0.7 < e < 1.5$ .

Figure 6-1 shows an example of the geometry of the 3D models without bevel. The backfill was modelled with identical geometry and properties as the backfill in the model of the swelling test (Chapter 3). In order to help convergence a collar that limited the radial swelling in the pellet filling was installed in the floor around the deposition hole. There was a small difference to the models shown in Chapter 5 since there was no stiff plate between the buffer and the backfill. The other models had no collar.

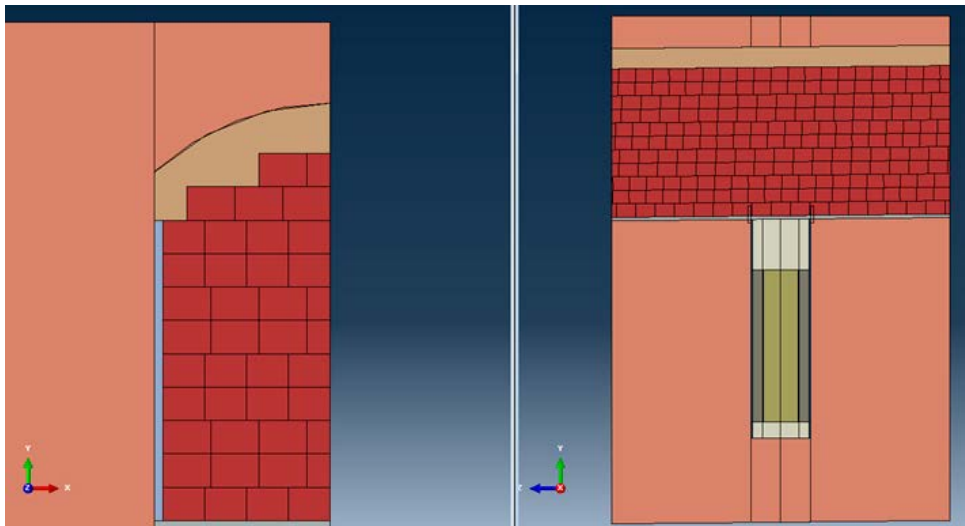


**Figure 6-1.** Sketch of the geometry of the 3D model.

## 6.2 Case 3e (10 MPa swelling pressure and 50 cm pellet filling)

This calculation runs for  $3.4 \times 10^8$  s (10.8 years) when it was interrupted due to convergence problems. At this time the pore pressure was not completely equilibrated but a negative pore pressure of about 1 MPa was still remaining above the canister. The results are though correct up to 10.8 years and are therefore described.

All results refer to the end state after 10.8 years. The vertical displacements are shown in Figure 6-2, both for a large part of the model in the axial vertical symmetry plane and as a detail around the upper part of the deposition hole. The vertical displacements in the pellet filling in the ceiling and wall are shown in Figure 6-3 and the vertical displacements and the vertical stresses in the backfill blocks are shown in Figure 6-4.

The void ratio and dry density in the buffer are shown in Figure 6-5 and the average effective stress and vertical total stress are shown in Figure 6-6. The model is by mistake given the wrong name (3b instead of 3e) in the pictures.

The average void ratio and density at saturation according to the new criterion (see Section 4.5) are

$$e=0.745$$

$$\rho_m=2020 \text{ kg/m}^3$$

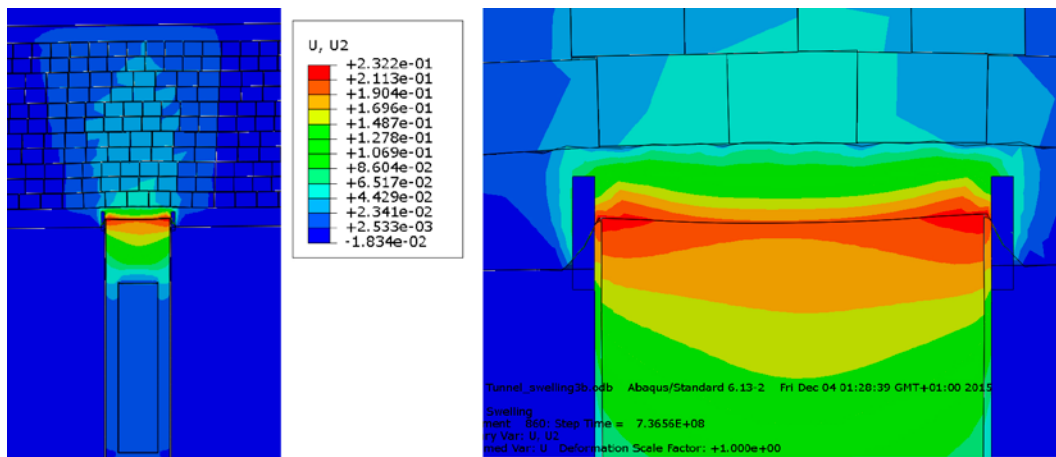


Figure 6-2. Vertical displacements (m) in the axial vertical symmetry plane.

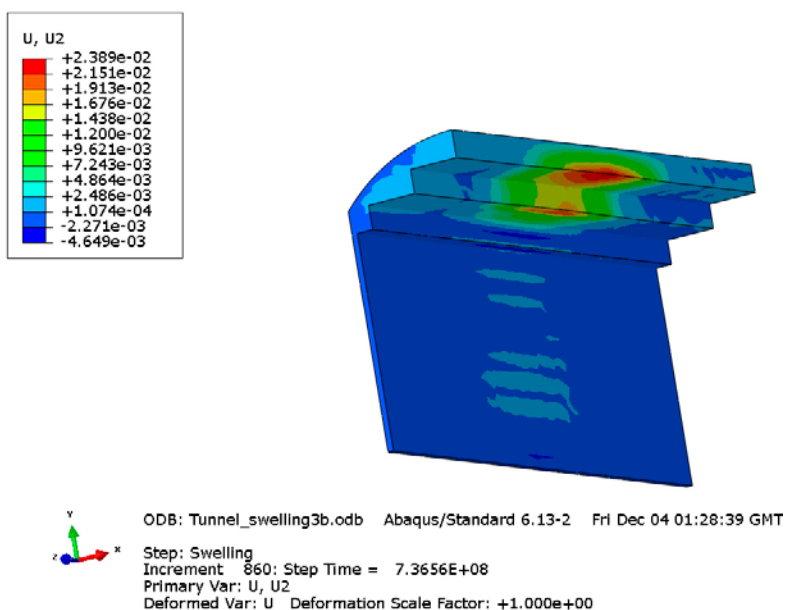
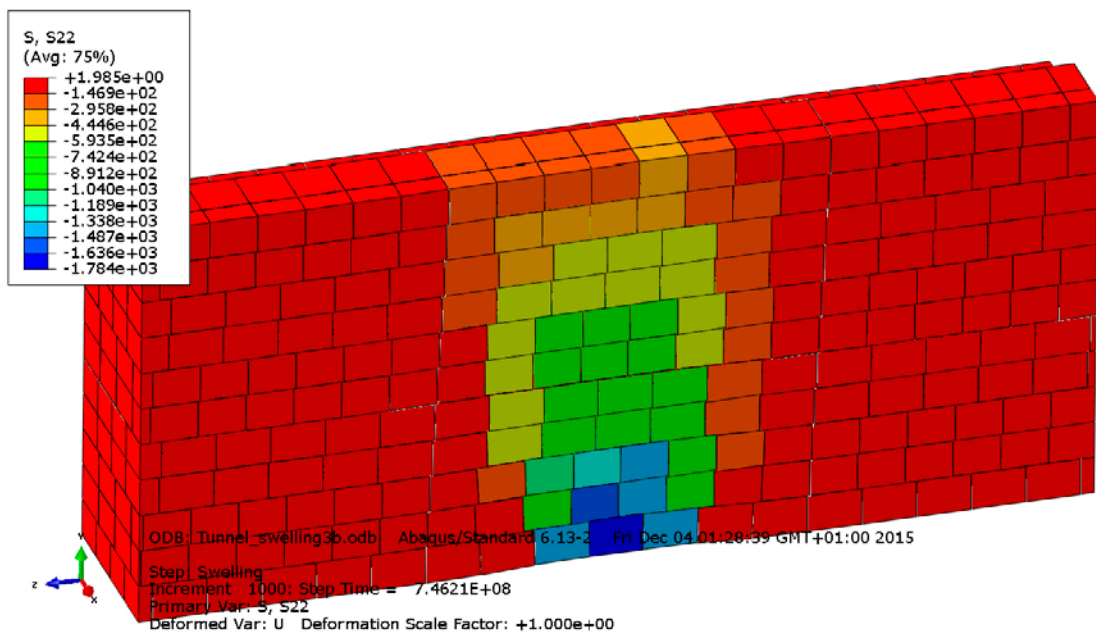
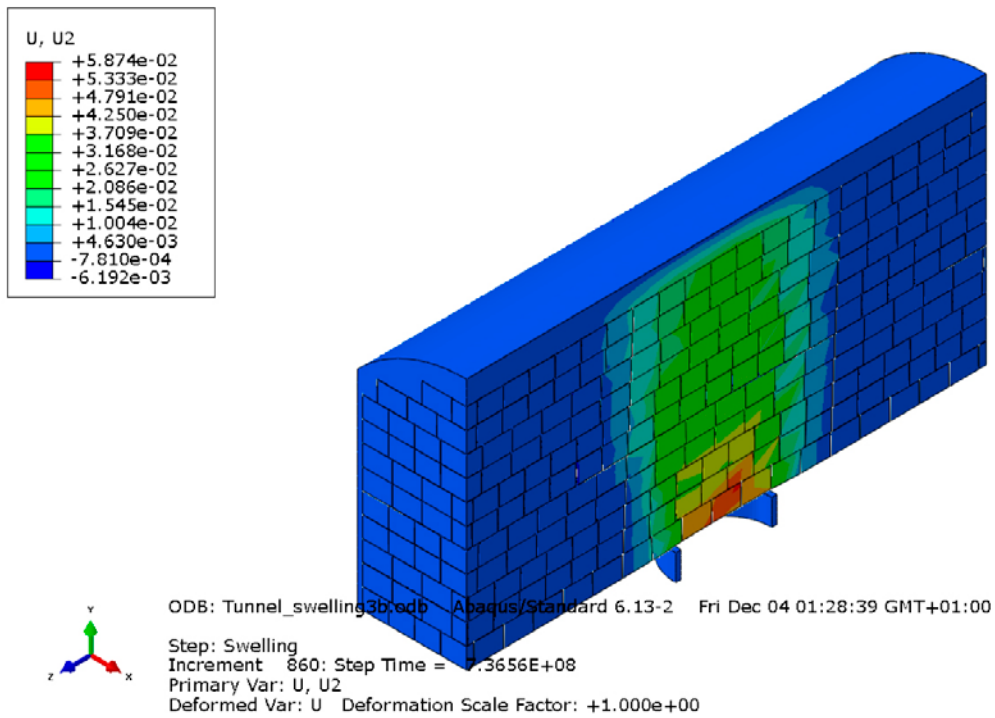


Figure 6-3. Vertical displacements (m) in the pellet filling in the ceiling and wall.



**Figure 6-4.** Vertical displacements (m) in the backfill (upper) and vertical stresses (kPa) in the backfill blocks in the tunnel.

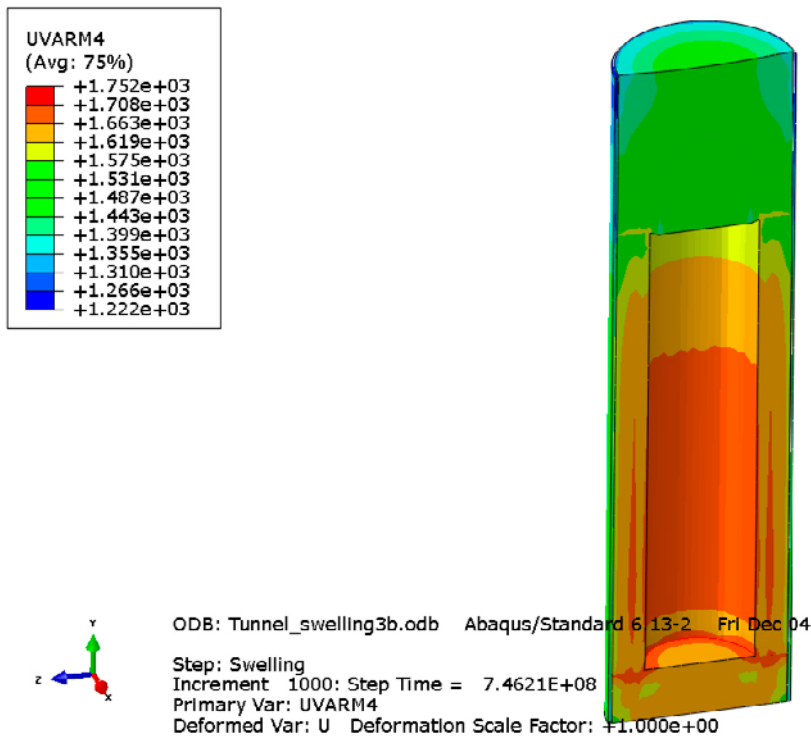
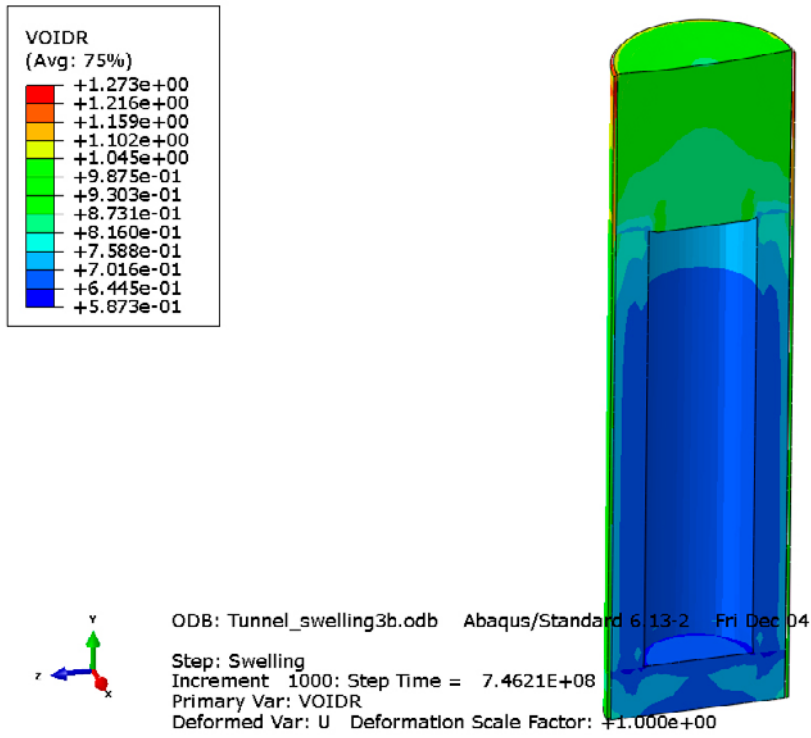


Figure 6-5. Void ratio (upper) and dry density ( $\text{kg/m}^3$ ) in the buffer.

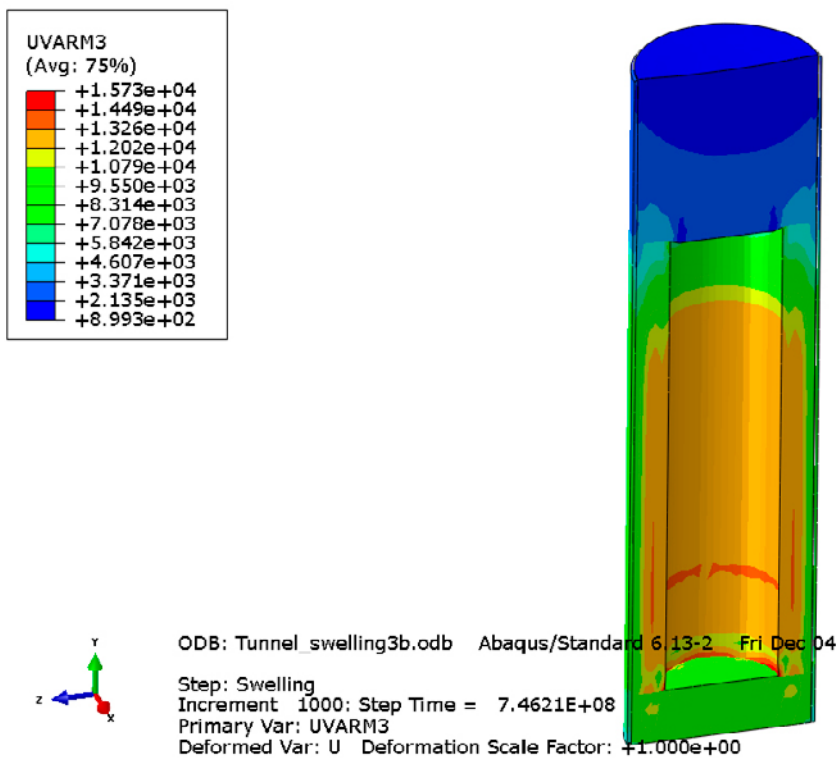
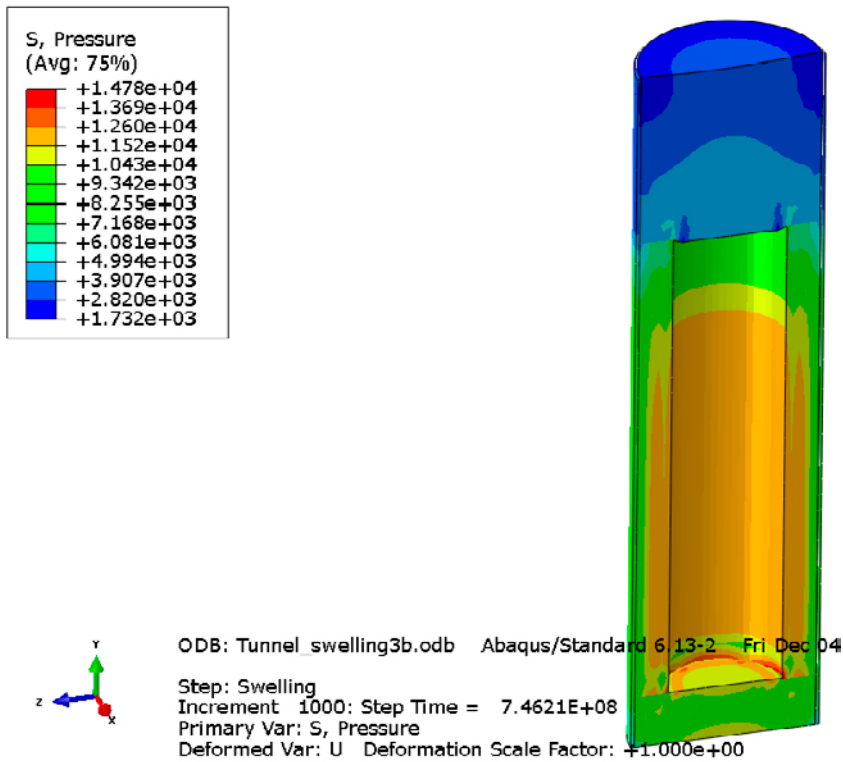


Figure 6-6. Average effective stress (upper) and vertical total stress (kPa) in the buffer.

### 6.3 Case 3a (10 MPa swelling pressure and 10 cm pellet filling)

This calculation is identical to the previous one (Section 6.2) with exception of the thickness of the pellet filling. Also this calculation was interrupted in advance ( $1.3 \times 10^9$  s or 41 years) due to convergence problems with a not completely equilibrated negative pore pressure of about 0.35 MPa still remaining above the canister. The results are though correct up to 41 years and are therefore described. All results refer to this time.

Figure 6-7 shows the vertical displacements, Figure 6-8 shows the vertical displacements and the total vertical stresses in the backfill blocks and Figure 6-9 shows the vertical displacements in the pellet filling in the ceiling and wall. The void ratio and dry density in the buffer are shown in Figure 6-10 and the average effective stress and vertical total stress are shown in Figure 6-11.

The axial displacements of the surface located 0.5 m above the canister are shown in Figure 6-12.

The average void ratio and density at saturation according to the new criterion (see Section 4.5) are

$$e=0.727$$

$$\rho_m=2031 \text{ kg/m}^3$$

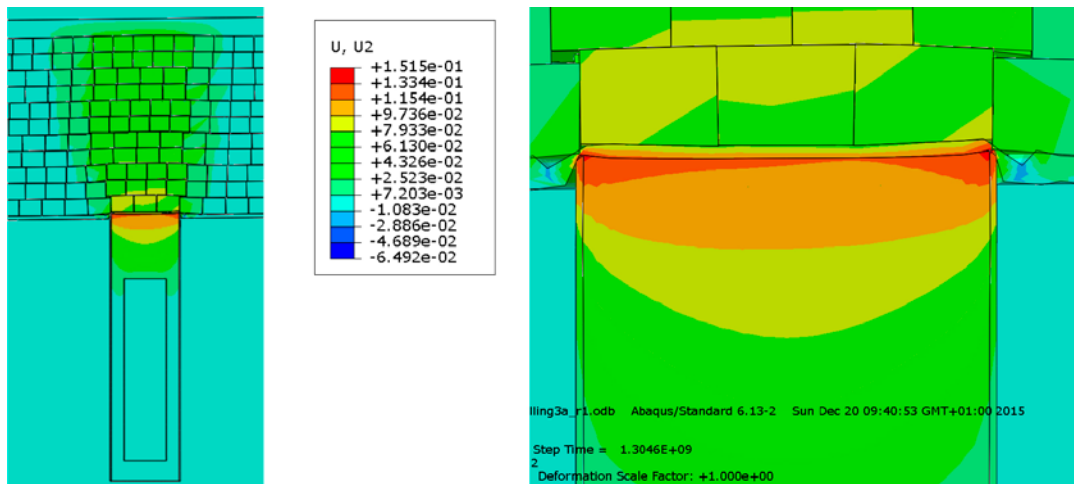
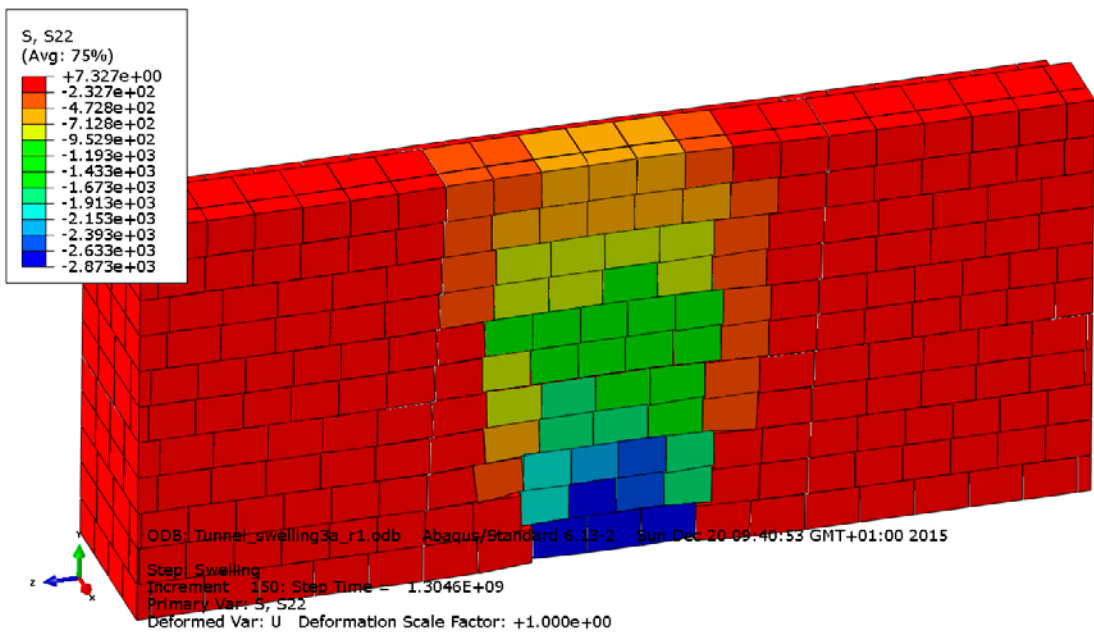
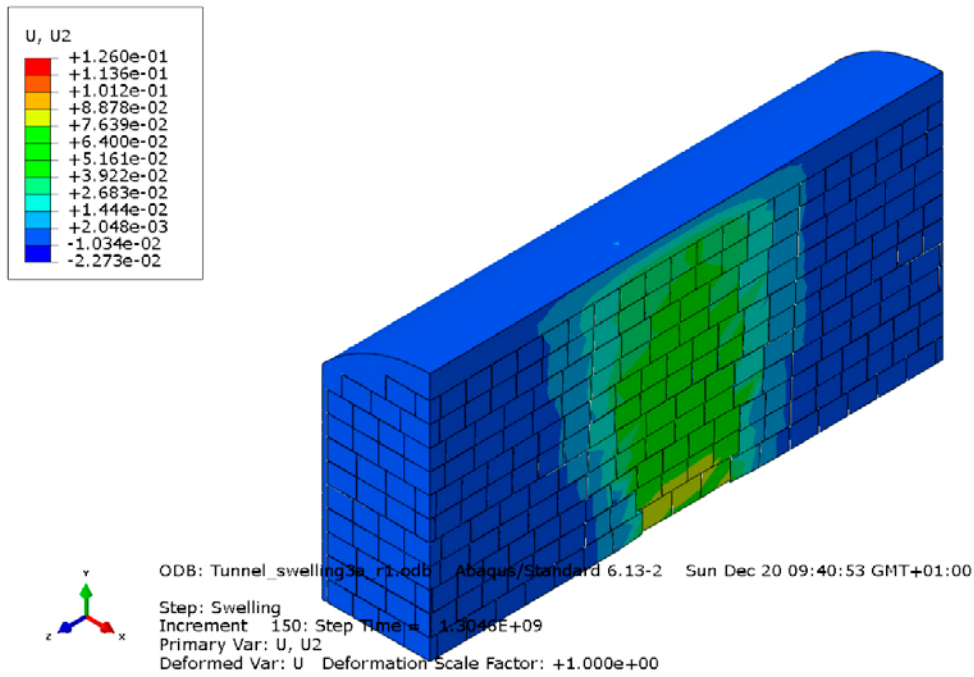
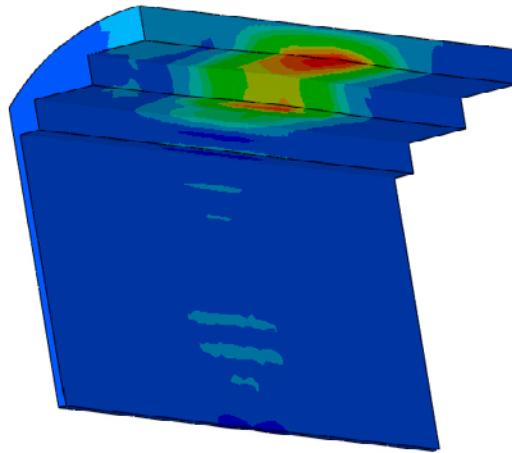
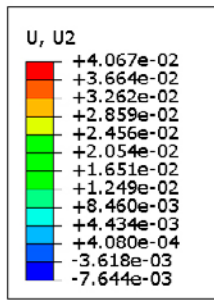


Figure 6-7. Vertical displacements (m) in the axial vertical symmetry plane.



**Figure 6-8.** Vertical displacements (m) in the backfill in the tunnel (upper) and vertical stresses (kPa) in the backfill blocks.



ODB: Tunnel\_swelling3a\_r1.odb Abaqus/Standard 6.13-2 Sun Dec 20 09:40:53

Step: Swelling  
 Increment 150: Step Time = 1.3046E+09  
 Primary Var: U, U2  
 Deformed Var: U Deformation Scale Factor: +1.000e+00

*Figure 6-9. Vertical displacements (m) in the pellet filling in the ceiling and wall.*



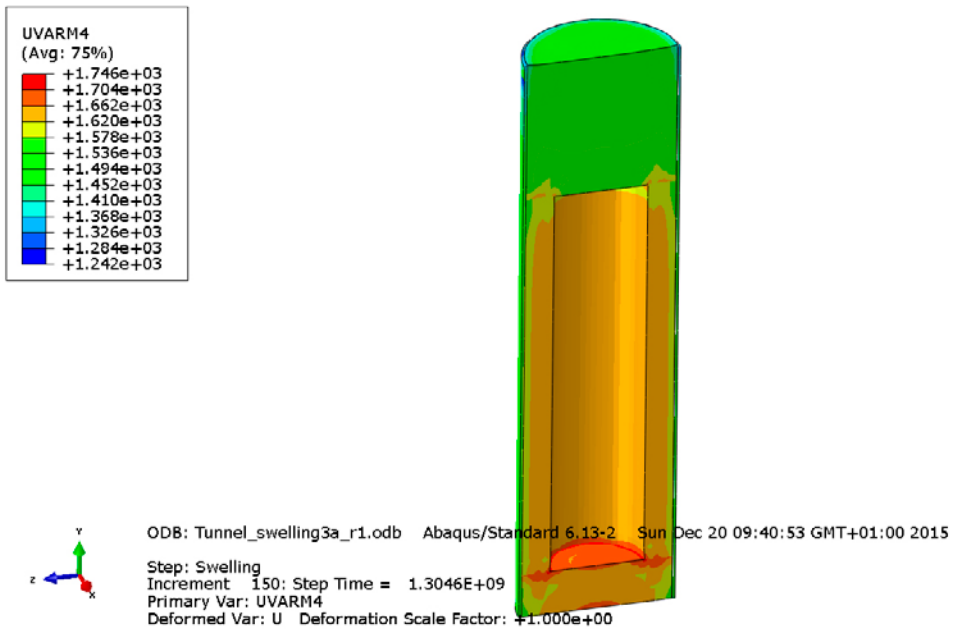
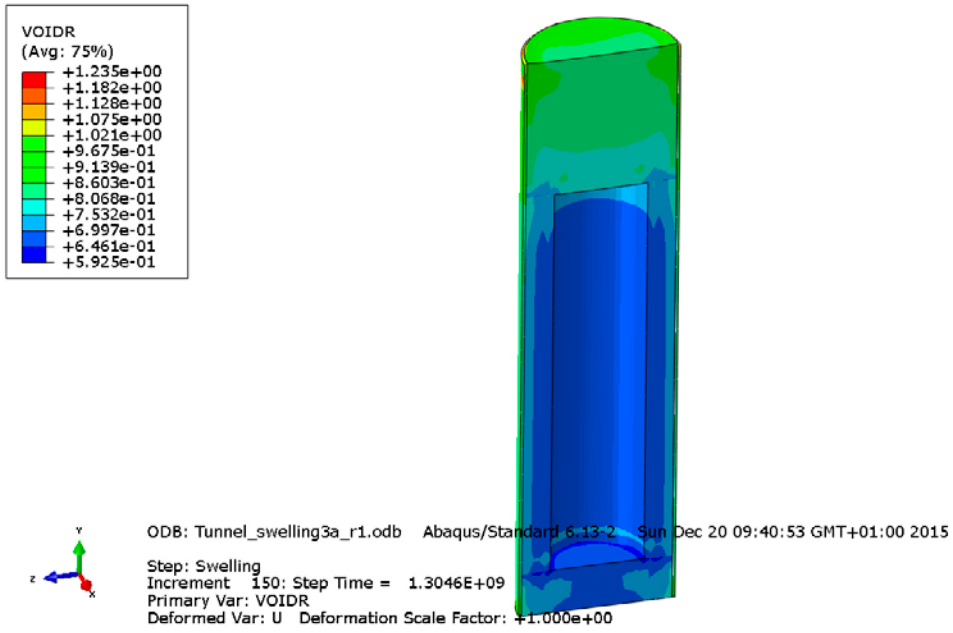
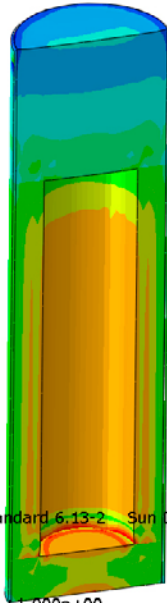
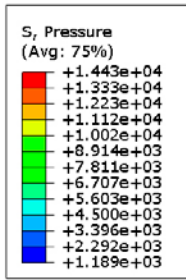
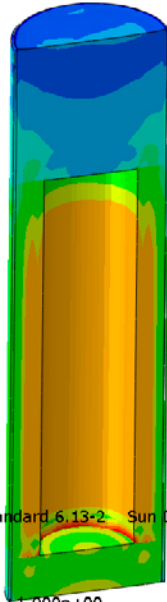
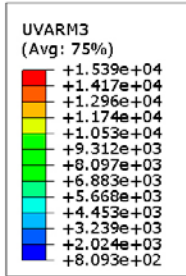


**Figure 6-10.** Void ratio (upper) and dry density (kg/m<sup>3</sup>) in the buffer.



ODB: Tunnel\_swelling3a\_r1.odb Abaqus/Standard 6.13-2 Sun Dec 20 09:40:53 GMT+01:00 2015

Step: Swelling  
Increment: 150; Step Time = 1.3046E+09  
Primary Var: S, Pressure  
Deformed Var: U Deformation Scale Factor: +1.000e+00



ODB: Tunnel\_swelling3a\_r1.odb Abaqus/Standard 6.13-2 Sun Dec 20 09:40:53 GMT+01:00 2015

Step: Swelling  
Increment: 150; Step Time = 1.3046E+09  
Primary Var: UVARM3  
Deformed Var: U Deformation Scale Factor: +1.000e+00

Figure 6-11. Average effective stress (upper) and vertical total stress (kPa) in the buffer.

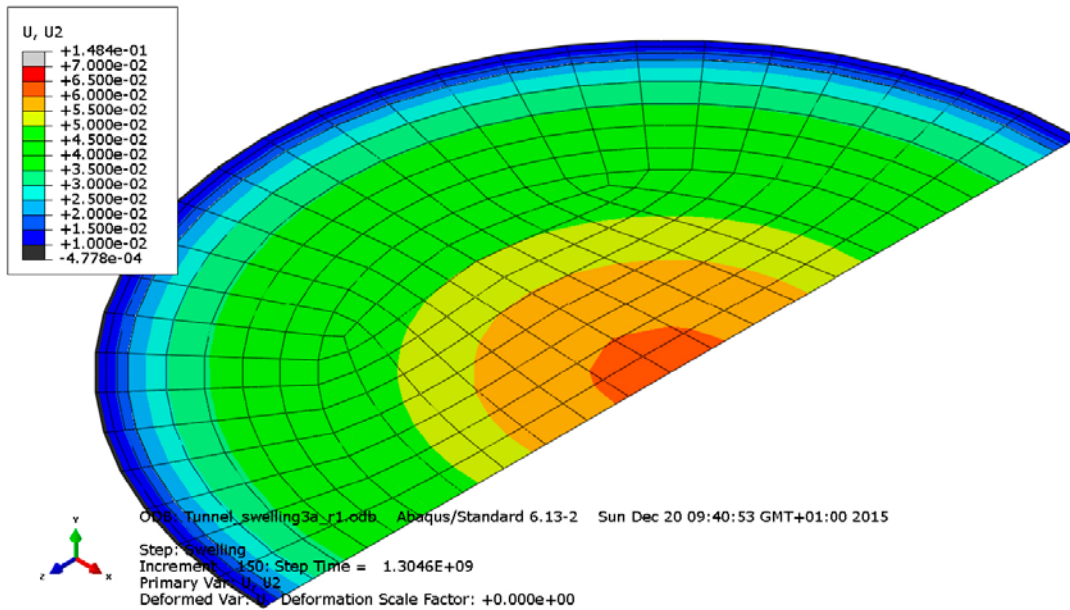


Figure 6-12. Axial displacements (m) of the surface located 0.5 m above the canister.

## 6.4 Comments and conclusions

Table 6-2 summarises the results and shows the density after swelling according to the new criterion

Table 6-2 Results and comparison of the 2D and 3D calculations.

Case	$\rho_m$ kg/m <sup>3</sup> New criterion		$p$ above canister lid		Buffer swelling		Pore pressure
	2D	3D	2D	3D	2D	3D	3D
3e	2000	2020	2.5 MPa	5 MPa	27 cm	21 cm	-1 MPa
3a	2016	2031	3 MPa	6 MPa	18 cm	12 cm	-0.35 MPa

Table 6-2 shows that the agreement is rather poor. For case 3e the displacement of the contact buffer/backfill is in average about 21 cm in the 3D model while it is about 27 cm in the 2D model. In agreement with this the average stress on top of the canister is higher in the 3D case (about 5 MPa) than in the 2D model (about 2.5 MPa). The same poor agreement applies for case 3a. The displacement of the contact buffer/backfill is about 12 cm in the 3D model while it is about 18 cm in the 2D model. This difference yields that the average stress above the canister is about 6 MPa in the 3D model and only about 3 MPa in the 2D model.

The comparison thus shows that the 3D model for both cases yields less upwards swelling, higher remaining density above the canister than the 2D model and higher average density according to the new criterion. The major reason for this difference is that the 3D calculations were interrupted before equilibrium.



## 7 3D model for studying the influence of the width of the pellet filled slot at the ceiling

### 7.1 General

In order to study the influence of the thickness of the pellet filling at the ceiling two 3D calculations were done. Both calculations refer to case 2b, i.e. 7 MPa swelling pressure and 25 cm pellet filling in the floor. The two calculations were identical with the only difference that the pellet filling at the ceiling was 60 cm in one model and 45 cm in the other.

### 7.2 60 cm slot at the ceiling (*Tunnel\_swelling2b*)

Modelling of case 2b (7 MPa swelling pressure and 25 cm pellet filling in the floor) has been done with a full 3D model without bevel and with a pellet filling in the ceiling that is 15 cm thicker than in the base geometry. The geometry and material models are identical to those in the calculation described in Chapter 6. The initial conditions of the blocks and pellets are described in Table 7-1.

**Table 7-1. Initial conditions of the buffer parts.**

Case	Void ratio $e_0$	Pressure $p_0$ and Pore pressure $-u_0$ (MPa)	Remarks
<b>Blocks</b>			
(2) 7 MPa	0.683	10.9	Recalculated <sup>1</sup>
<b>Rings</b>			
(2) 7 MPa	0.591	18.4	Recalculated <sup>1</sup>
<b>Pellet filling</b>			
1-3	1.78	0.022	Recalculated <sup>1</sup>

<sup>1</sup> Recalculated means that the pressure  $p_0$  has been adapted to the yield the correct swelling pressure at the desired average density. This must be done the blocks and the pellets since the validity of the Porous Elastic model is limited to  $0.7 < e < 1.5$ .

The calculation was run to complete pore pressure equalization ( $3.5 \times 10^{10}$  s or 1 100 years). All results refer to the end stage.

Figure 7-1 shows the vertical displacements, Figure 7-2 shows the vertical displacements in the pellet filling in the ceiling and wall and Figure 7-3 shows the vertical displacements and the total vertical stresses in the backfill blocks. The void ratio and dry density in the buffer are shown in Figure 7-4 and the average effective stress and vertical total stress are shown in Figure 7-5.

The average void ratio and density at saturation according to the new criterion (see Section 4.5) are

$$e=0.796$$

$$\rho_m=1\,991\text{ kg/m}^3$$

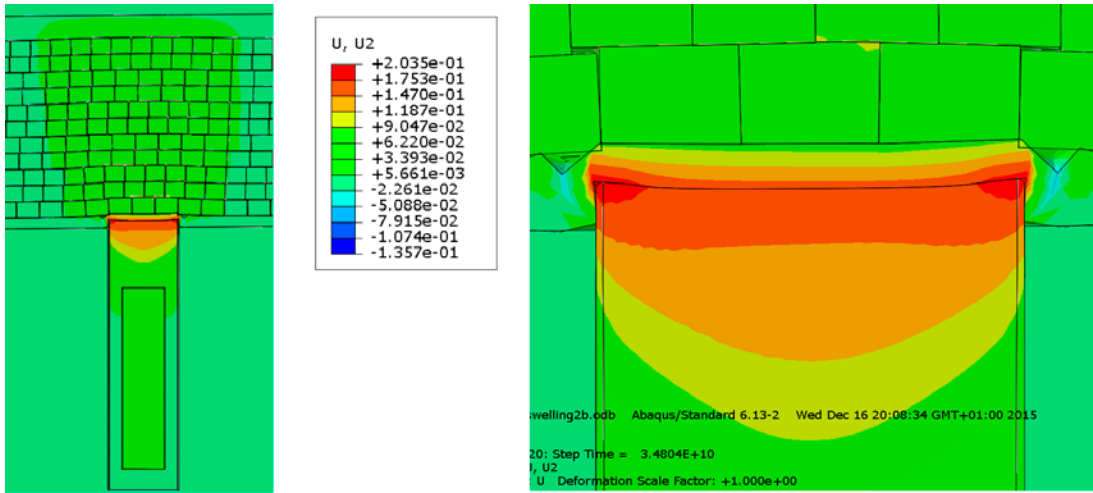


Figure 7-1. Vertical displacements (m) in the axial vertical symmetry plane.

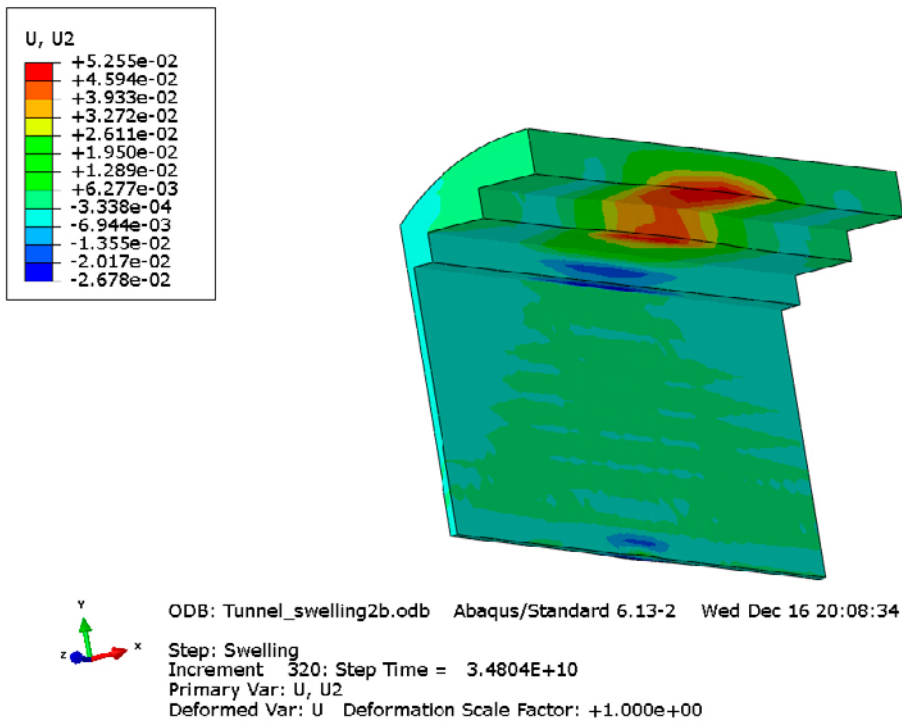
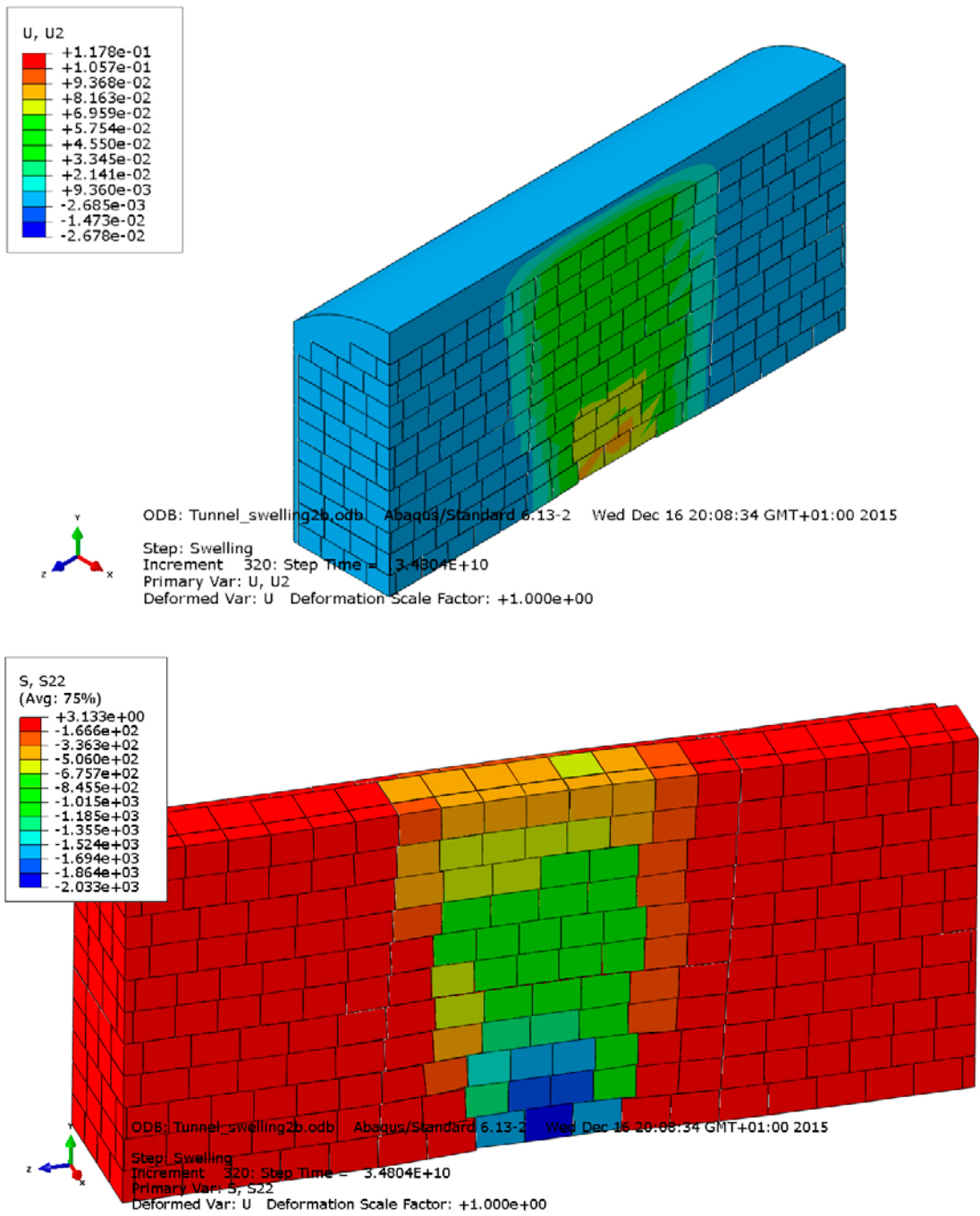
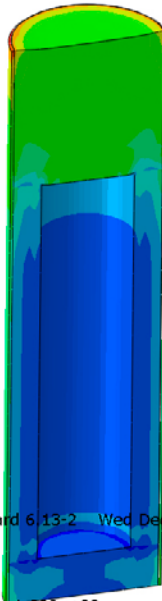
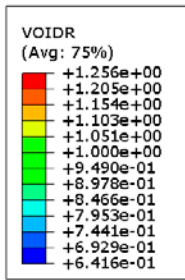


Figure 7-2. Vertical displacements (m) in the pellet filling in the ceiling and wall.

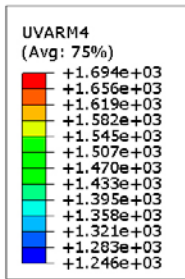


**Figure 7-3.** Vertical displacements (m) in the backfill in the tunnel (upper) and vertical stresses (kPa) in the backfill blocks.



ODB: Tunnel\_swelling2b.odb Abaqus/Standard 6.13-2 Wed Dec 16 20:08:34 GMT+01:00 2015

Step: Swelling  
Increment 320: Step Time = 3.4804E+10  
Primary Var: VOIDR  
Deformed Var: U Deformation Scale Factor: +1.000e+00



ODB: Tunnel\_swelling2b.odb Abaqus/Standard 6.13-2 Wed Dec 16 20:08:34 GMT+01:00 2015

Step: Swelling  
Increment 320: Step Time = 3.4804E+10  
Primary Var: UARM4  
Deformed Var: U Deformation Scale Factor: +1.000e+00

Figure 7-4. Void ratio (upper) and dry density ( $\text{kg/m}^3$ ) in the buffer.



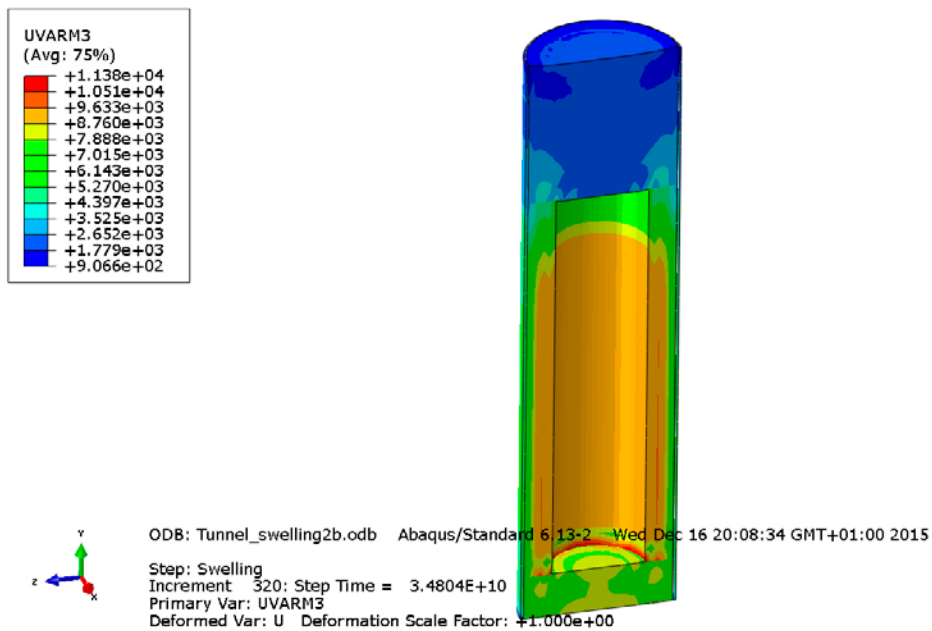
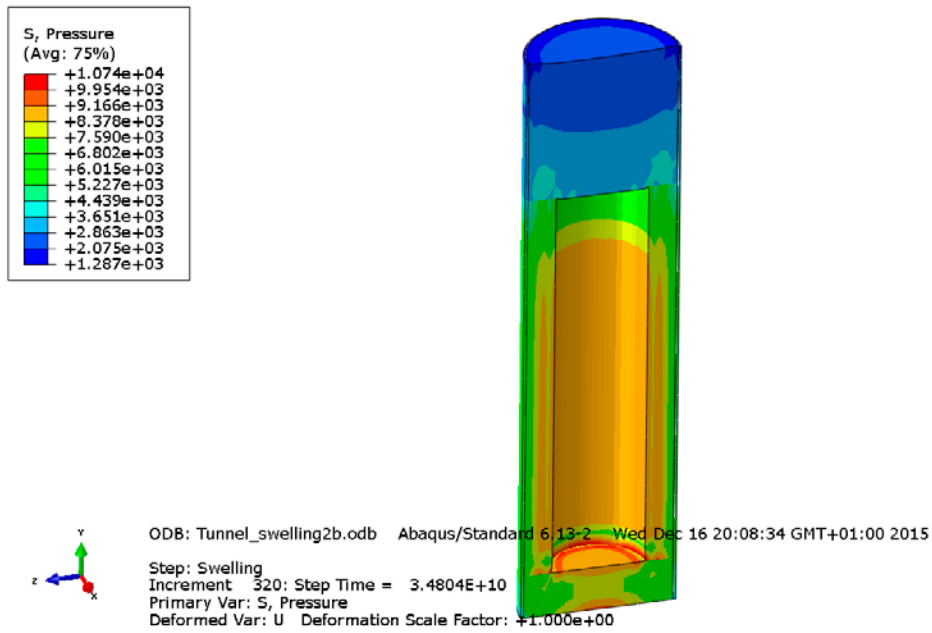


*Figure 7-5. Average effective stress (upper) and vertical total stress (kPa) in the buffer.*

### 7.3 Base case with 45 cm slot at the ceiling (Tunnel\_swelling2b\_standard)

In order to be able to study the influence of the thickness of the pellet filled slot between the rock ceiling and the backfill blocks also the base case was modelled. The calculation was identical to the previous one with exception of the thickness of the pellet filled slot at the ceiling. This calculation was run to complete pore pressure equalization ( $3.65 \times 10^{10}$  s or 1 160 years). All results refer to the end stage.

Figures 7-6 shows the vertical displacements, Figure 7-7 shows the vertical displacements in the pellet filling in the ceiling and wall and Figure 7-8 shows the vertical displacements and the total vertical stresses in the backfill blocks. The void ratio and dry density in the buffer are shown in Figure 7-9 and the average effective stress and vertical total stress are shown in Figure 7-10.

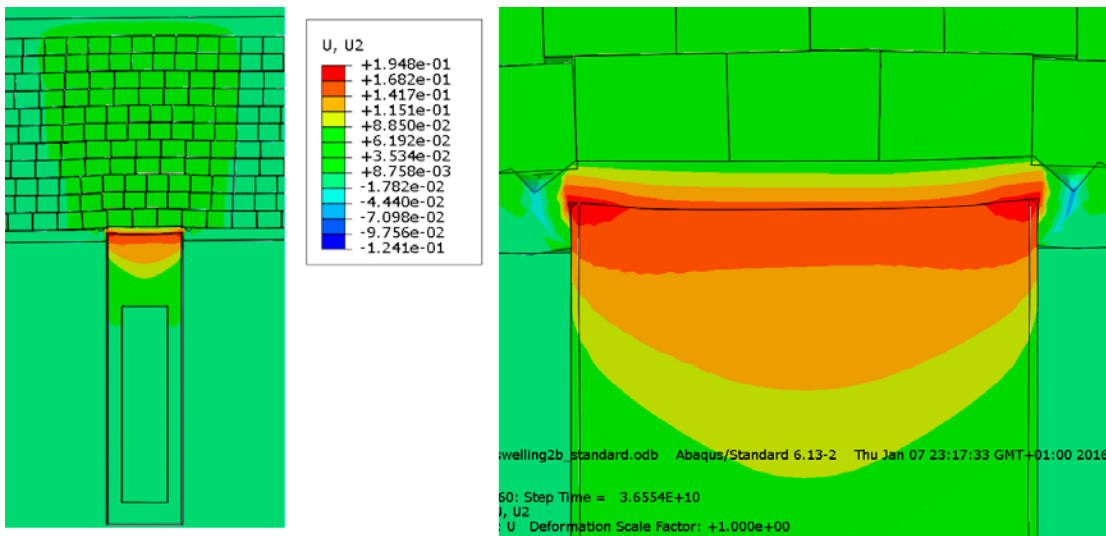


Figure 7-6. Vertical displacements (m) in the axial vertical symmetry plane.

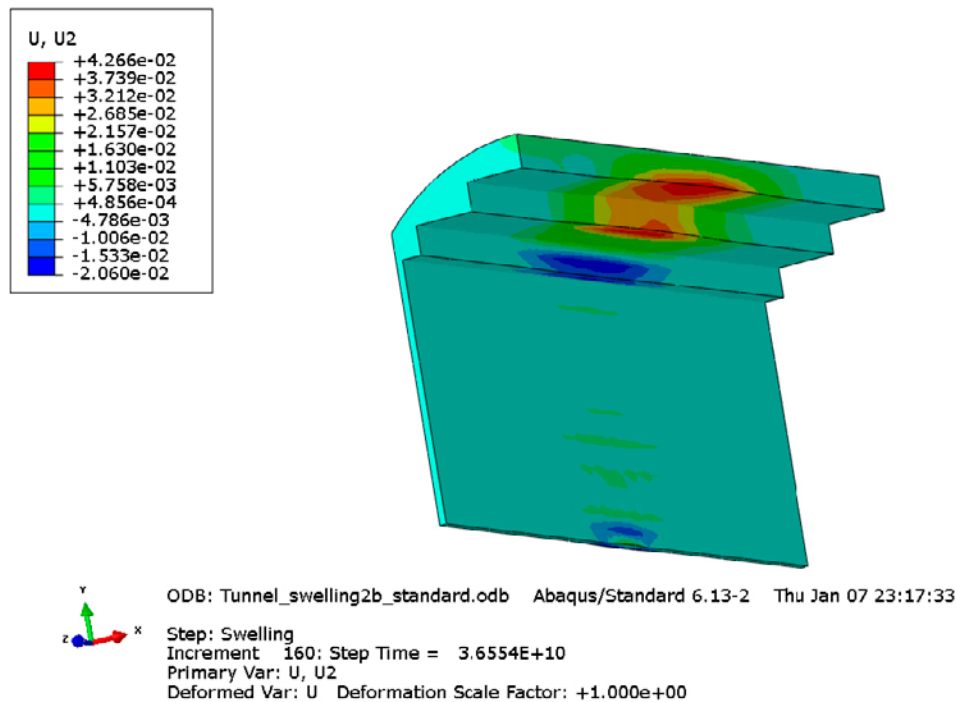
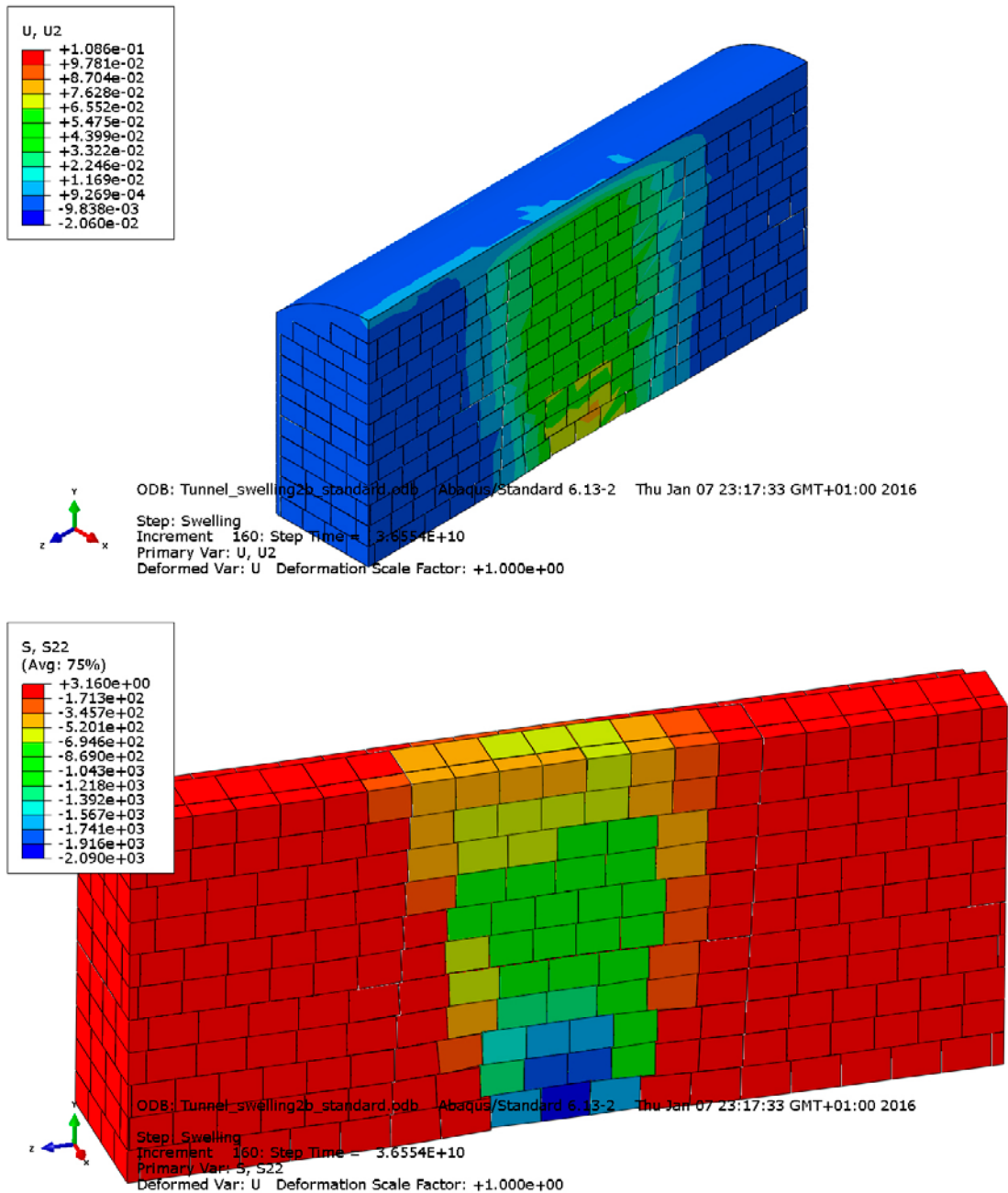


Figure 7-7. Vertical displacements (m) in the pellet filling in the ceiling and wall.



**Figure 7-8.** Vertical displacements (m) in the backfill in the tunnel (upper) and vertical stresses (kPa) in the backfill blocks.

The average void ratio and density at saturation according to the new criterion (see Section 4.5) are

$$e=0.795$$

$$\rho_m=1992 \text{ kg/m}^3$$

Comparing the results with the model with 60 cm slot instead of 45 cm shows rather small difference. Table 7-2 compares some data of the two models.

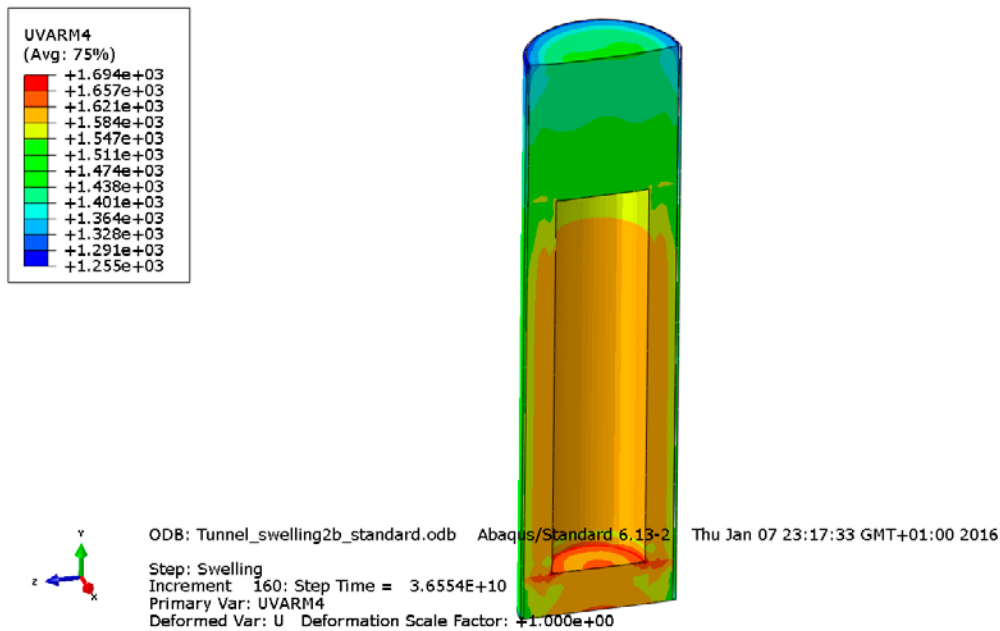
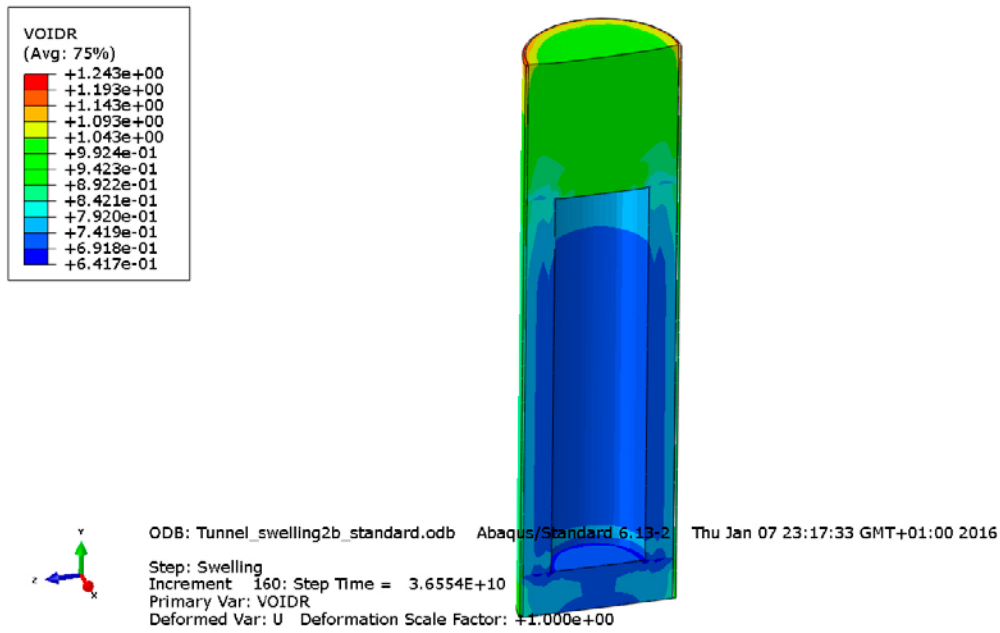


Figure 7-9. Void ratio (upper) and dry density ( $\text{kg/m}^3$ ) in the buffer.

Table 7-2. Influence of the slot width at the ceiling.

Variable	45 cm slot	60 cm slot
$\rho_m$ ( $\text{kg/m}^3$ ) according to the new criterion	1992	1991
Max vertical displacement of the buffer/rock interface (cm)	19.5	20.4
Max vertical displacement of the backfill blocks (cm)	10.9	11.8
Max vertical compression of the pellets in the ceiling (cm)	4.3	5.3
Minimum pressure on the canister (MPa)	~2.5	~2.5

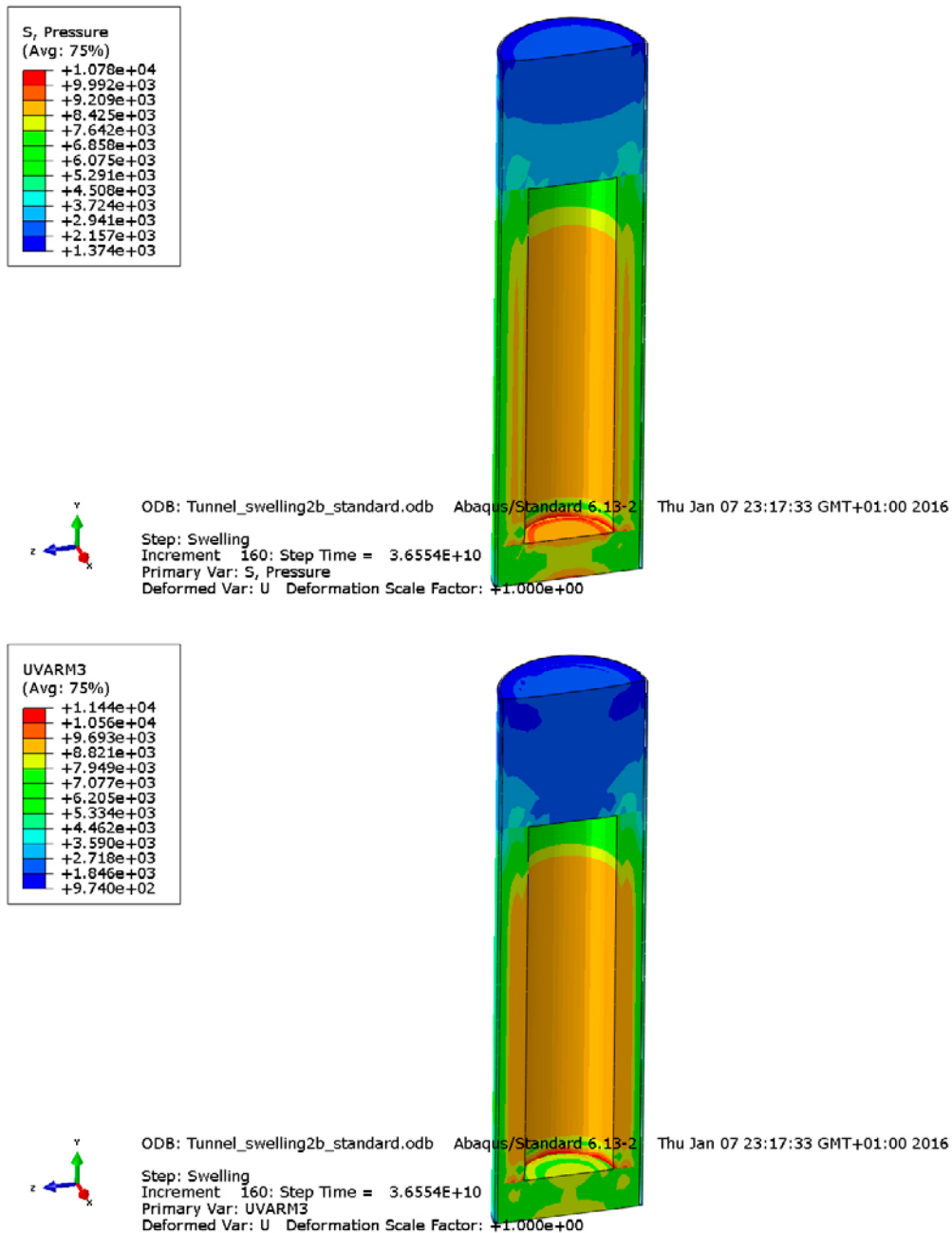


Figure 7-10. Average effective stress (upper) and vertical total stress (kPa) in the buffer.

## 7.4 Comments and conclusions

The comparison between the results of the effect of buffer upwards swelling against a dry tunnel filled with backfill blocks and pellets show that the influence of the width of the pellet filled slot at the ceiling is rather small. This is good for the concept since the rock surface at the ceiling can be very irregular.

The lateral spreading of the stress through the block masonry is quite efficient yielding a rather low vertical stress at the ceiling (300–500 kPa).

The  $E$ -modulus of the pellet filling can be converted to an  $M$ -modulus (oedometer modulus) according to Equation 7-1.

$$M = \frac{E(1-\nu)}{(1+\nu)(1-2\nu)} \quad (7-1)$$

The M-modulus relates to one dimensional compression.

Applying the compression modulus of the pellet filling  $M=5.25$  MPa (corresponding to the E-modulus  $E=3.9$  MPa) yields the following compression of the pellet filling for the two cases:

45 cm slot:

$$\delta = S_w \cdot \Delta\sigma / M = 0.45 \cdot 0.5 / 5.25 = 0.043 \text{ m}$$

where

$S_w$  = slot width

$\Delta\sigma$  = stress increase

60 cm slot:

$$\delta = S_w \cdot \Delta\sigma / M = 0.6 \cdot 0.5 / 5.25 = 0.057 \text{ m}$$

The difference is reduced by the fact that larger compression means lower stresses for the 60 cm slot.

This simplified calculation thus agrees well with the modelling results. The conclusion is thus that the influence of the slot width is not strong but also that the geometry of the masonry is important. If there is no overlapping of the blocks the stress will continue through the block without spreading and with retained stress level.

## 8 Modelling of the case with backfill block failure

### 8.1 General

In Chapter 5 the buffer upwards swelling for 15 different cases with varying buffer density and backfill geometry was modelled by simulating the response of the backfill blocks and pellet filling in the ceiling with a spring that had the same properties as the extrapolated stress-displacement relation measured in the Buffer Swelling Test. However, the stresses reached a peak after 8 cm upwards displacement due to cracking and failure of the backfill blocks. In all calculations described in this report it has been presumed that the blocks can be made of higher density and shear strength so that cracking can be avoided. Since it could be interesting to see what the effect would be on the buffer if cracking takes place a new 2D simulation has been done.

### 8.2 Model

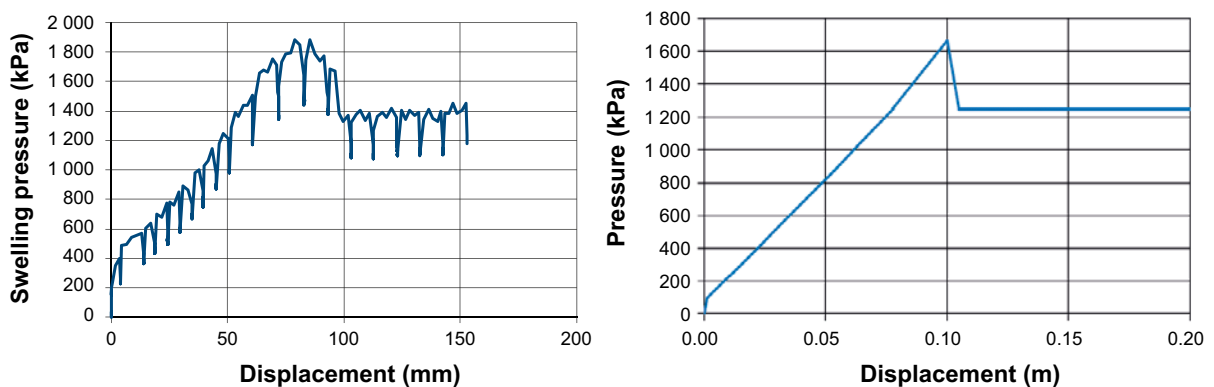
Case 2b with 7 MPa swelling pressure and 25 cm pellet filling at the floor has been modelled. All properties and geometries have been identical to that model described in Chapter 5. The only difference is that the stress-strain curve has followed the stress strain curve measured in the Buffer swelling test (Chapter 3).

Figure 8-1 shows the measured stress-displacement relation and the relation used in the calculation. Due to a mistake the maximum peak stress was simulated to take place after 10 cm displacement instead of measured 8 cm but the effect on the results of this difference is judged to be small.

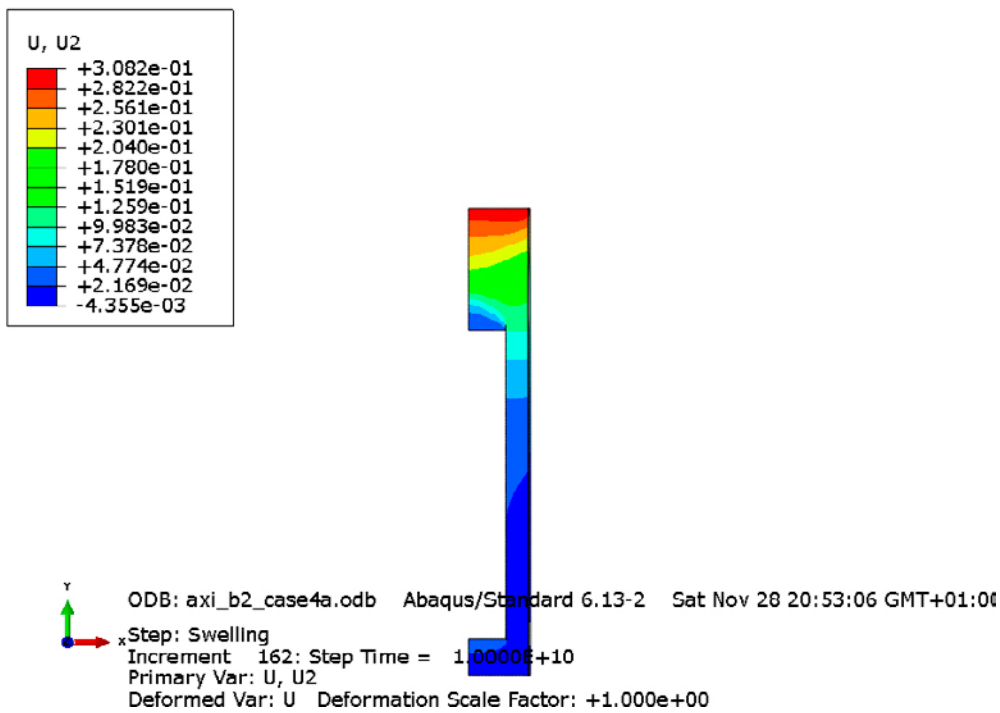
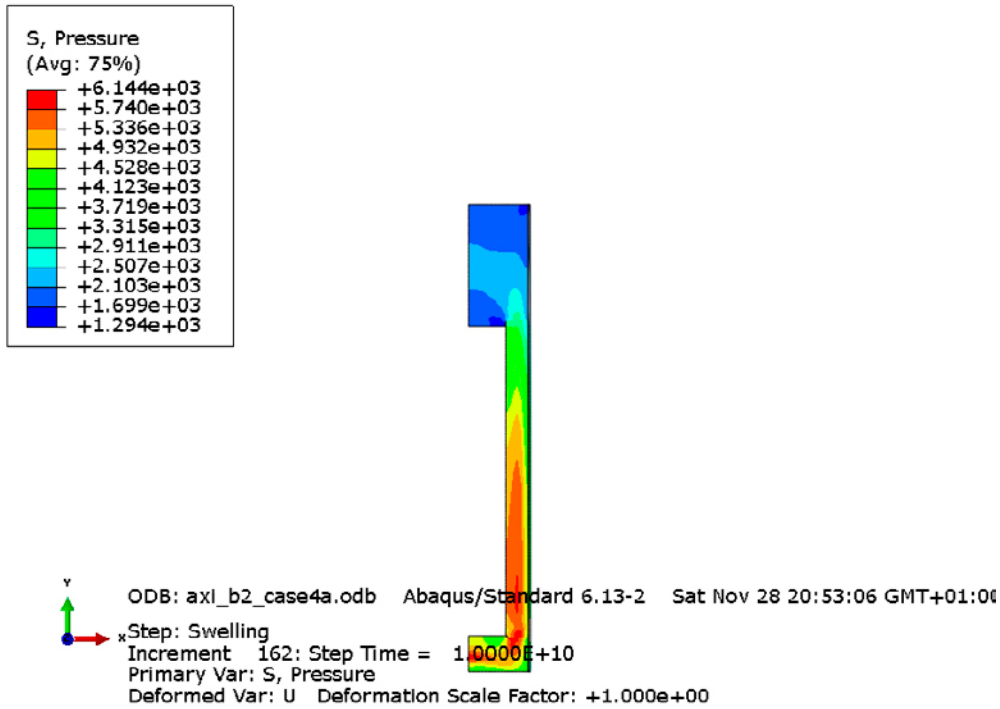
### 8.3 Results

Figure 8-2 shows the modelled average stress and axial displacement at the end while Figure 8-3 shows the modelled dry density, void ratio, radial stress and axial stress at the end.

The figures show that the effect on the buffer is rather large. The swelling of the buffer/backfill interface is increased from 15 to slightly over 30 cm and the average stress above the canister lid is decreased from about 3 MPa to about 1.6 MPa.



*Figure 8-1. Measured stress-displacement relation of the backfill block in the deposition hole in the Buffer Swelling Test (left) and the relation used in the model.*



**Figure 8-2.** Average stress (kPa) and vertical displacements (m) at the end.

The average void ratio and density at saturation according to the new criterion (see Section 4.5) are

$$e=0.842$$

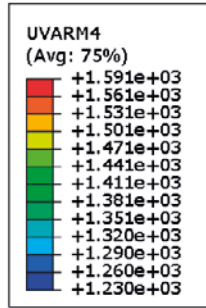
$$\rho_m=1966 \text{ kg/m}^3$$

$$(\rho_m=1985 \text{ kg/m}^3 \text{ without block failure})$$

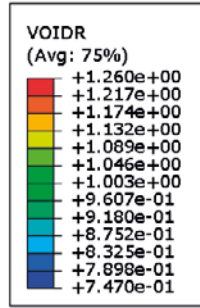
The consequences of block failure for this case 2a are thus that the swelling pressure on the canister lid is less than 2 MPa but acceptable according to the new criterion.



Dry density (kg/m<sup>3</sup>)



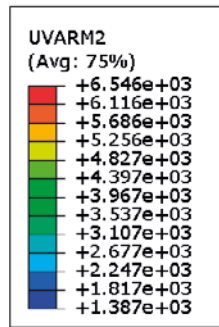
Void ratio



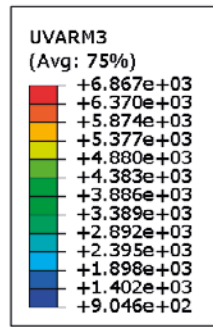
ODB: axi\_b2\_case4a.odb Abaqus/Stand  
 xStep: Swelling  
 Increment 162: Step Time = 1.0000E-  
 Primary Var: UVARM4  
 Deformed Var: U Deformation Scale Fac

ODB: axi\_b2\_case4a.odb Abaqus/Standard 6  
 xStep: Swelling  
 Increment 162: Step Time = 1.0000E+10  
 Primary Var: VOIDR  
 Deformed Var: U Deformation Scale Factor: 4

Radial stress (kPa)



Axial stress (kPa)



ODB: axi\_b2\_case4a.odb Abaqus/Stand  
 xStep: Swelling  
 Increment 162: Step Time = 1.0000E-  
 Primary Var: UVARM2  
 Deformed Var: U Deformation Scale Fac

ODB: axi\_b2\_case4a.odb Abaqus/Stand  
 xStep: Swelling  
 Increment 162: Step Time = 1.0000E-  
 Primary Var: UVARM3  
 Deformed Var: U Deformation Scale Fac

Figure 8-3. End state of the calculation. Dry density, void ratio, radial stress and axial stress.



## 9 3D model with bevel of wet upper part of deposition hole

### 9.1 General

In Chapter 5 the effect of also having the upper part of the deposition hole and the pellet filled bevel wetted was investigated as cases *c* and *d*. But for those cases the pessimistic assumption was made that the entire backfill part (upper 1.25 m and the bevel) was homogenised which results in a rather low density in the deposition hole. In order to study how pessimistic those models are two 3D calculations were done.

The calculations refers to models 2c and 3c in Tables 5-1 and 5-4 with

- 10 cm pellets filling in the floor.
- 7 MPa swelling pressure of the buffer for model 2c.
- 10 MPa swelling pressure of the buffer for model 3c.
- Only pellets in the bevel.

The model is named *Tunnel\_swelling2c\_wedge\_2*.

Figure 9-1 shows the geometry of the deposition hole, the bevel and the pellet filling in the floor. The tunnel model is identical to the model used for the Buffer swelling test shown in Figure 3-4.

The geometry, material properties and calculation are identical to the base calculation in Chapter 7 (*Tunnel\_swelling2b\_standard*) except for the thickness of the pellet filling in the floor and the introduction of the pellet filled bevel. The pellet filling in the bevel has the same properties as the pellet filling between the buffer blocks and the rock in the deposition hole.

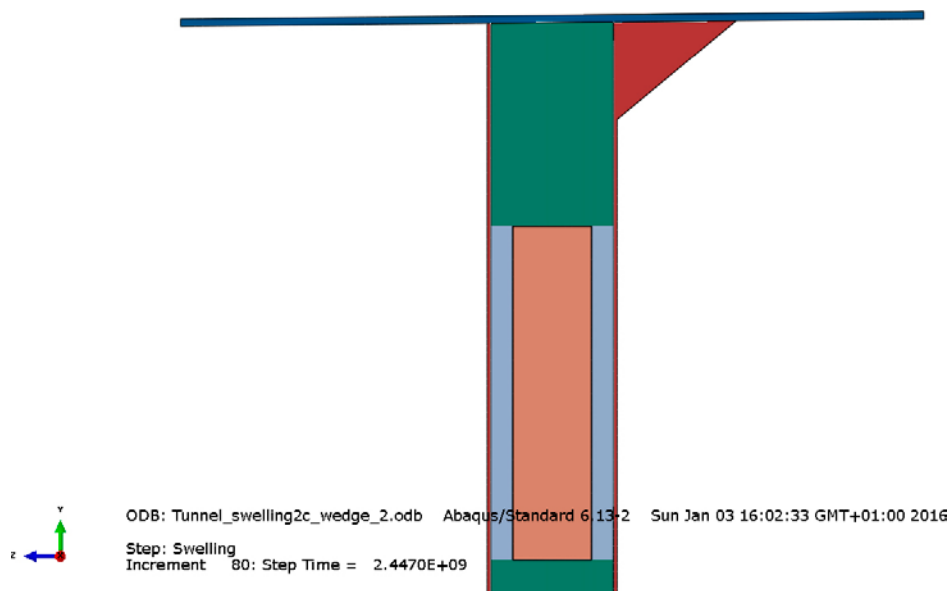


**Figure 9-1.** Geometry and material areas in the vertical symmetry plane. In addition there are also backfill blocks and pellets in the rest of the tunnel (see Figure 3-4).

## 9.2 Case 2c (swelling pressure 7 MPa)

The initial conditions are shown in Table 9-1.

**Table 9-1. Initial conditions of the buffer parts.**

Case	Void ratio $e_0$	Pressure $p_0$ and Pore pressure $-u_0$ (MPa)	Remarks
<b>Blocks</b>			
(2) 7 MPa	0.683	10.9	Recalculated <sup>1</sup>
<b>Rings</b>			
(2) 7 MPa	0.591	18.4	Recalculated <sup>1</sup>
<b>Pellet filling in the deposition hole and the bevel</b>			
1-3	1.78	0.022	Recalculated <sup>1</sup>

<sup>1</sup> Recalculated means that the pressure  $p_0$  has been adapted to the yield the correct swelling pressure at the desired average density. This must be done the blocks and the pellets since the validity of the Porous Elastic model is limited to  $0.7 < e < 1.5$ .

As expected the calculation has entailed large problems with convergence. Several attempts with changed strategy and stabilize factor have been done but complete pore pressure equalization was not reached. The best calculation reached  $4.93 \times 10^9$  s with a remaining maximum negative pore pressure in the buffer blocks above the canister of  $-63$  kPa, which is very close to equilibrium considering that the buffer started with a pore pressure of  $-18.4$  MPa (rings) and  $-10.9$  MPa (blocks). The time is judged to have been prolonged in the calculation due to the use of stabilize.

Unstable non-dynamic problems when using Abaqus can be stabilized by adding viscous forces. One technique is to use the parameter "Stabilize" where either an adaptive damping force could be used or by defining a constant damping coefficient. In the current analyses the latter method has been used and the coefficient has been tuned such that the effect on the solution is made as small as possible and still have a converged solution.

All results refer to the end stage. Figures 9-2 shows the vertical displacements and horizontal displacements in the deposition hole and bevel. Figure 9-3 shows the vertical displacements and the total vertical stresses in the backfill blocks.

The void ratio and dry density in the buffer are shown in Figure 9-4 and the average effective stress and vertical total stress are shown in Figure 9-5.

The average void ratio and density at saturation according to the new criterion (see Section 4.5) are  
 $e=0.773$

$$\rho_m=2004 \text{ kg/m}^3$$

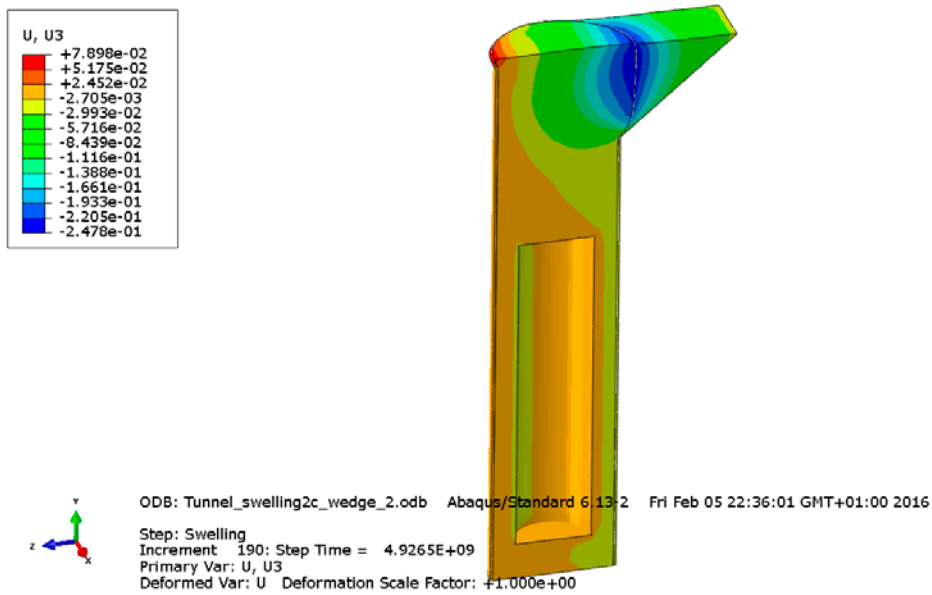
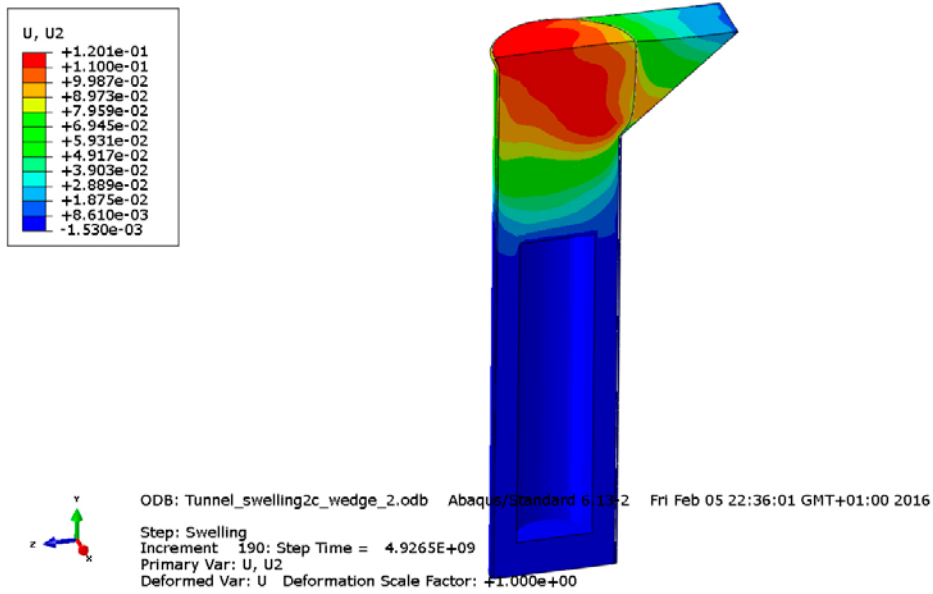


**Figure 9-2.** Vertical (upper) and horizontal displacements (m) in the axial vertical symmetry plane.

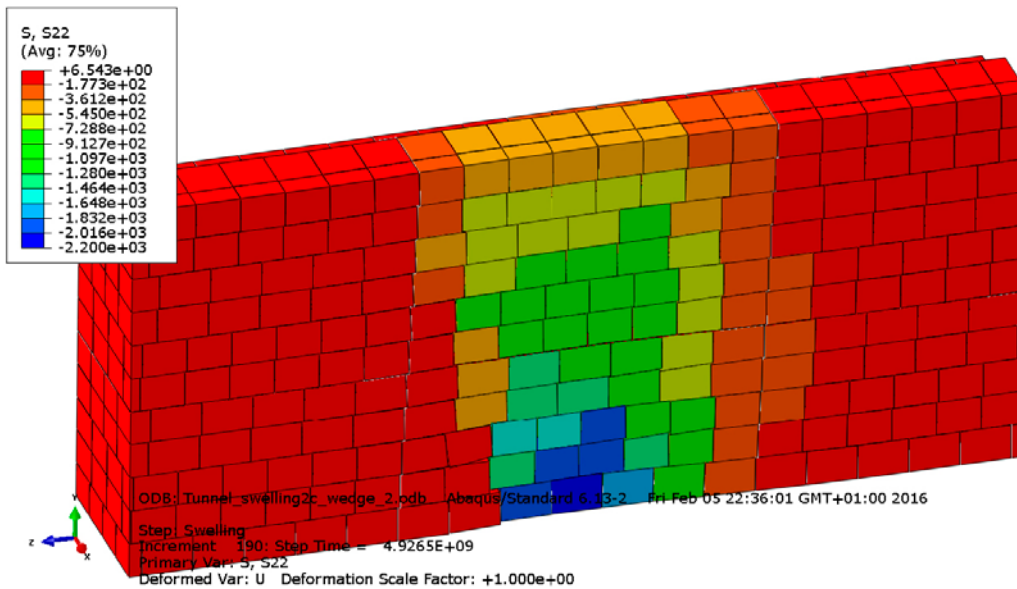
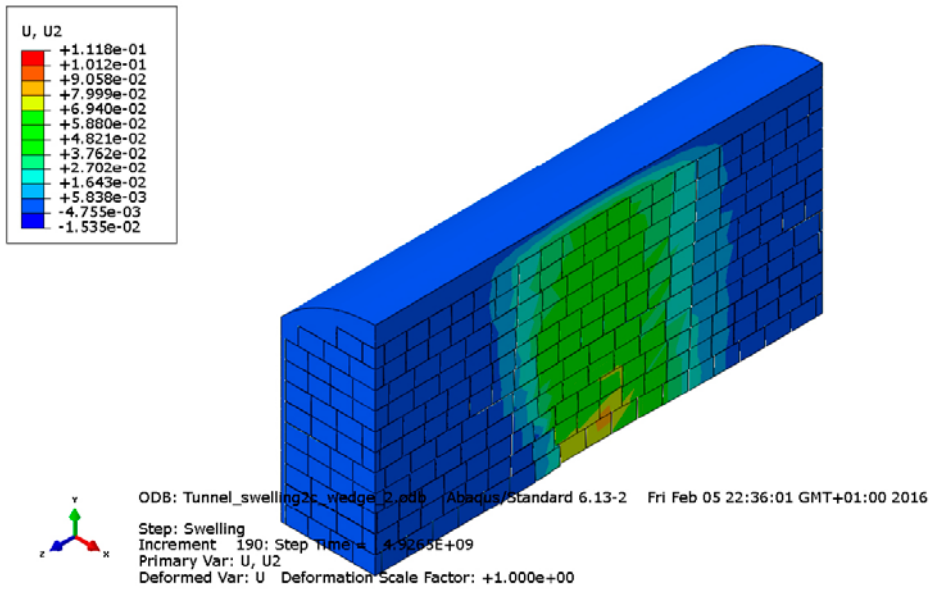


**Figure 9-3.** Vertical displacements (m) in the backfill in the tunnel (upper) and vertical stresses (kPa) in the backfill blocks.

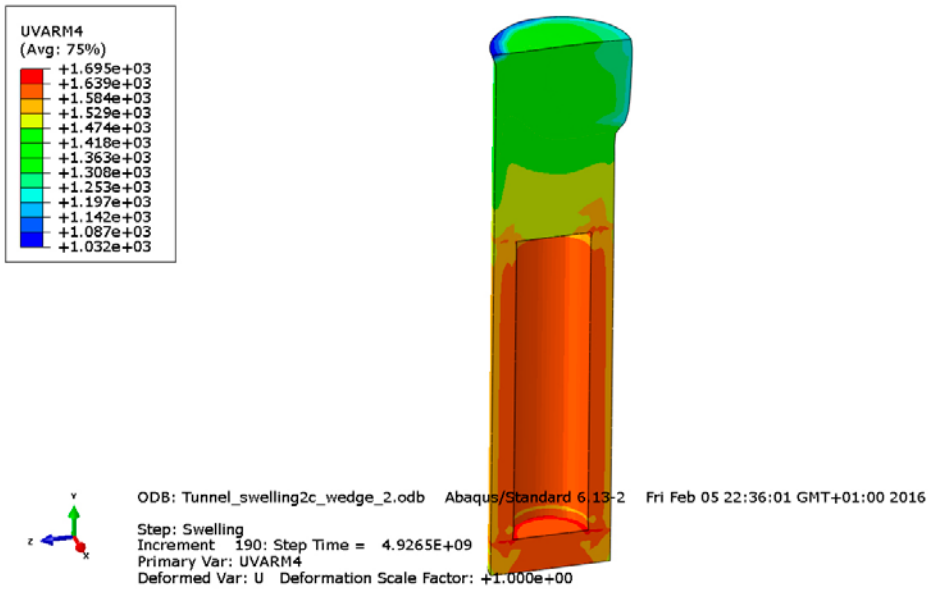
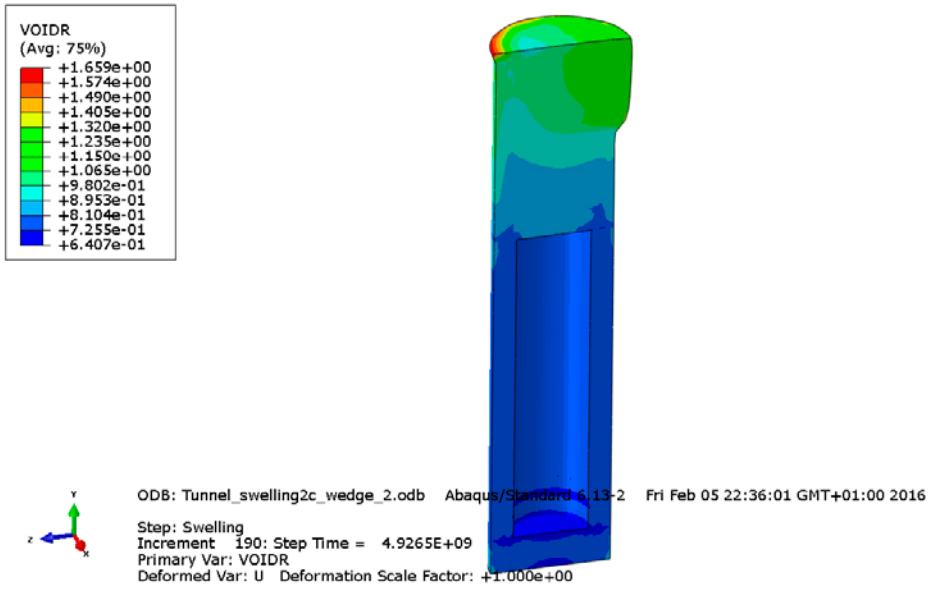
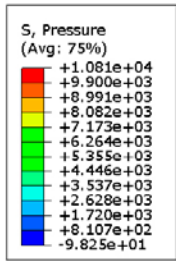
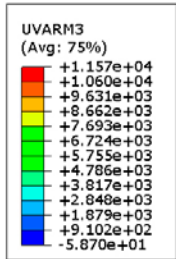


**Figure 9-4.** Void ratio (upper) and dry density ( $\text{kg/m}^3$ ) in the buffer.



ODB: Tunnel\_swelling2c\_wedge\_2.odb Abaqus/Standard 6.13-2 Fri Feb 05 22:36:01 GMT+01:00 2016  
 Step: Swelling  
 Increment 190: Step Time = 4.9265E+09  
 Primary Var: S, Pressure  
 Deformed Var: U Deformation Scale Factor: +1.000e+00



ODB: Tunnel\_swelling2c\_wedge\_2.odb Abaqus/Standard 6.13-2 Fri Feb 05 22:36:01 GMT+01:00 2016  
 Step: Swelling  
 Increment 190: Step Time = 4.9265E+09  
 Primary Var: UVARM3  
 Deformed Var: U Deformation Scale Factor: +1.000e+00

Figure 9-5. Average effective stress (upper) and vertical total stress (kPa) in the buffer.



### 9.3 Case 3c (swelling pressure 10 MPa)

The initial conditions are shown in Table 9-2.

**Table 9-2. Initial conditions of the buffer parts.**

Case	Void ratio $e_0$	Pressure $p_0$ and Pore pressure $-u_0$ (MPa)	Remarks
<b>Blocks</b>			
(3) 10 MPa	0.632	14.5	Recalculated <sup>1</sup>
<b>Rings</b>			
(3) 10 MPa	0.541	24.5	Recalculated <sup>1</sup>
<b>Pellet filling in the deposition hole and the bevel</b>			
1-3	1.78	0.022	Recalculated <sup>1</sup>

<sup>1</sup> Recalculated means that the pressure  $p_0$  has been adapted to the yield the correct swelling pressure at the desired average density. This must be done the blocks and the pellets since the validity of the Porous Elastic model is limited to  $0.7 < e < 1.5$ .

Also for this case the calculation entailed large problems with convergence. Several attempts with changed strategy and stabilize factor have been done but complete pore pressure equalization was not reached. The best calculation reached  $4.0 \times 10^9$  s with a remaining maximum negative pore pressure in the buffer blocks above the canister of  $-125$  kPa, which is also very close to equilibrium considering that the buffer started with a pore pressure of  $-24.5$  MPa (rings) and  $-14.5$  MPa (blocks). The time is judged to have been prolonged in the calculation due to the use of stabilize.

All results refer to the end stage. Figures 9-6 shows the vertical displacements and horizontal displacements in the deposition hole and bevel. Figure 9-7 shows the vertical displacements and the total vertical stresses in the backfill blocks.

The void ratio and dry density in the buffer are shown in Figure 9-8 and the average effective stress and vertical total stress are shown in Figure 9-9.

The average void ratio and density at saturation according to the new criterion (see Section 4.5) are

$$e=0.727$$

$$\rho_m=2031 \text{ kg/m}^3$$

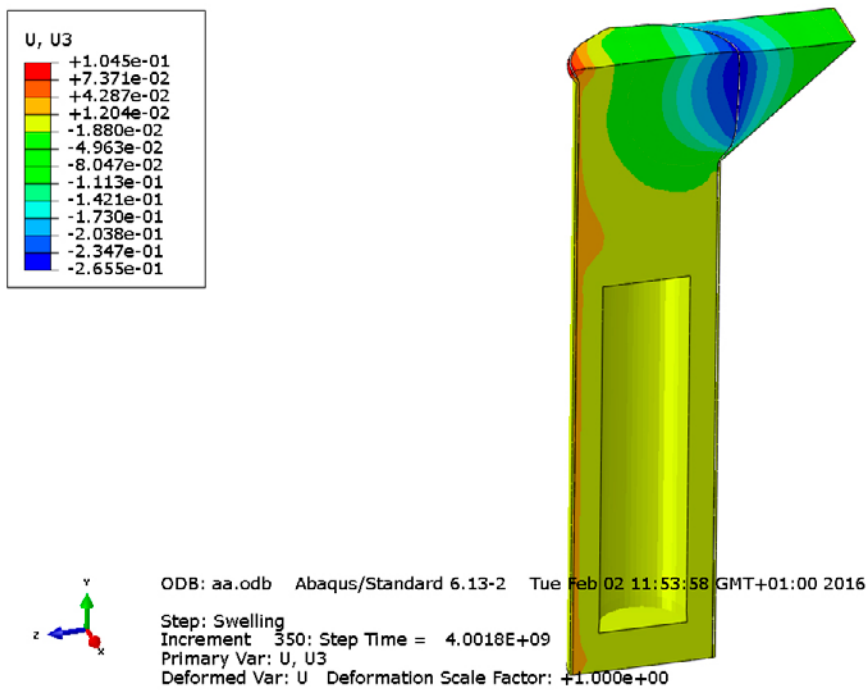
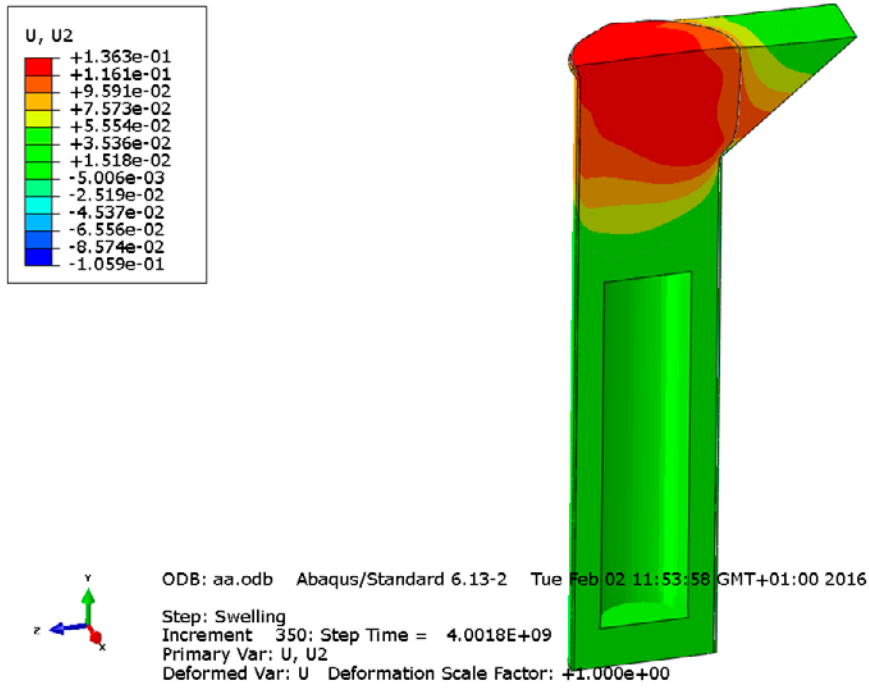
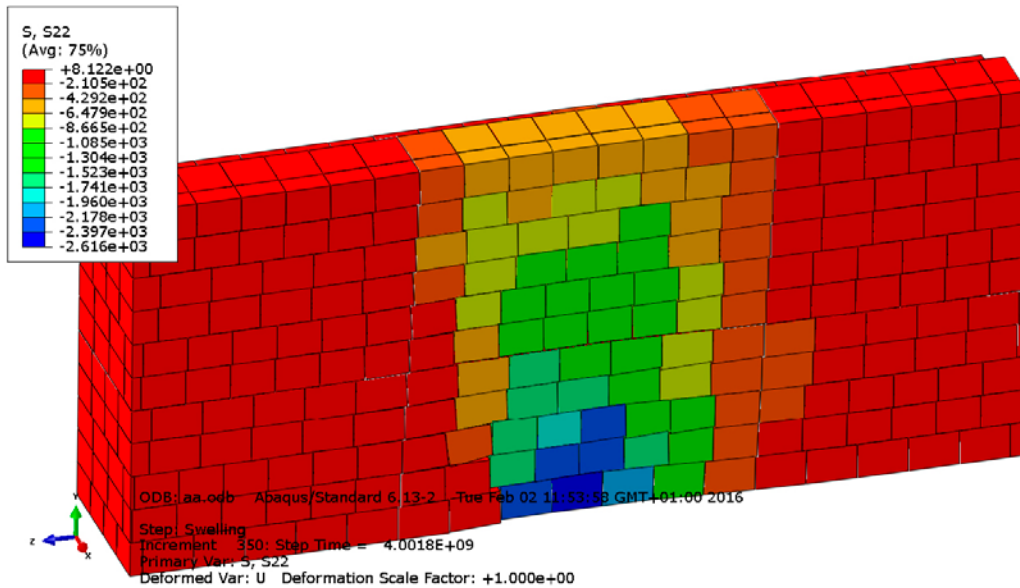
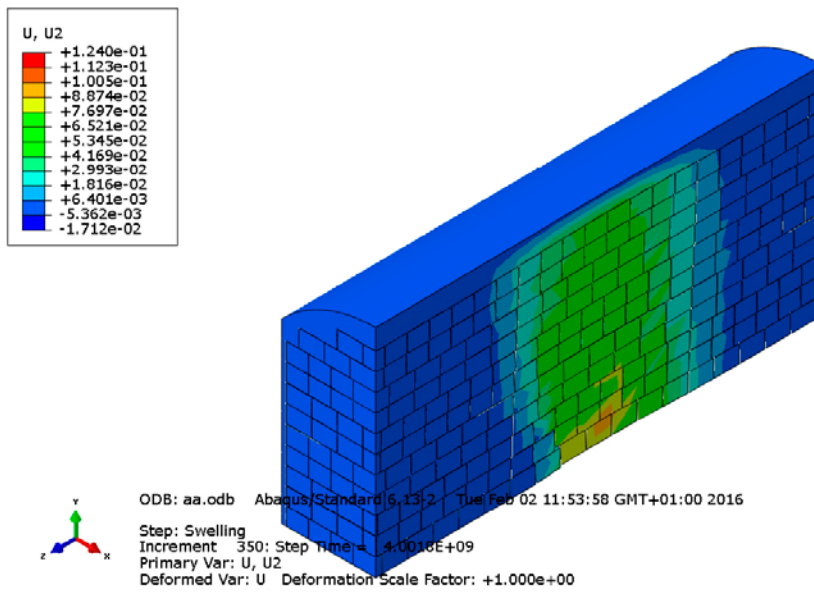
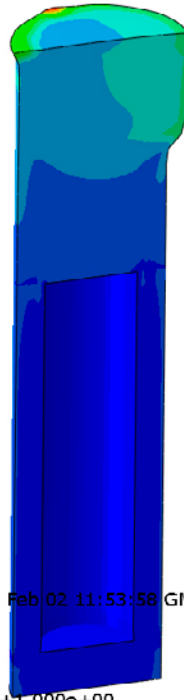
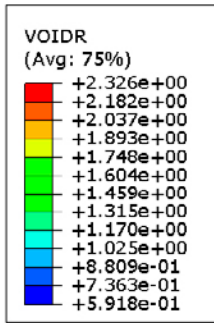


Figure 9-6. Vertical (upper) and horizontal displacements (m) in the axial vertical symmetry plane.

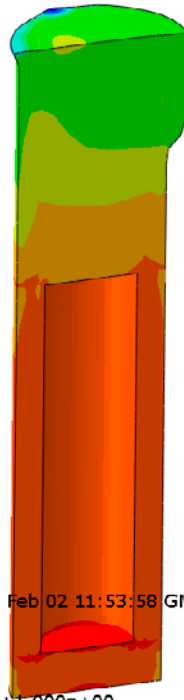
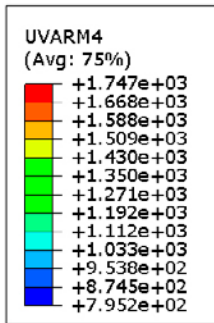


**Figure 9-7.** Vertical displacements (m) in the backfill in the tunnel (upper) and vertical stresses (kPa) in the backfill blocks.



ODB: aa.odb Abaqus/Standard 6.13-2 Tue Feb 02 11:53:58 GMT+01:00 2016

Step: Swelling  
Increment 350: Step Time = 4.0018E+09  
Primary Var: VOIDR  
Deformed Var: U Deformation Scale Factor: +1.000e+00



ODB: aa.odb Abaqus/Standard 6.13-2 Tue Feb 02 11:53:58 GMT+01:00 2016

Step: Swelling  
Increment 350: Step Time = 4.0018E+09  
Primary Var: UARM4  
Deformed Var: U Deformation Scale Factor: +1.000e+00

Figure 9-8. Void ratio (upper) and dry density ( $\text{kg/m}^3$ ) in the buffer.

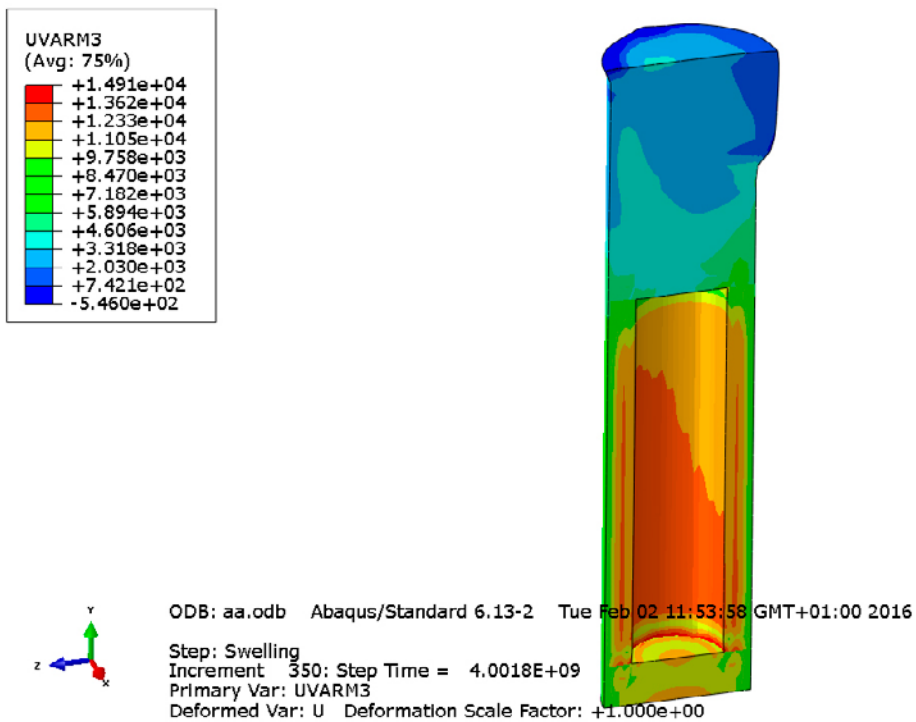
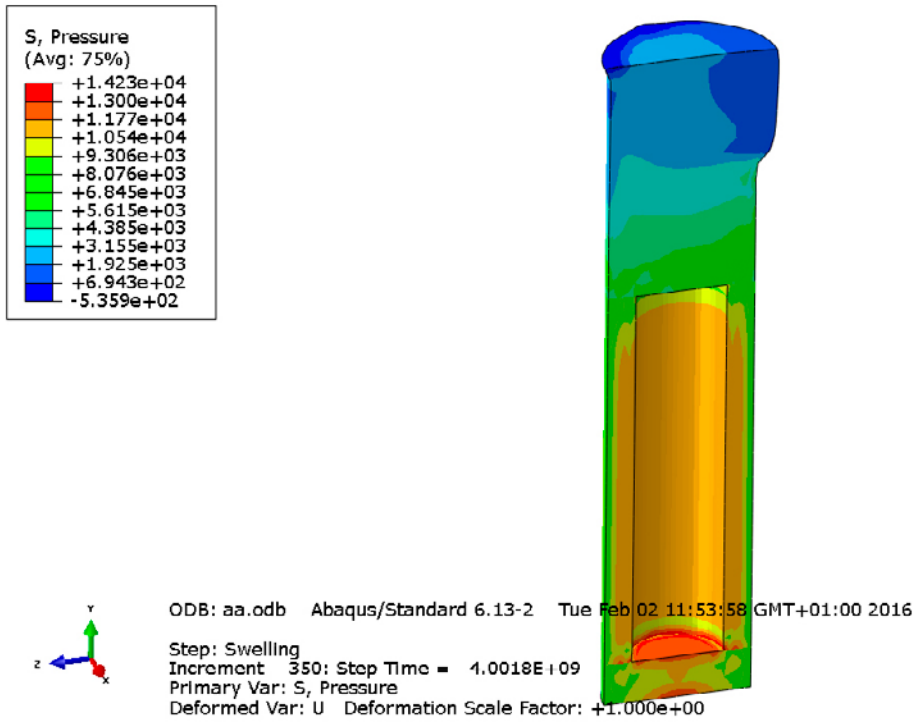


**Figure 9-9.** Average effective stress (upper) and vertical total stress (kPa) in the buffer.

## 9.4 Comments and conclusions

The numerical problems of these calculations are well illustrated for case 3c in Figure 9-8, where a local swelling has occurred in the contact between the wet upper bentonite in the deposition hole and the dry pellet filling in the floor, which results in locally very low density. It is difficult to say how much the incomplete pore pressure equalization means for the end state but the rather low remaining negative pore pressure indicates that the effect is small.

Figures 9-2 and 9-6 show that the axial displacements are rather small compared to the results of the simplified calculations in Chapter 5. The axial displacement is about 12 and 13 cm for case 2c and 3c. However, the lateral swelling of the upper bentonite bocks into the bevel is rather large or about 25 and 26 cm.

The average stress above the canister and the density according to the new criterion are much higher for this model than the simplified models in Chapter 5. Table 9-3 shows a comparison.

**Table 9-3. Comparison between the model with the bevel and the homogenized model.**

Model	Variable	Actual bevel (3D)	Simplified bevel (2D)	Remaining pore pressure
2c (7 MPa)	Average stress above the canister	$p=5$ MPa	$p=3$ MPa	-63 kPa
3c (10 MPa)	Average stress above the canister	$p=6.5$ MPa	$p=4$ MPa	-125 kPa
2c (7 MPa)	Density with new criterion	$\rho_m=2004$ kg/m <sup>3</sup>	$\rho_m=1990$ kg/m <sup>3</sup>	
3c (10 MPa)	Density with new criterion	$\rho_m=2031$ kg/m <sup>3</sup>	$\rho_m=2014$ kg/m <sup>3</sup>	

In spite of the large horizontal swelling the density distribution is still very inhomogeneous in the upper part of the deposition hole and the bevel. This shows that the assumption of complete homogenization that cases *c* and *d* in Chapter 5 is based on is very pessimistic and the results not reliable.

The conclusion of the modelling of two cases with wet upper part of the deposition hole and bevel that is only filled with pellets is that the large remaining inhomogeneity of the bentonite in the bevel results in a rather high density and high counter pressure in the upper 1.25 m of the deposition hole that prevent buffer upwards swelling to critical levels. All cases with 10 cm pellet filling in the floor are acceptable.

## 10 Summary and conclusions

### 10.1 General

One important task for the backfill is to restrict upwards swelling of the buffer in deposition holes. If the buffer can swell upwards it will lose density and by that also important properties. A possible scenario is the so called dry case of buffer/backfill interaction meaning that the water inflow into the deposition tunnel is very low and the backfill kept dry but at the same time there is a fast wetting of a deposition hole.

The report describes the modelling efforts of the mechanical interaction between the buffer and the backfill at a dry backfill that were made in 2015. All calculations were done with the finite element code Abaqus.

### 10.2 Modelled cases

#### ***The buffer swelling test in Äspö HRL***

This full scale test was used to check the response of a dry backfill to an upwards swelling of the buffer. Instead of buffer a bentonite block in a deposition hole was forced to move upwards by four cylinders and the force and displacement measured. The backfill was designed as the reference backfill in a deposition tunnel. By modelling this test the modelled response of the backfill could be checked against the measured response and the backfill model could be validated.

Comparison between modelled and measured results of the swelling test showed a very good agreement up to 8 cm displacement, after which cracking of the blocks took place and the model was invalid. Sensitivity analyses showed that the stiffness and thickness of the pellet filling in the floor and ceiling were the factors most sensitive to changes. For further modelling the models and parameters used are adequate to use. For 2D axial symmetry models the test results can be used as a simplified model of the dry backfill if proper account is taken to changes in slot width and pellet stiffness in the ceiling and floor. The models require of course that improved quality of the backfill blocks can be made so that cracking will not take place.

#### ***Modelling of the buffer and backfill mechanical interaction with different initial conditions and different material models of the buffer***

The base case with a density at saturation of 2000 kg/m<sup>3</sup> and the swelling pressure 7 MPa with the same backfill as in the field test was modelled as having a completely homogeneous buffer from start. Both the old mechanical material model for saturated buffer materials with Drucker-Prager plasticity model (used in SR-Site) and the new Plastic Cap model derived in the TF EBS have been used for comparison. The backfill response was modelled with the extrapolated test results and with changes in geometry taken into account.

The same base case corresponding to a buffer with an average density at saturation of 2000 kg/m<sup>3</sup> and the average swelling pressure 7 MPa with the same backfill as in the field test was modelled with the initial densities of the buffer in the deposition hole, i.e. buffer blocks, buffer rings and pellets. Also for this case both the old mechanical material model for saturated buffer material (used in SR-Site) and the new material model derived in the TF EBS has been used for comparison. The backfill response was modelled with the extrapolated test results and with changes in geometry taken into account.

A comparison between the results when the D-P model was used and when the Plastic Cap model was used show that the difference is small. It seems as the introduction of a cap and a curved failure envelope does not affect the results very much at the type of swelling that takes place at this type of upwards swelling.

The density distribution under and along the canister differs very much for the two initial conditions. The inhomogeneous model has a remaining very strong density spreading in comparison with the homogeneous model. Above the canister, where the large swelling takes place, there is also a clear difference with a much stronger swelling for the inhomogeneous model.

A general conclusion is that the inhomogeneous model should be used if possible. Underestimation of the swelling may otherwise be the case.

### ***Influence of buffer density and backfill geometry***

15 cases with different average density and swelling pressure of the buffer and different geometry of the backfill were modelled with the new material model and initially inhomogeneous buffer. The purpose was to study the sensitivity to changes in geometry and density. The backfill response was modelled with the extrapolated test results and with changes in geometry taken into account. Six cases with wet backfill blocks in the upper part of the deposition hole were modelled with simplified models that took the density loss into the bevel into account.

The results showed that the influence of the pellet filling in the floor and the influence of the bevel are rather strong but for most cases not critical. Only two cases (1b and 1e modelling the pellet filled bevel and the 50 cm pellet filling in the floor at the initial average swelling pressure 4 MPa) resulted in an average stress above the canister that was below 2 MPa.

These cases also yield too low density  $\rho_m < 1950 \text{ kg/m}^3$  according to the new criterion.

All simplified pessimistic cases with the bevel (c and d) fullfills the requirements with  $p > 2 \text{ MPa}$  above the canister lid and  $\rho_m \geq 1950 \text{ kg/m}^3$ .

The new buffer criterion seems to capture the low density at the top of the canister quite well.

General conclusions are that:

- Pellets filling thickness in the floor influences the results more than the bevel.
- Only low density buffer yields problems.
- Cases with bevel and 10 cm pellet filling thickness fullfills the requirements.

### ***3D model for checking the backfill compression model***

In order to check that the extrapolation of the stress-strain behaviour of the backfill used in the analyses is a valid model, 3D analyses of two of the cases in the sensitivity analysis were performed. The same backfill block configuration as in the field test and an inhomogeneous buffer were modelled and compared with the simplified 2D calculation.

The results show that the agreement is rather poor. For case 3e the displacement of the contact buffer/backfill is in average about 21 cm in the 3D model while it is about 27 cm in the 2D model. In agreement with this the average stress is on top of the canister is higher in the 3D case (about 5 MPa) than in the 2D model (about 2.5 MPa). The same poor agreement applies for case 3a. The displacement of the contact buffer/backfill is about 12 cm in the 3D model while it is about 18 cm in the 2D model. This difference yields that the average stress above the canister is about 6 MPa in the 3D model and only about 3 MPa in the 2D model.

The comparison thus shows that the 3D model for both cases yields less upwards swelling and higher remaining density above the canister than the 2D model. The main reason for this difference is that the 3D calculations were interrupted before equilibrium.

### ***3D model for studying the influence of the width of the pellet filled slot at the ceiling***

The sensitivity analysis was done with the same backfill geometry as in the field test. In order to study the influence of the width of the pellet filled slot at the ceiling 3D-models with two different slot widths in a backfilled dry tunnel was simulated. The comparison between the results show that the influence of the width of the pellet filled slot at the ceiling is rather small. This is good for the concept since the rock surface at the ceiling can be very irregular.



The conclusion is that the influence of the slot width is not strong but also that the geometry of the masonry is important. If there is no overlapping of the blocks the stress will continue through the block without spreading and with retained stress level.

### ***Modelling of the case with backfill block failure***

The backfill blocks in the field test cracked after about 10 cm displacement of the simulated buffer. In order to study the effect of block cracking case 2b in the sensitivity analysis was modelled with the results of the field test after 10 cm displacement as backfill response. The results show that the effect on the buffer is rather large. The swelling of the buffer/backfill interface was slightly over 30 cm and the average stress above the canister lid was about 1.5 MPa in the case of block failure. However, the density according to the new criterion was 1 966 kg/m<sup>3</sup> and thus acceptable.

### ***3D model with bevel of wet upper part of the deposition hole***

In the sensitivity analyses the effect of also having the upper part of the deposition hole and the pellet filled bevel wetted was investigated as cases *c* and *d*. But for those cases the pessimistic assumption was made that the entire backfill part (upper 1.25 m and the bevel) was homogenised which results in a rather low density in the deposition hole. In order to study the relevance of those models two 3D calculations of two of the cases including the bevel filled with bentonite pellets were performed.

The results show that the density loss in the buffer above the canister is much lower in the 3D case. In spite of the large horizontal swelling the density distribution after equilibrium is still very inhomogeneous in the upper part of the deposition hole and the bevel. The assumption of complete homogenization used for cases *c* and *d* in Chapter 5 is thus very pessimistic and the results not reliable.

The conclusion of the modelling of two cases with wet upper part of the deposition hole and bevel that is only filled with pellets is that the large remaining inhomogeneity of the bentonite in the bevel prevents buffer upwards swelling to critical levels. All cases with 10 cm pellet filling in the floor are acceptable.

## **10.3 New buffer criterion**

All modelling results have been evaluated according to the recently proposed buffer density criteria, which says that only the buffer located between the bottom of the deposition hole and the 0.5 m above the canister shall be used for calculating the average density. The results show that the criterion rather well captures the critical cases at upwards swelling scenarios. All cases with a swelling pressure above the canister lid  $\leq 2$  MPa gave average densities according to the new criterion  $\leq 1 950$  kg/m<sup>3</sup> at water saturation, which corresponds to a swelling pressure of about 3 MPa.

Only in one case the new buffer criterion failed to discover a critical case with swelling pressure above the canister lid less than 2 MPa. This case was the case of backfill block failure.



## References

SKB's (Svensk Kärnbränslehantering AB) publications can be found at [www.skb.com/publications](http://www.skb.com/publications).

**Andersson L, Sandén T, 2012.** Optimization of backfill pellet properties. ÅSKAR DP2. Laboratory tests. SKB R-12-18, Svensk Kärnbränslehantering AB.

**Börgesson L, Johannesson L-E, Sandén T, Hernelind J, 1995.** Modelling of the physical behaviour of water saturated clay barriers. Laboratory tests, material models and finite element application. SKB TR 95-20, Svensk Kärnbränslehantering AB.

**Börgesson L, Dueck A, Johannesson L-E, 2010.** Material model for shear of the buffer – evaluation of laboratory test results. SKB TR-10-31, Svensk Kärnbränslehantering AB.

**Börgesson L, Åkesson M, Hernelind J, 2015.** EBS TF – THM modelling. Homogenisation Task. SKB P-18-05, Svensk Kärnbränslehantering AB.

**Börgesson L, Åkesson M, Kristensson O, Dueck A, Hernelind J, 2016.** EBS TF – THM modelling. BM2 – Large scale field tests. SKB TR-13-07, Svensk Kärnbränslehantering AB.

**Johannesson L-E, 2008.** Backfill and closure of the deep repository. Phase 3 – pilot tests to verify engineering feasibility. Geotechnical investigations made on unsaturated backfill materials. SKB R-08-131, Svensk Kärnbränslehantering AB.

**Martino L, Börgesson L, Keto P, 2016.** Numerical modelling of the buffer swelling test in Äspö HRL. Validation of numerical models with the ÅSKAR test data. SKB TR-17-03, Svensk Kärnbränslehantering AB.

**Posiva SKB, 2017.** Safety functions, performance targets and technical design requirements for a KBS-3V repository Conclusions and recommendations from a joint SKB and Posiva working group. SKB Posiva Report 01, Posiva Oy, Svensk Kärnbränslehantering AB.

**Sandén T, Dueck A, Nilsson, Jensen V, Börgesson L, 2015.** Full scale Buffer Swelling Test at dry backfill conditions in Äspö HRL. In situ test and related laboratory tests. SKB TR-16-07, Svensk Kärnbränslehantering AB.

**Åkesson M, Kristensson O, Börgesson L, Dueck A, Hernelind J, 2010a.** THM modeling of buffer, backfill and other system components. Critical processes and scenarios. SKB TR-10-11, Svensk Kärnbränslehantering AB.

**Åkesson M, Börgesson L, Kristensson O, 2010b.** SR-Site Data report. THM modeling of buffer, backfill and other system components. SKB TR-10-44, Svensk Kärnbränslehantering AB.

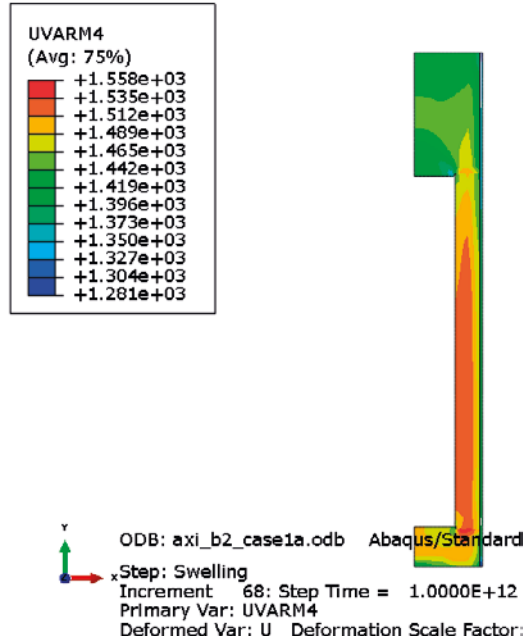


Results of the sensitivity analyses

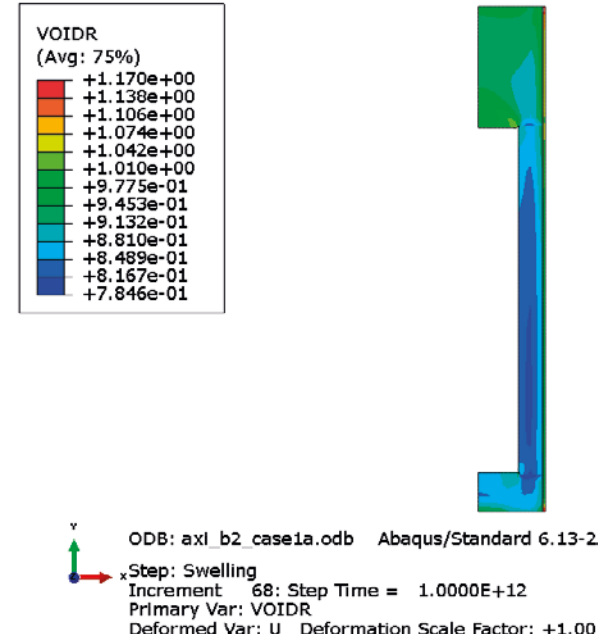
Case 1a ( $\sigma=4$  MPa,  $t_p=10$ cm)

Total displacement (buffer top): 11 cm

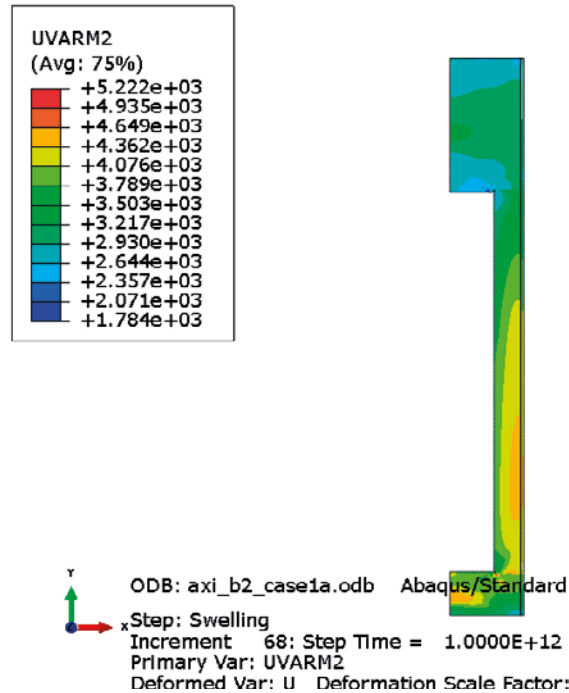
Dry density (kg/m<sup>3</sup>)



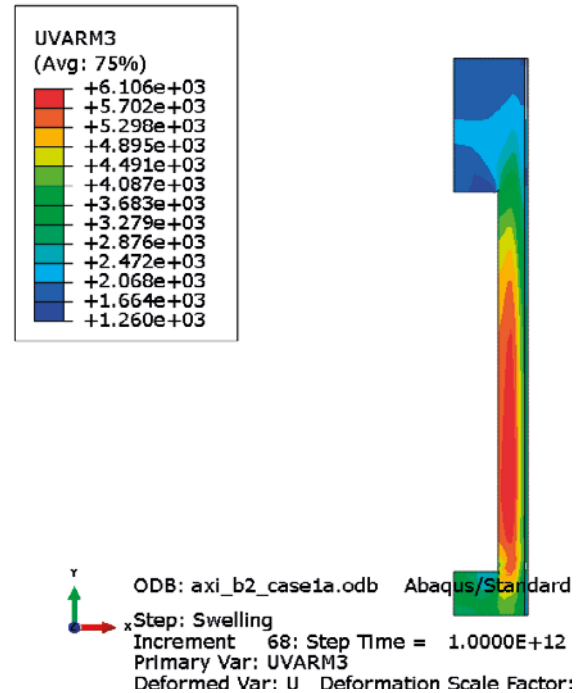
Void ratio



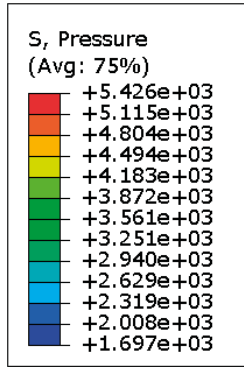
Radial stress (kPa)




Axial stress (kPa)

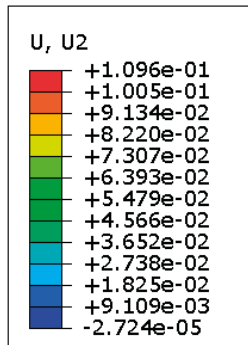



**Average stress (kPa)**




 ODB: axi\_b2\_case1a.odb    Abaqus/Standard 6.13-2    Thu Oct 22 17:32:27 GMT+02:00  
 Step: Swelling  
 Increment    68: Step Time =    1.0000E+12  
 Primary Var: S, Pressure  
 Deformed Var: U    Deformation Scale Factor: +1.000e+00

**Axial displacements (m)**

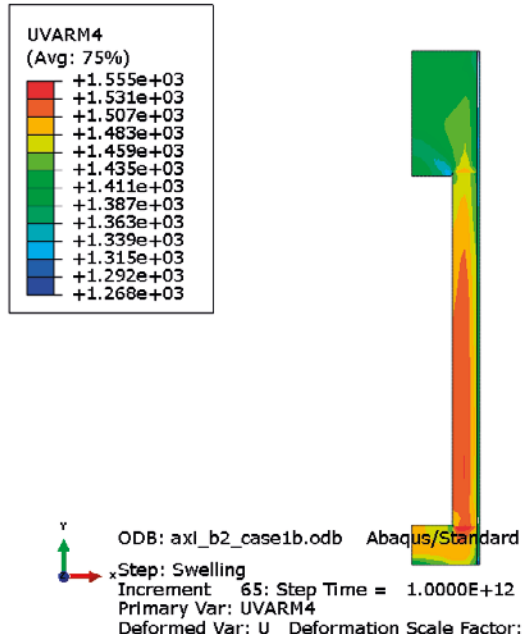



 ODB: axi\_b2\_case1a.odb    Abaqus/Standard 6.13-2    Thu Oct 22 17:32:27 GMT+02:00  
 Step: Swelling  
 Increment    68: Step Time =    1.0000E+12  
 Primary Var: U, U2  
 Deformed Var: U    Deformation Scale Factor: +1.000e+00

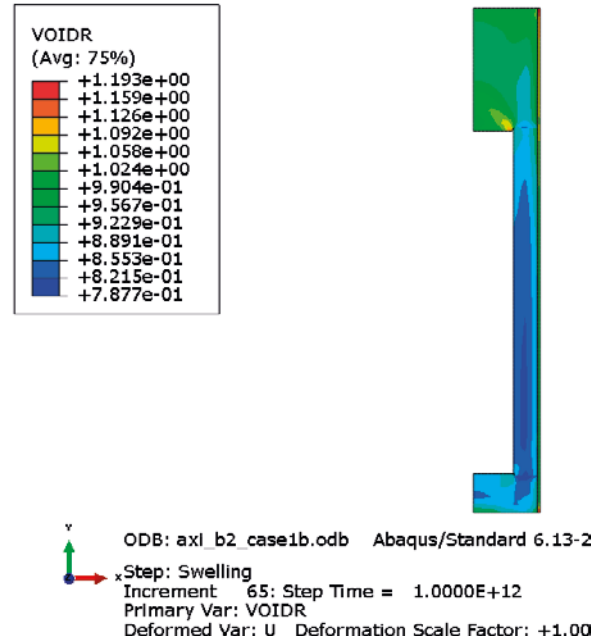
**Case 1b ( $\sigma=4$  MPa,  $t_p=25$  cm)**

**Total displacement (buffer top): 14 cm**

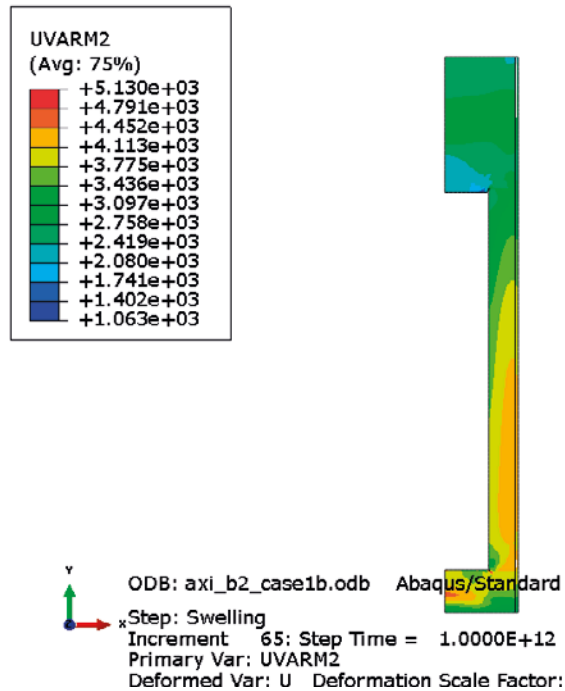
**Dry density (kg/m<sup>3</sup>)**



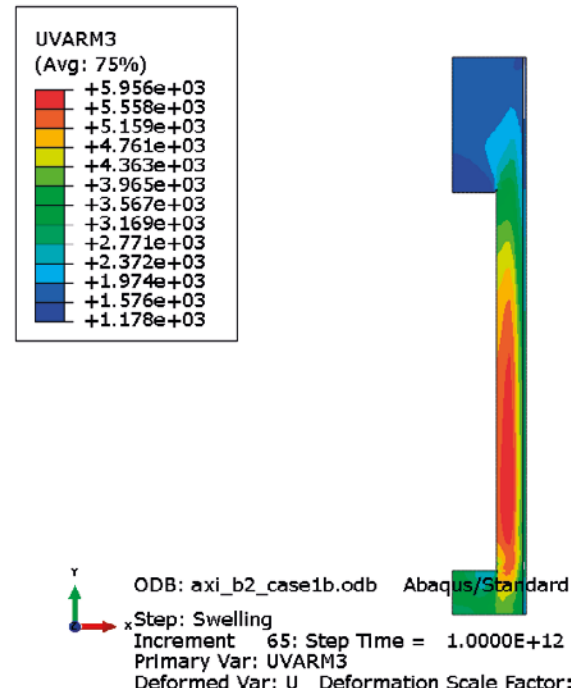
**Void ratio**



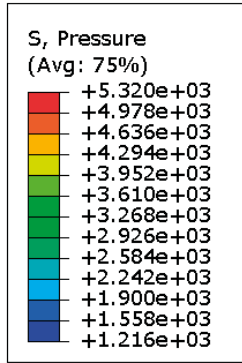
**Radial stress (kPa)**

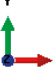


**Axial stress (kPa)**

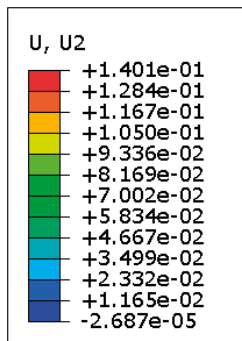



**Average stress (kPa)**




 ODB: axi\_b2\_case1b.odb    Abaqus/Standard 6.13-2    Thu Oct 22 15:22:27 GMT+02:00  
 Step: Swelling  
 Increment    65: Step Time = 1.0000E+12  
 Primary Var: S, Pressure  
 Deformed Var: U    Deformation Scale Factor: +1.000e+00

**Axial displacements (m)**



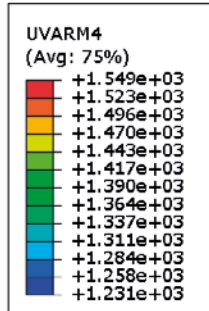

 ODB: axi\_b2\_case1b.odb    Abaqus/Standard 6.13-2    Thu Oct 22 15:22:27 GMT+02:00  
 Step: Swelling  
 Increment    65: Step Time = 1.0000E+12  
 Primary Var: U, U2  
 Deformed Var: U    Deformation Scale Factor: +1.000e+00



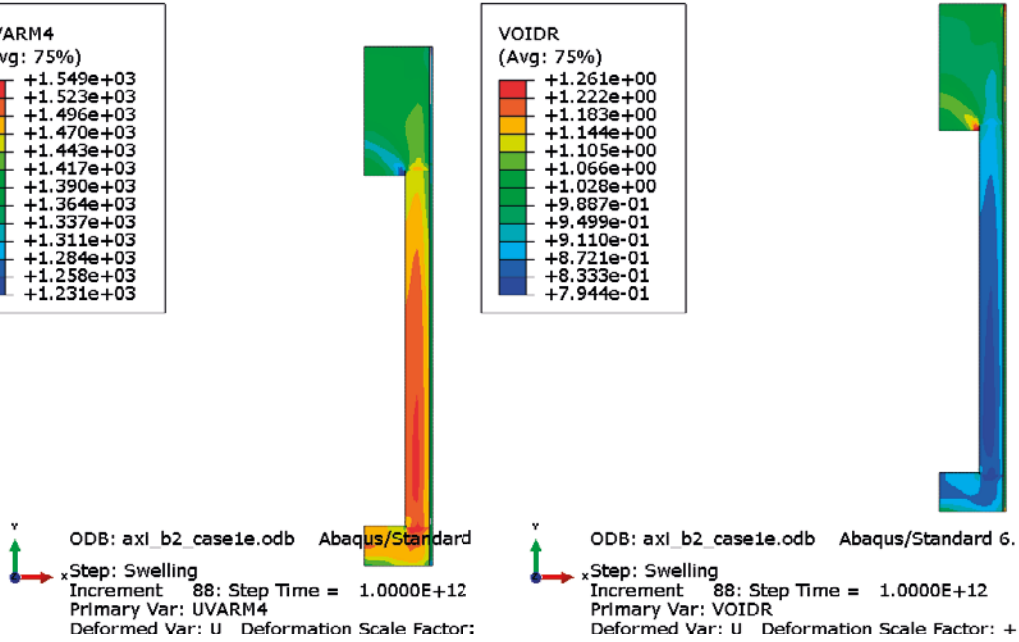
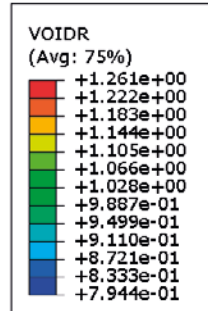
**Case 1e ( $\sigma=4$  MPa,  $t_p=50$  cm)**

**Total displacement (buffer top): 19 cm**

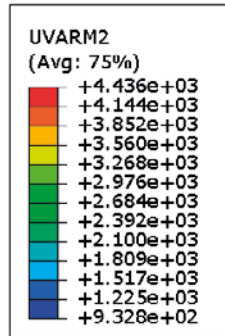
**Dry density ( $\text{kg/m}^3$ )**



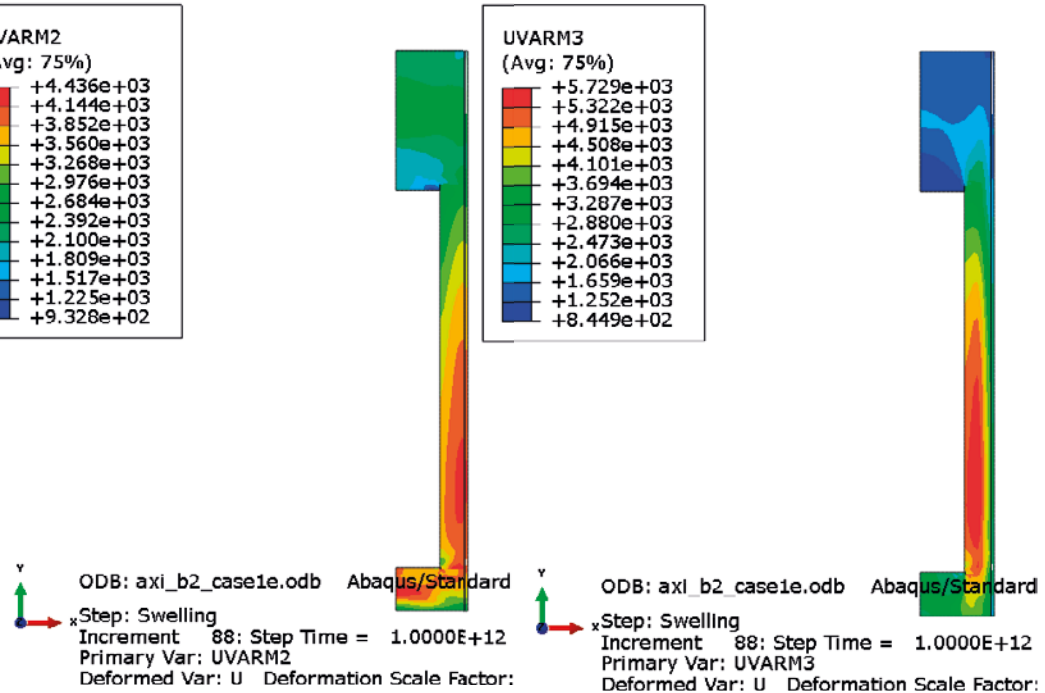
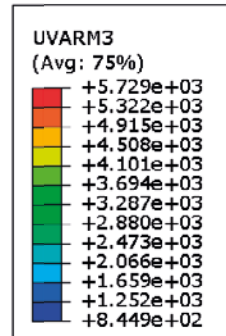
**Void ratio**



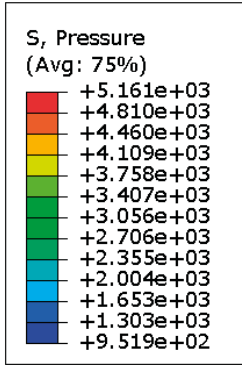
**Radial stress (kPa)**




**Axial stress (kPa)**

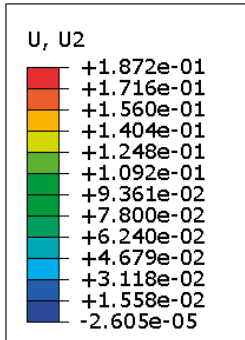



**Average stress (kPa)**




 ODB: axi\_b2\_case1e.odb    Abaqus/Standard 6.13-2    Sun Oct 25 14:27:28 GMT+01:00  
 Step: Swelling  
 Increment 88: Step Time = 1.0000E+12  
 Primary Var: S, Pressure  
 Deformed Var: U    Deformation Scale Factor: +1.000e+00

**Axial displacements (m)**

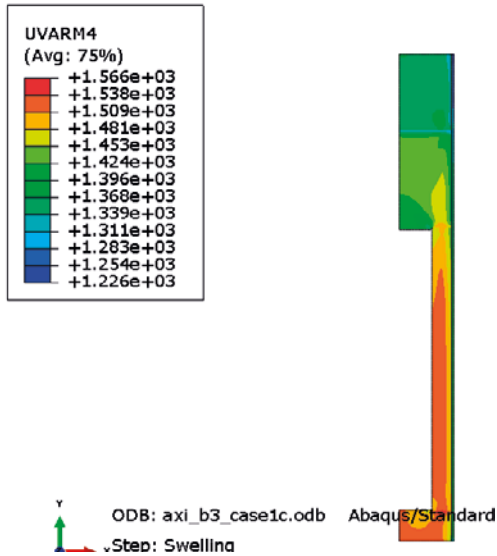



 ODB: axi\_b2\_case1e.odb    Abaqus/Standard 6.13-2    Sun Oct 25 14:27:28 GMT+01:00  
 Step: Swelling  
 Increment 88: Step Time = 1.0000E+12  
 Primary Var: U, U2  
 Deformed Var: U    Deformation Scale Factor: +1.000e+00

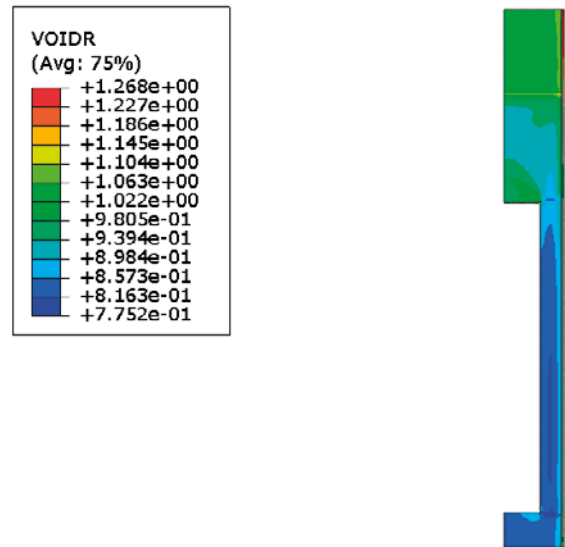
**Case 1c ( $\sigma=4$  MPa,  $t_p=10$  cm + bevel)**

Total displacement (buffer top): 11 cm

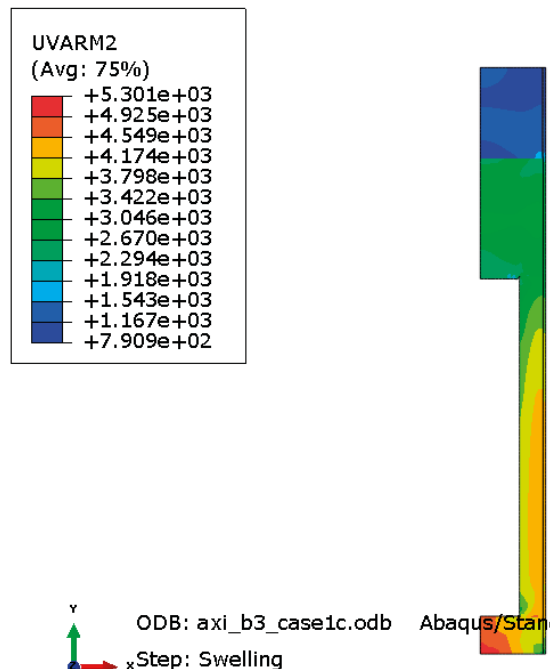
**Dry density (kg/m<sup>3</sup>)**



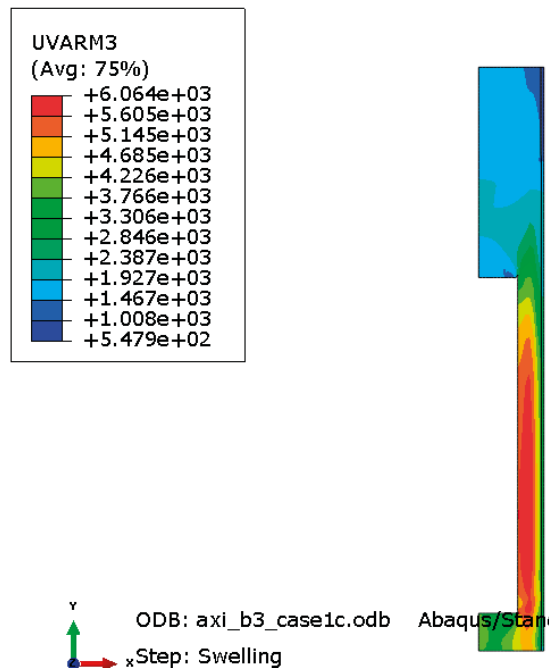
**Void ratio**



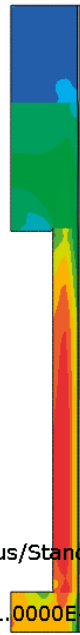
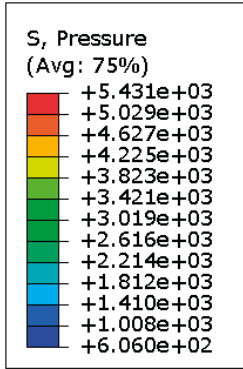
**Radial stress (kPa)**

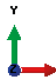


**Axial stress (kPa)**

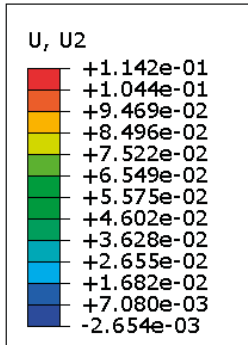



**Average stress (kPa)**




 ODB: axi\_b3\_case1c.odb    Abaqus/Standard 6.13-2    Thu Nov 05 19:37:48 GMT+01:00  
 Step: Swelling  
 Increment 67: Step Time = 1.0000E+12  
 Primary Var: S, Pressure  
 Deformed Var: U    Deformation Scale Factor: +1.000e+00

**Axial displacements (m)**

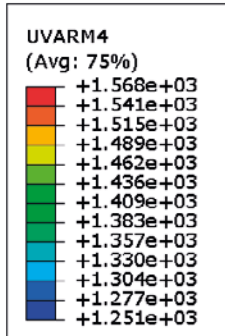



 ODB: axi\_b3\_case1c.odb    Abaqus/Standard 6.13-2    Thu Nov 05 19:37:48 GMT+01:00  
 Step: Swelling  
 Increment 67: Step Time = 1.0000E+12  
 Primary Var: U, U2  
 Deformed Var: U    Deformation Scale Factor: +1.000e+00

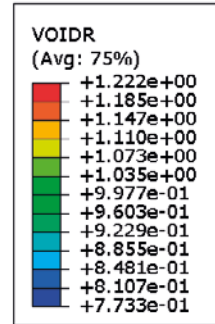
**Case 1d ( $\sigma=4$  MPa,  $t_p=10$  cm + bevel + blocks)**

**Total displacement (buffer top): 7 cm**

**Dry density (kg/m<sup>3</sup>)**

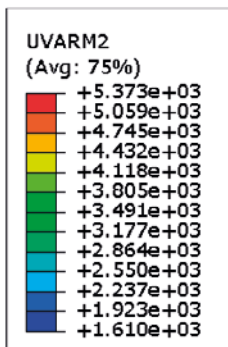


**Void ratio**

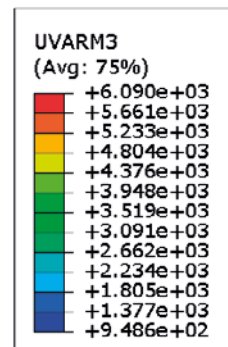


ODB: axi\_b3\_case1d.odb Abaqus/Stan  
Step: Swelling

**Radial stress (kPa)**



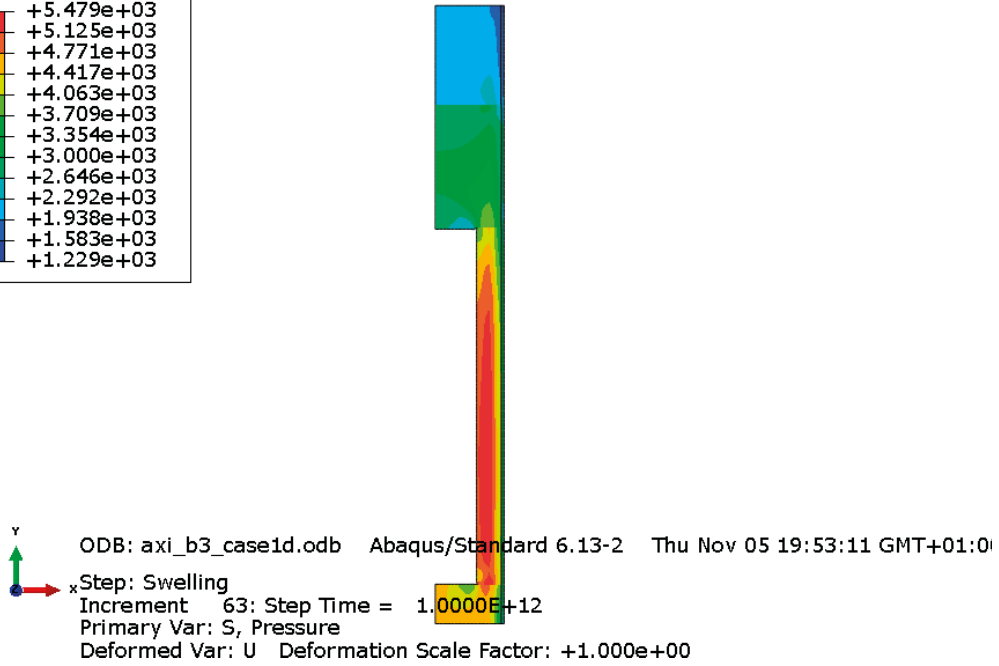
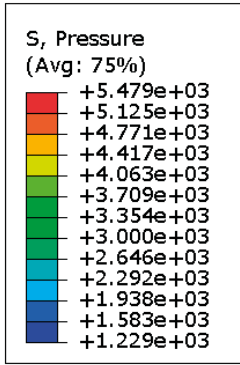
**Axial stress (kPa)**



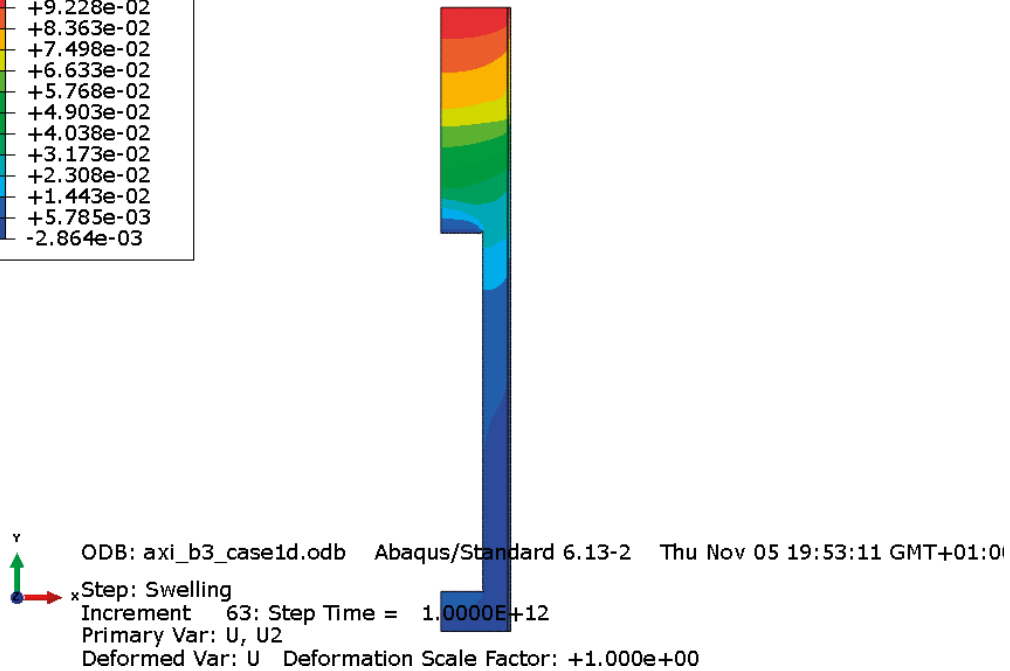
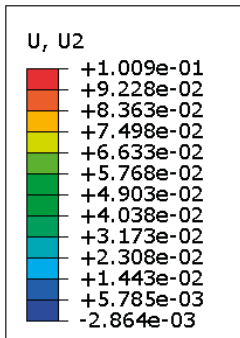
ODB: axi\_b3\_case1d.odb Abaqus/Stan  
Step: Swelling

ODB: axi\_b3\_case1d.odb Abaqus/Stan  
Step: Swelling

Average stress (kPa)



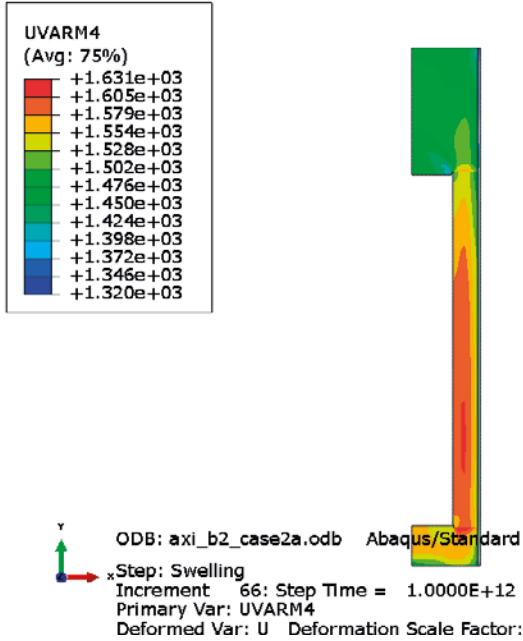
Axial displacements (m)



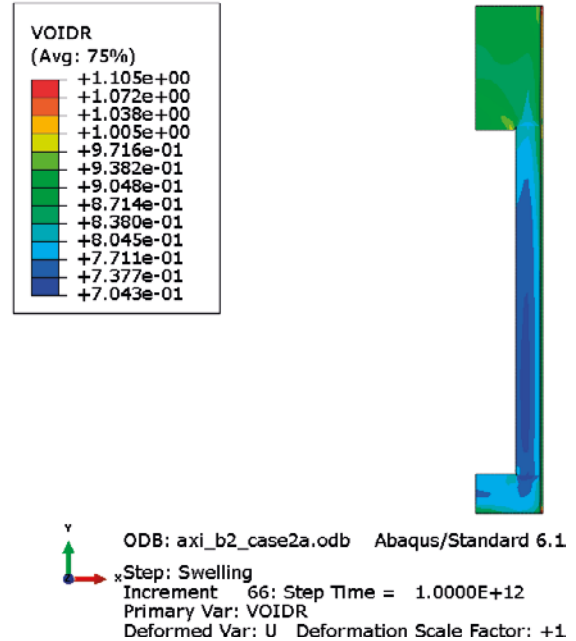
**Case 2a ( $\sigma=7$  MPa,  $t_p=10$  cm)**

**Total displacement (buffer top): 15 cm**

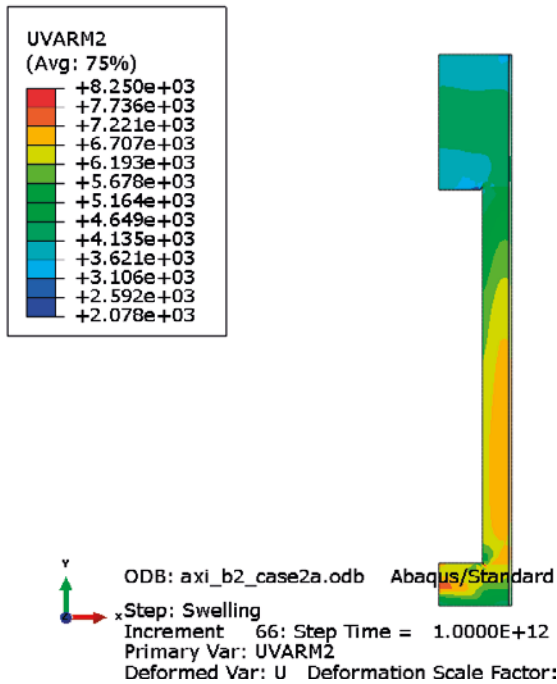
**Dry density (kg/m<sup>3</sup>)**



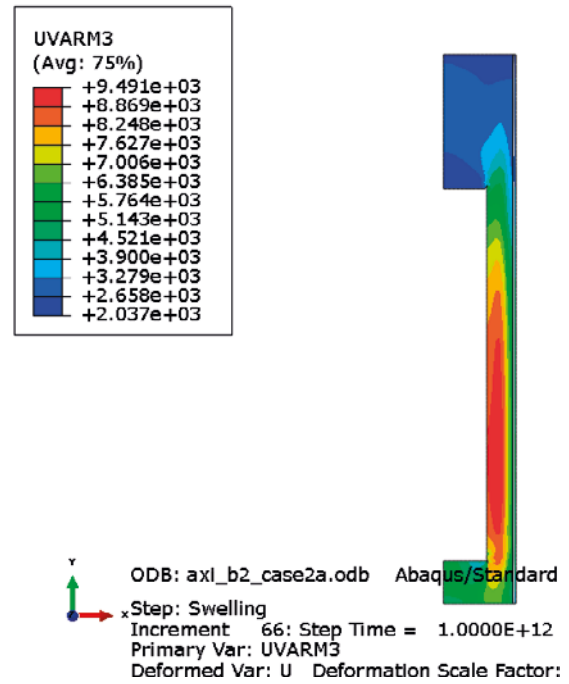
**Void ratio**



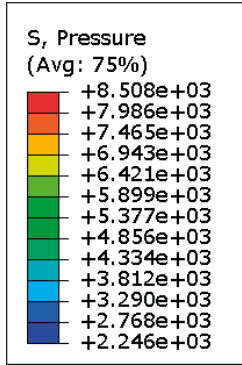
**Radial stress (kPa)**



**Axial stress (kPa)**

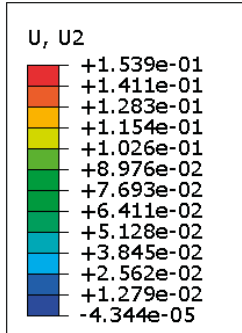


### Average stress (kPa)



ODB: axi\_b2\_case2a.odb    Abaqus/Standard 6.13-2    Thu Oct 22 15:25:42 GMT+02:00  
Step: Swelling  
Increment 66: Step Time = 1.0000E+12  
Primary Var: S, Pressure  
Deformed Var: U    Deformation Scale Factor: +1.000e+00

### Axial displacements (m)



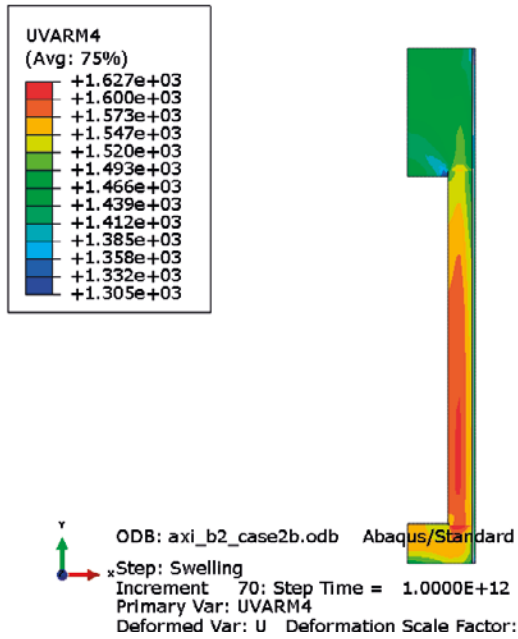
ODB: axi\_b2\_case2a.odb    Abaqus/Standard 6.13-2    Thu Oct 22 15:25:42 GMT+02:00  
Step: Swelling  
Increment 66: Step Time = 1.0000E+12  
Primary Var: U, U2  
Deformed Var: U    Deformation Scale Factor: +1.000e+00



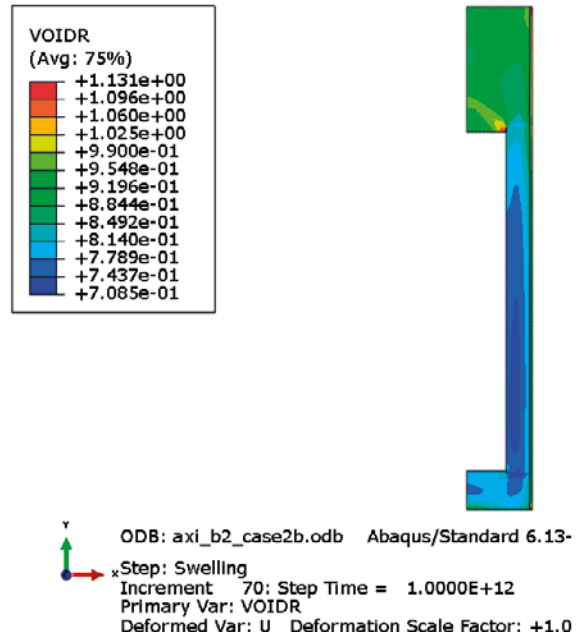
**Case 2b ( $\sigma=7$  MPa,  $t_p=25$  cm)**

Total displacement (buffer top): 19 cm

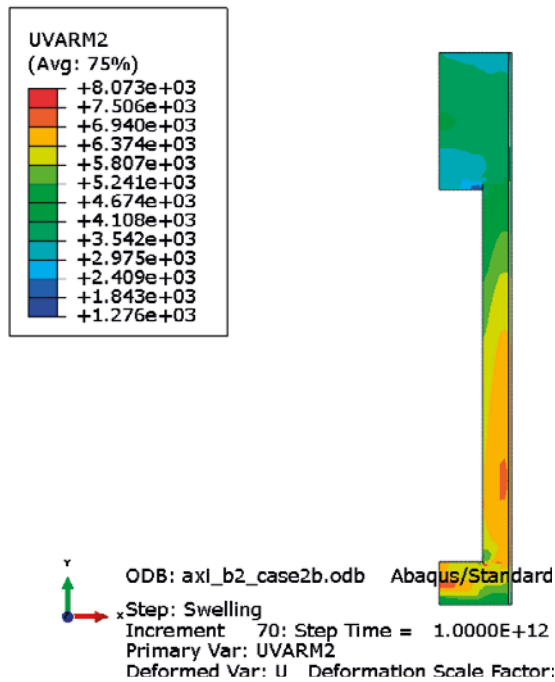
**Dry density (kg/m<sup>3</sup>)**



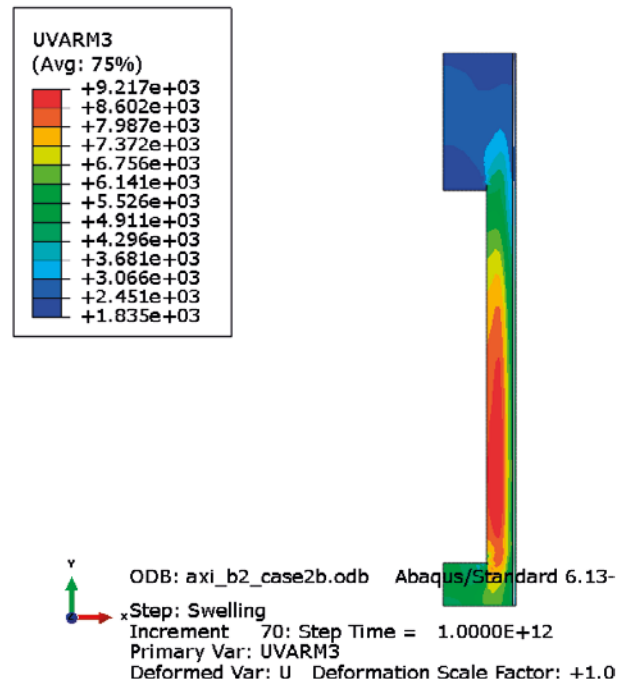
**Void ratio**



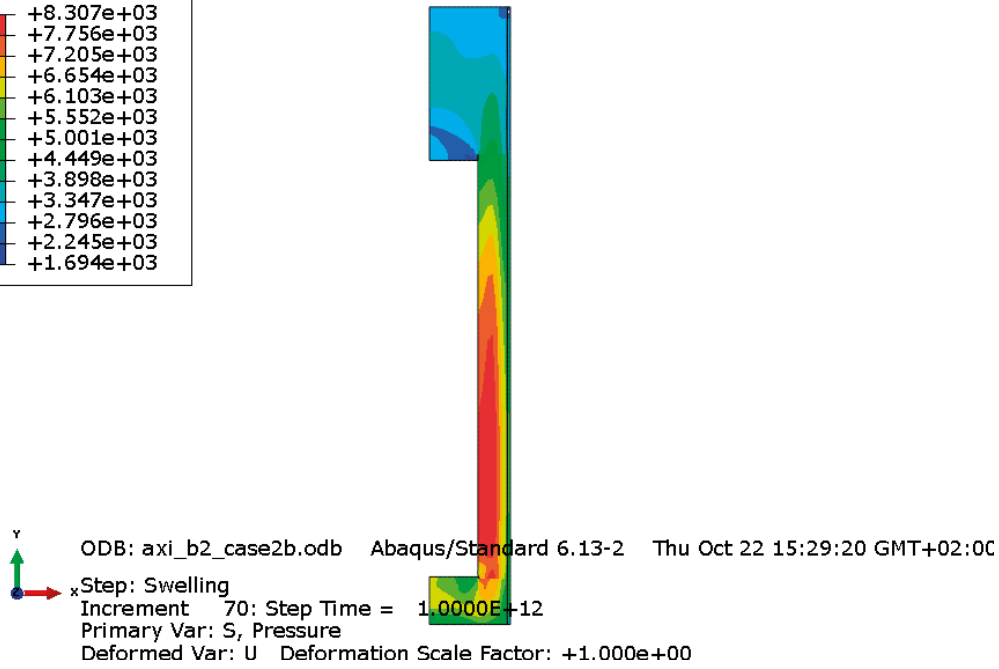
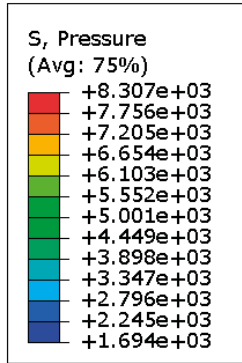
**Radial stress (kPa)**



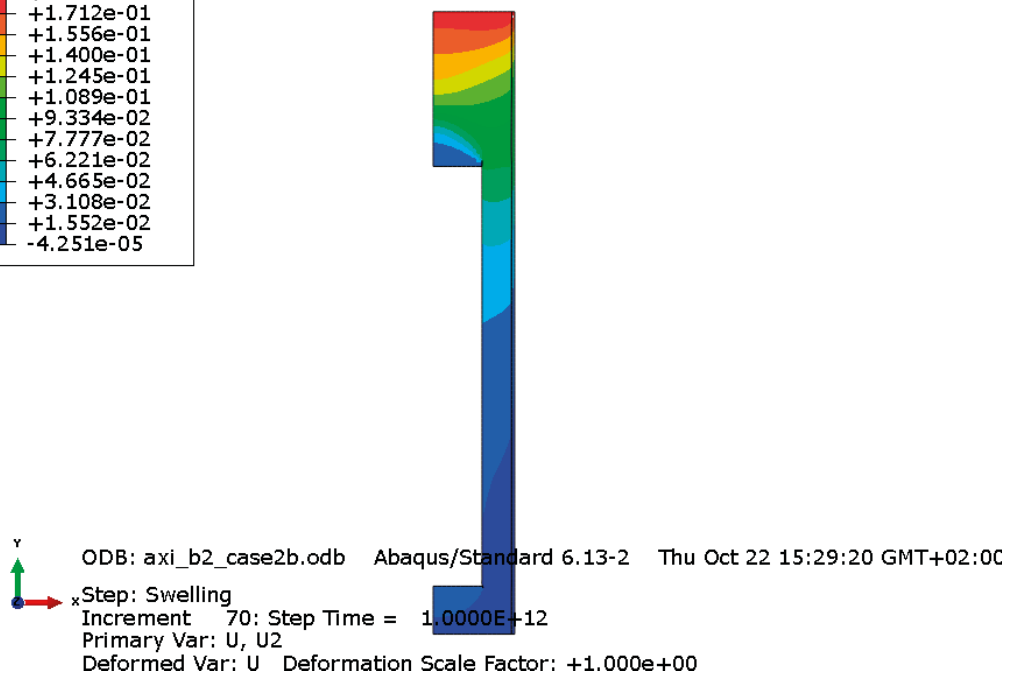
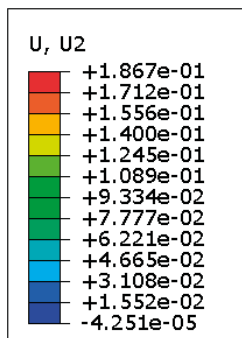
**Axial stress (kPa)**



### Average stress (kPa)



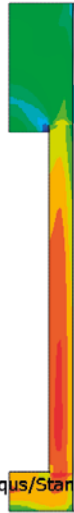
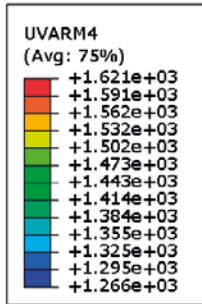
### Axial displacements (m)



**Case 2e ( $\sigma=7$  MPa,  $t_p=50$  cm)**

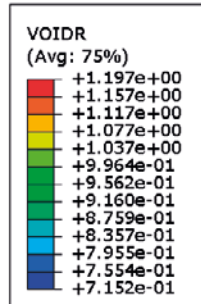
**Total displacement (buffer top): 24 cm**

**Dry density (kg/m<sup>3</sup>)**



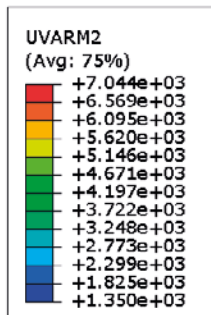
ODB: axi\_b2\_case2e.odb Abaqus/Standard  
 xStep: Swelling  
 Increment 82: Step Time = 1.0000E+12  
 Primary Var: UVARM4  
 Deformed Var: U Deformation Scale Factor:

**Void ratio**



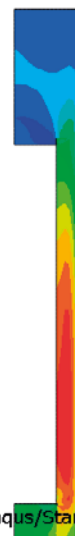
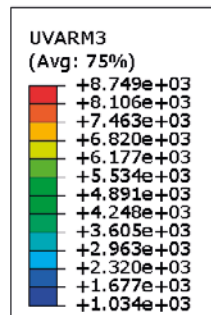
ODB: axi\_b2\_case2e.odb Abaqus/Standard 6.13-2  
 xStep: Swelling  
 Increment 82: Step Time = 1.0000E+12  
 Primary Var: VOIDR  
 Deformed Var: U Deformation Scale Factor: +1.00

**Radial stress (kPa)**



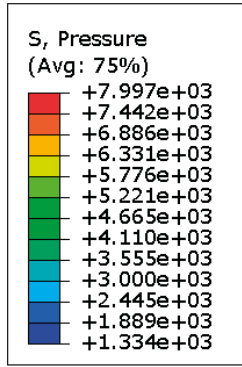
ODB: axi\_b2\_case2e.odb Abaqus/Standard  
 xStep: Swelling  
 Increment 82: Step Time = 1.0000E+12  
 Primary Var: UVARM2  
 Deformed Var: U Deformation Scale Factor:

**Axial stress (kPa)**



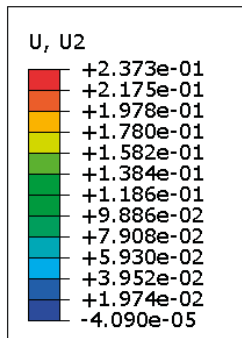
ODB: axi\_b2\_case2e.odb Abaqus/Standard  
 xStep: Swelling  
 Increment 82: Step Time = 1.0000E+12  
 Primary Var: UVARM3  
 Deformed Var: U Deformation Scale Factor:

### Average stress (kPa)



ODB: axi\_b2\_case2e.odb    Abaqus/Standard 6.13-2    Thu Oct 29 17:17:01 GMT+01:00  
Step: Swelling  
Increment    82: Step Time = 1.0000E+12  
Primary Var: S, Pressure  
Deformed Var: U    Deformation Scale Factor: +1.000e+00

### Axial displacements (m)

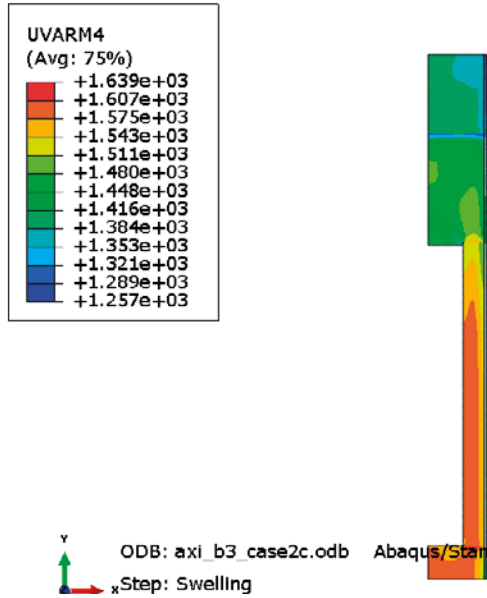


ODB: axi\_b2\_case2e.odb    Abaqus/Standard 6.13-2    Thu Oct 29 17:17:01 GMT+01:00  
Step: Swelling  
Increment    82: Step Time = 1.0000E+12  
Primary Var: U, U2  
Deformed Var: U    Deformation Scale Factor: +1.000e+00

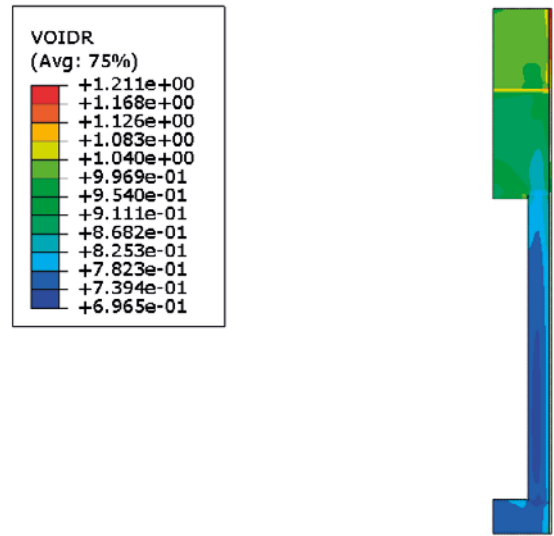
**Case 2c ( $\sigma=7$  MPa,  $t_p=10$  cm + bevel)**

**Total displacement (buffer top): 16 cm**

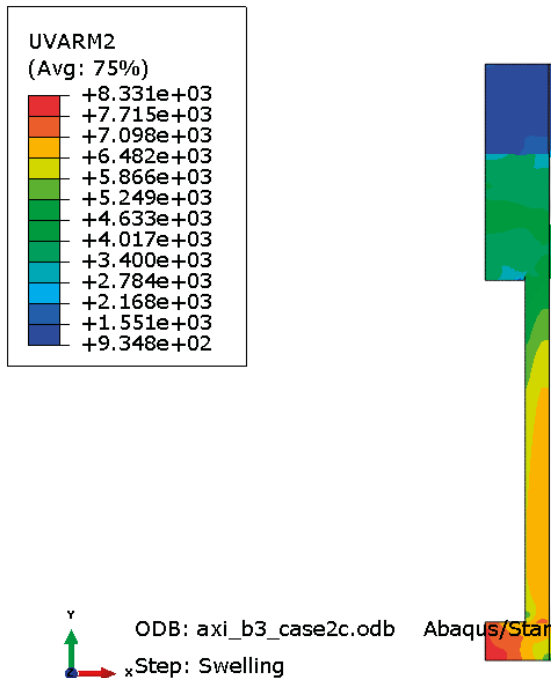
**Dry density (kg/m<sup>3</sup>)**



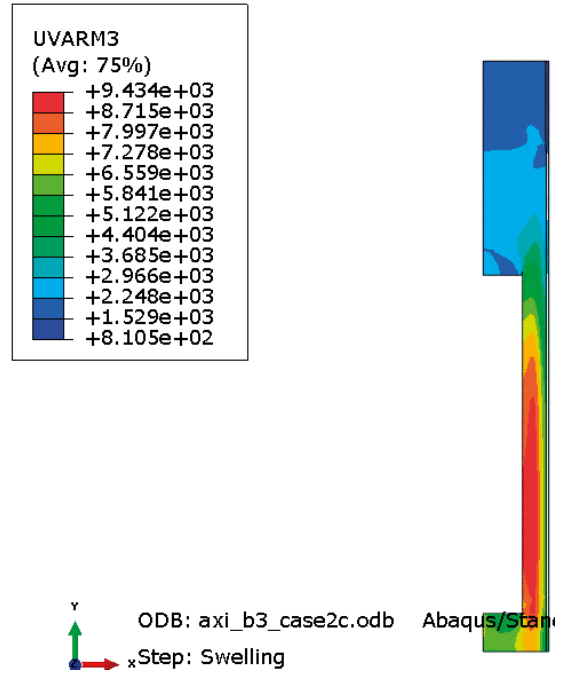
**Void ratio**



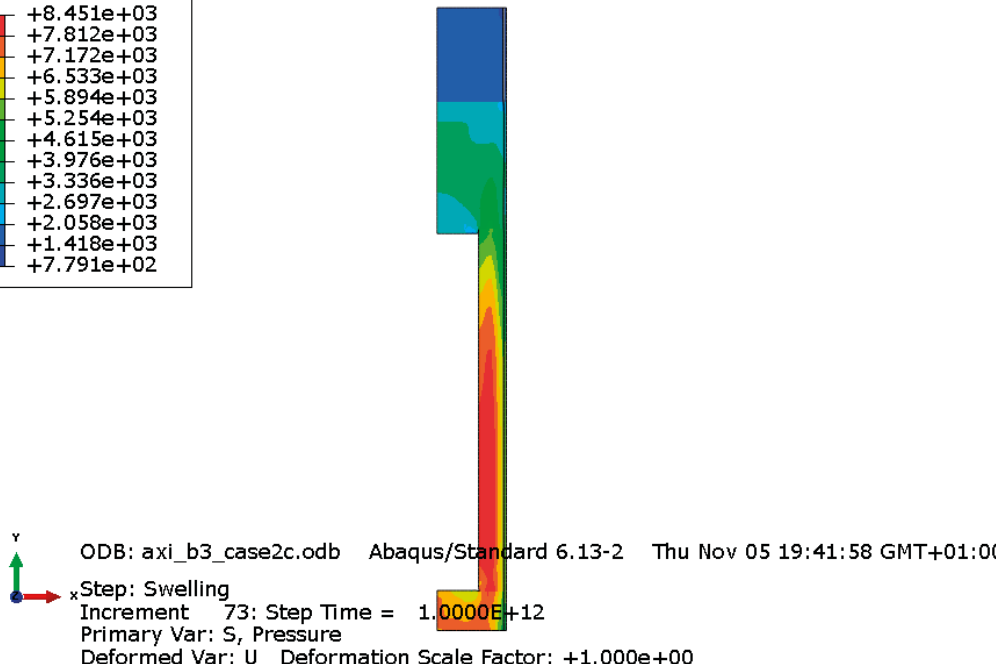
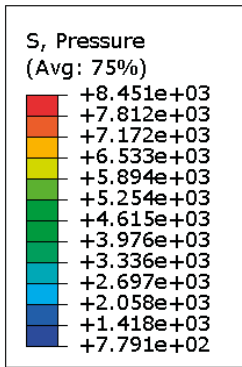
**Radial stress (kPa)**



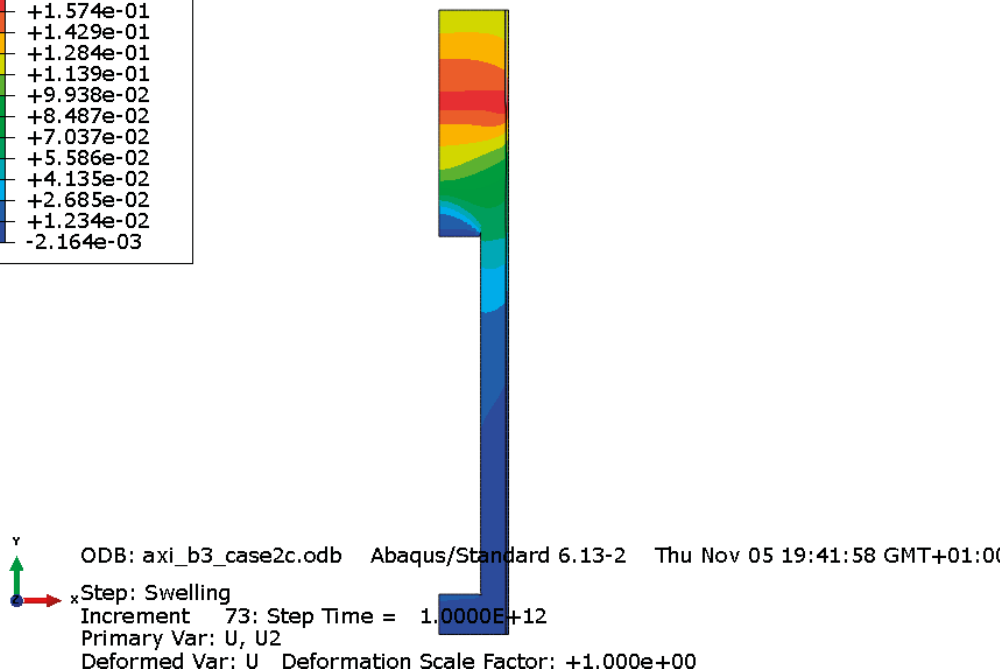
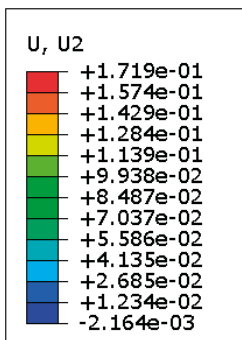
**Axial stress (kPa)**



Average stress (kPa)



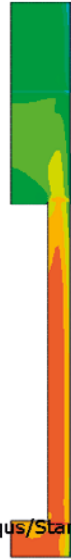
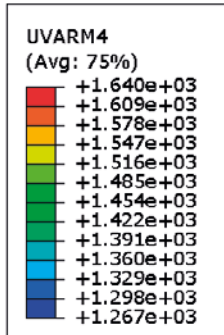
Axial displacements (m)



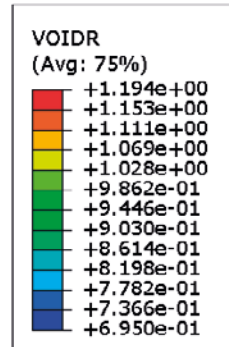
**Case 2d ( $\sigma=7$  MPa,  $t_p=10$  cm + bevel + blocks)**

**Total displacement (buffer top): 12 cm**

**Dry density (kg/m<sup>3</sup>)**

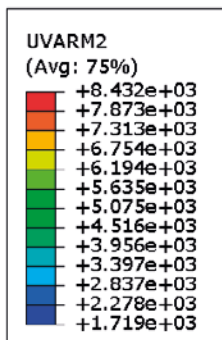


**Void ratio**

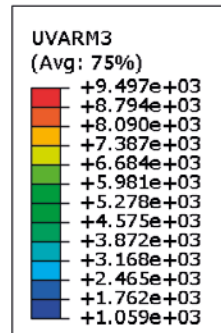


Y ODB: axi\_b3\_case2d.odb Abaqus/Stan  
x Step: Swelling

**Radial stress (kPa)**



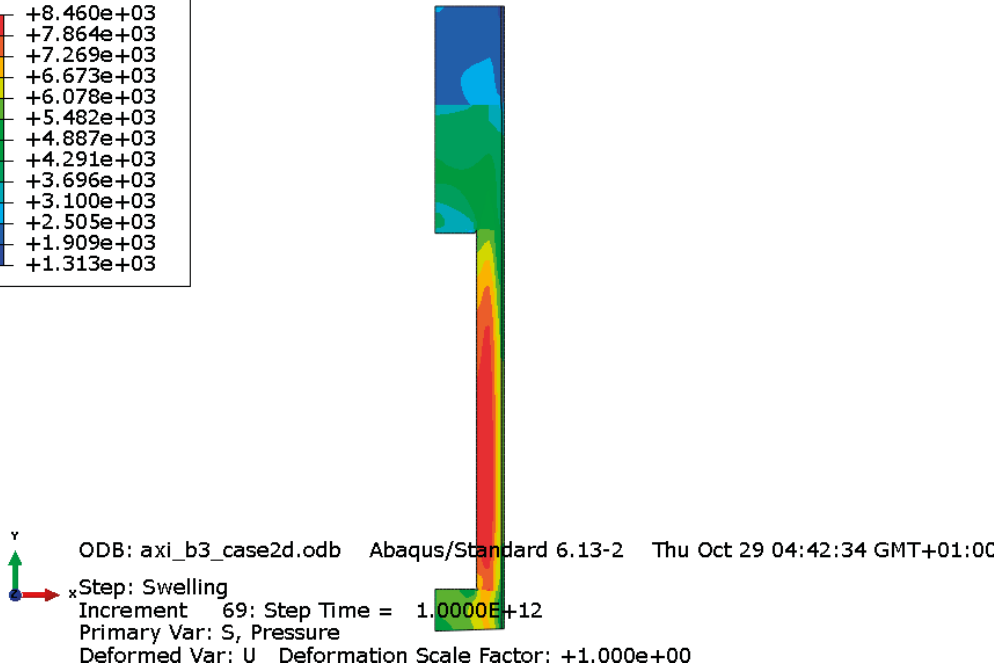
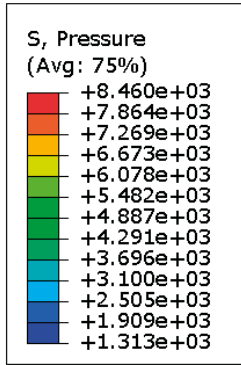
**Axial stress (kPa)**



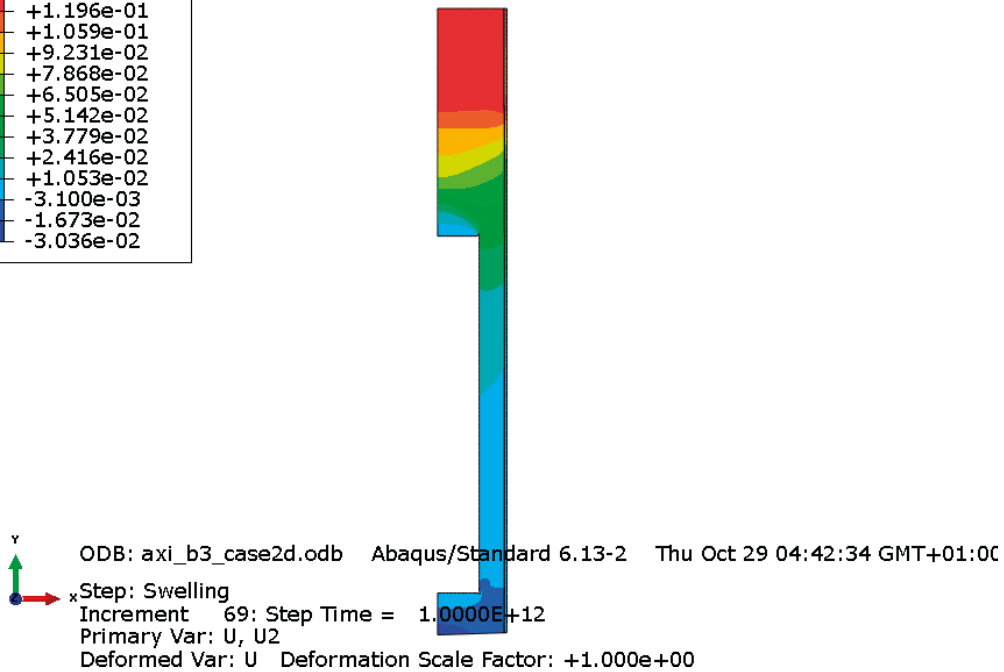
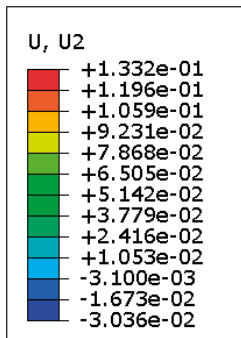
Y ODB: axi\_b3\_case2d.odb Abaqus/Stan  
x Step: Swelling

Y ODB: axi\_b3\_case2d.odb Abaqus/Stan  
x Step: Swelling

### Average stress (kPa)



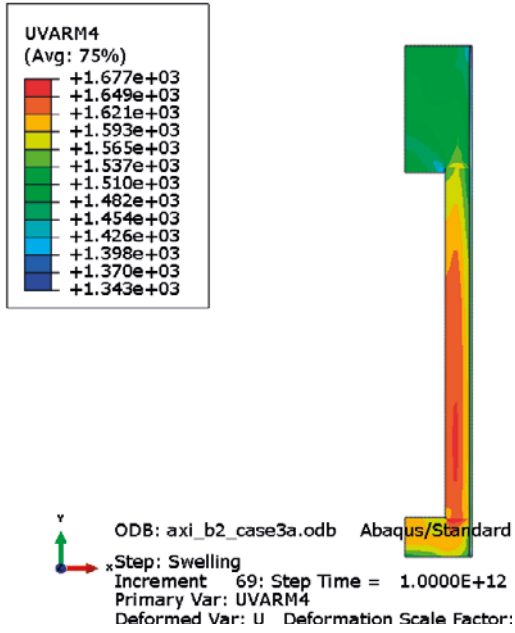
### Axial displacements (m)



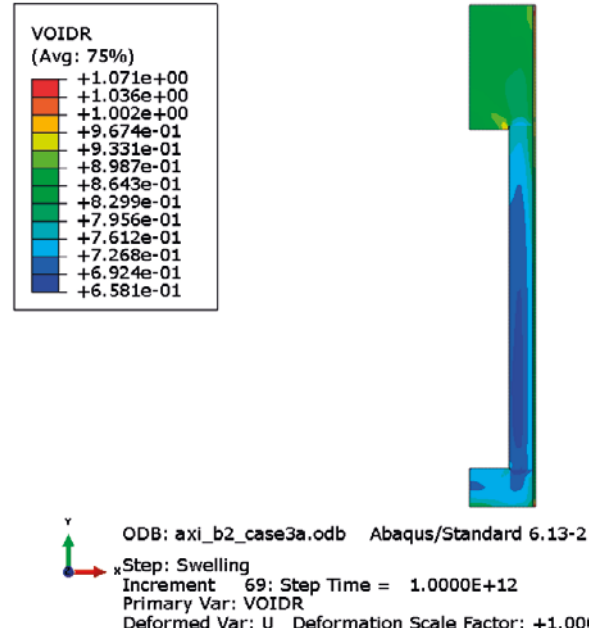


**Case 3a ( $\sigma=10$  MPa,  $t_p=10$  cm)**  
**Total displacement (buffer top): 18 cm**

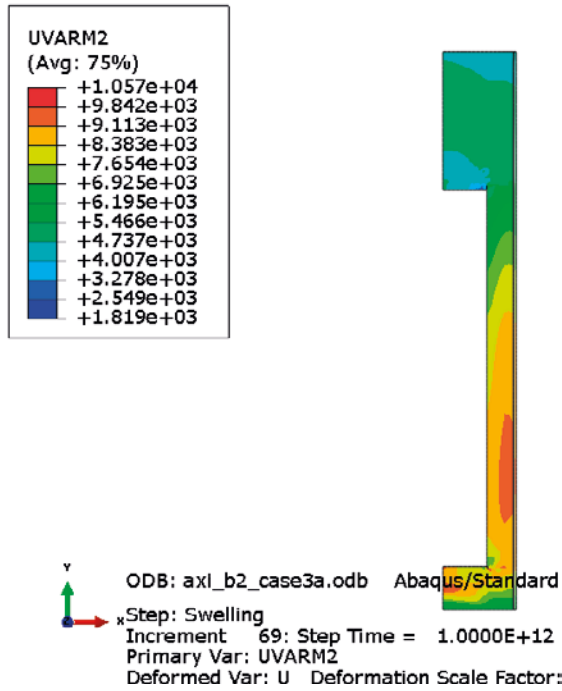
**Dry density ( $\text{kg/m}^3$ )**



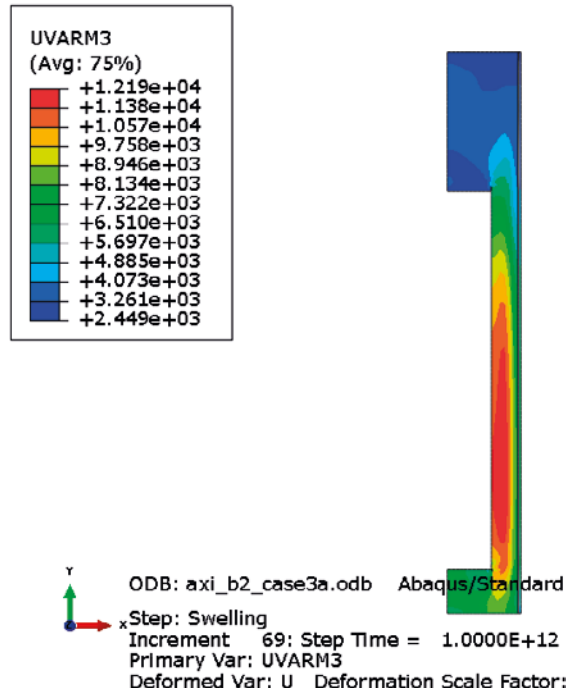
**Void ratio**



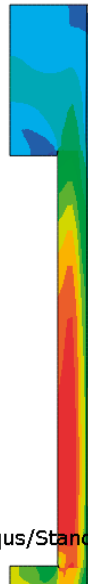
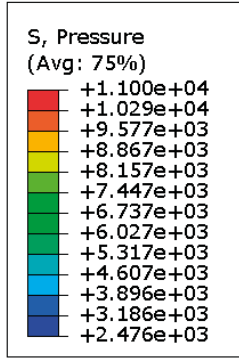
**Radial stress (kPa)**

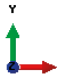


**Axial stress (kPa)**

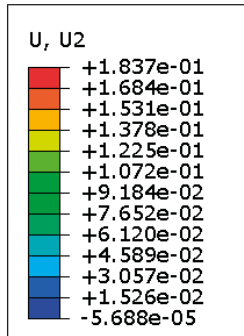



**Average stress (kPa)**




 ODB: axi\_b2\_case3a.odb Abaqus/Standard 6.13-2 Thu Oct 22 16:46:55 GMT+02:00  
 Step: Swelling  
 Increment 69: Step Time = 1.0000E+12  
 Primary Var: S, Pressure  
 Deformed Var: U Deformation Scale Factor: +1.000e+00

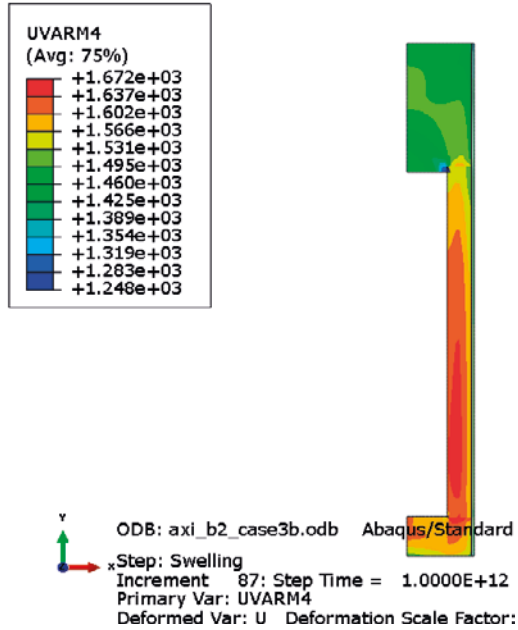
**Axial displacements (m)**



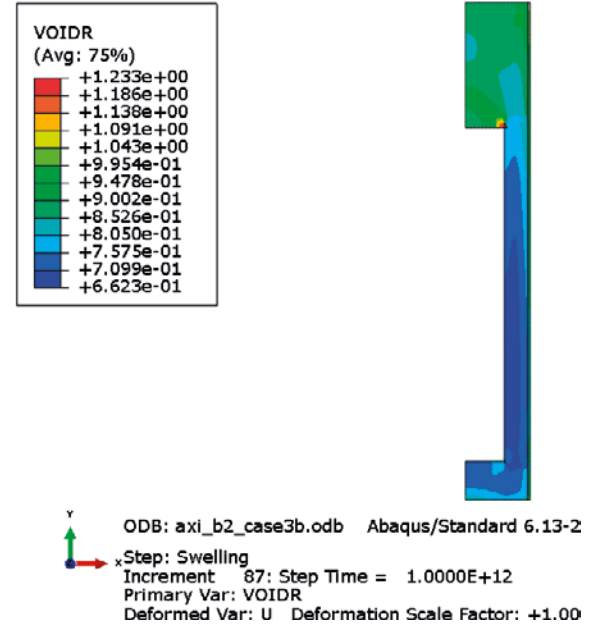

 ODB: axi\_b2\_case3a.odb Abaqus/Standard 6.13-2 Thu Oct 22 16:46:55 GMT+02:00  
 Step: Swelling  
 Increment 69: Step Time = 1.0000E+12  
 Primary Var: U, U2  
 Deformed Var: U Deformation Scale Factor: +1.000e+00

**Case 3b ( $\sigma=10$  MPa,  $t_p=25$  cm)**  
**Total displacement (buffer top): 22 cm**

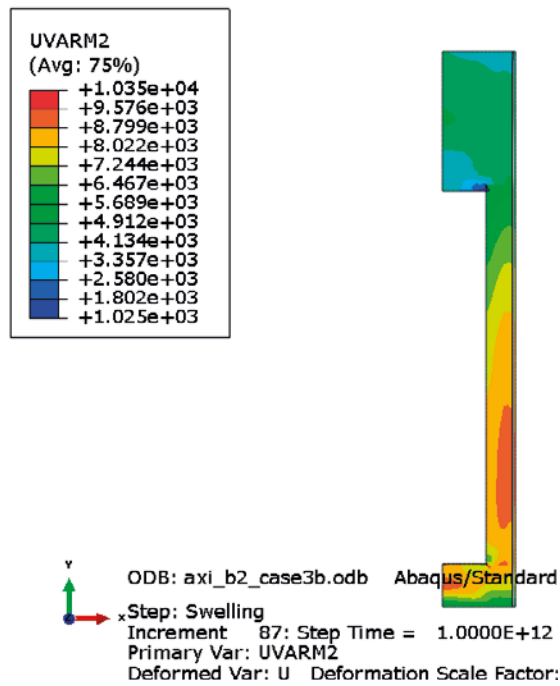
**Dry density (kg/m<sup>3</sup>)**



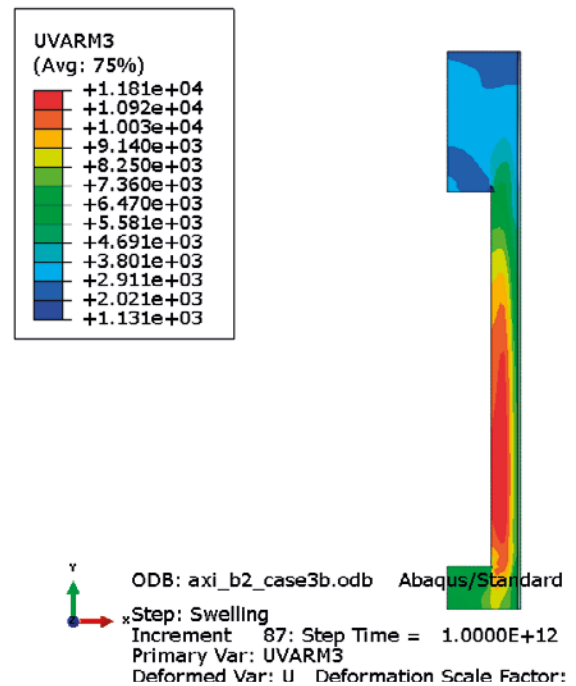
**Void ratio**



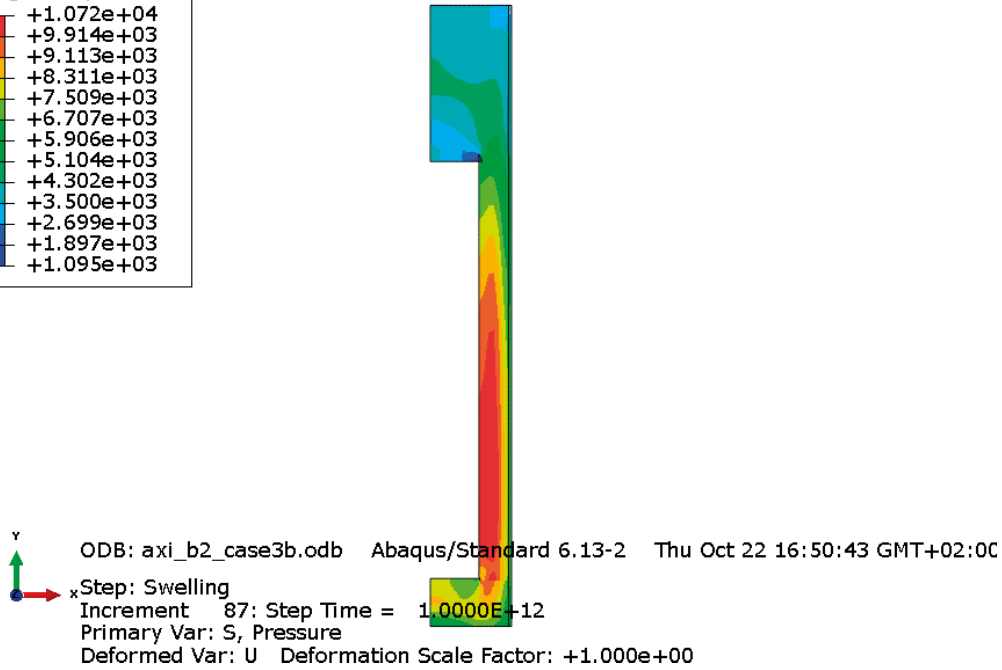
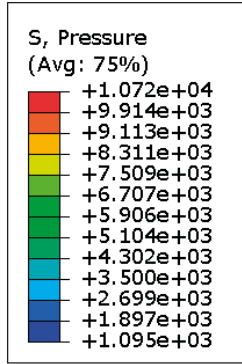
**Radial stress (kPa)**



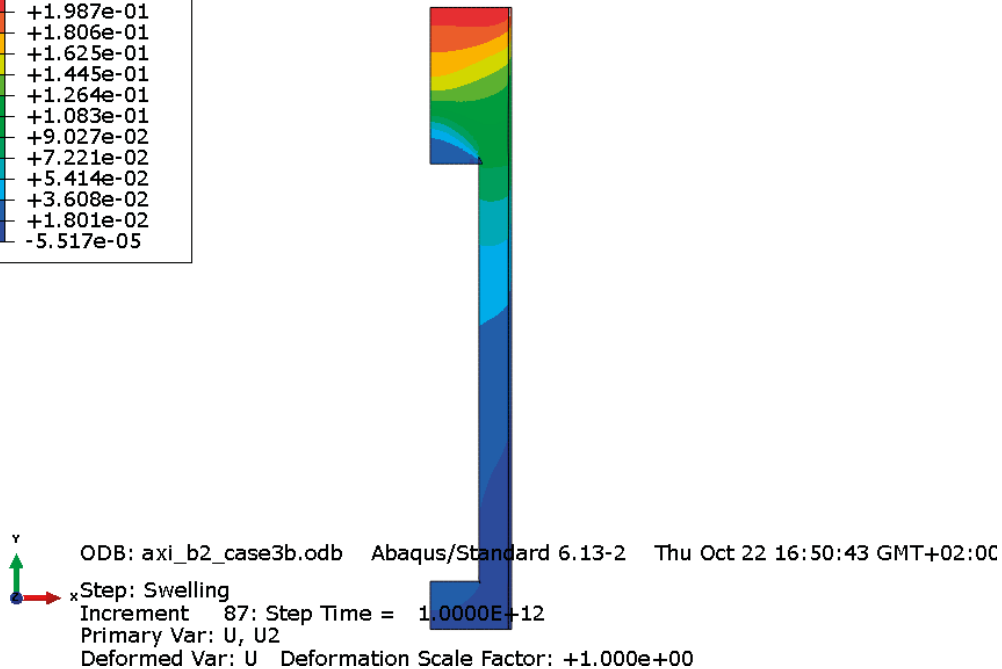
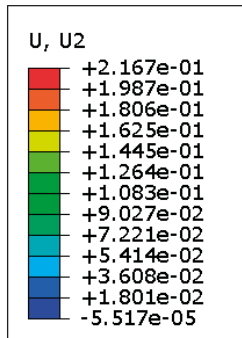
**Axial stress (kPa)**



Average stress (kPa)



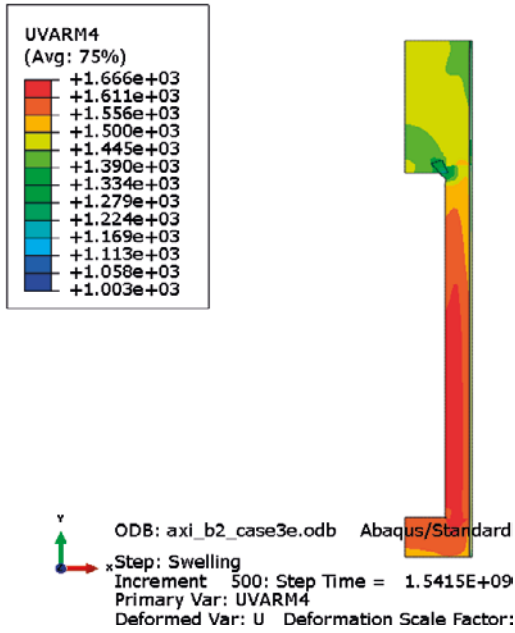
Axial displacements (m)



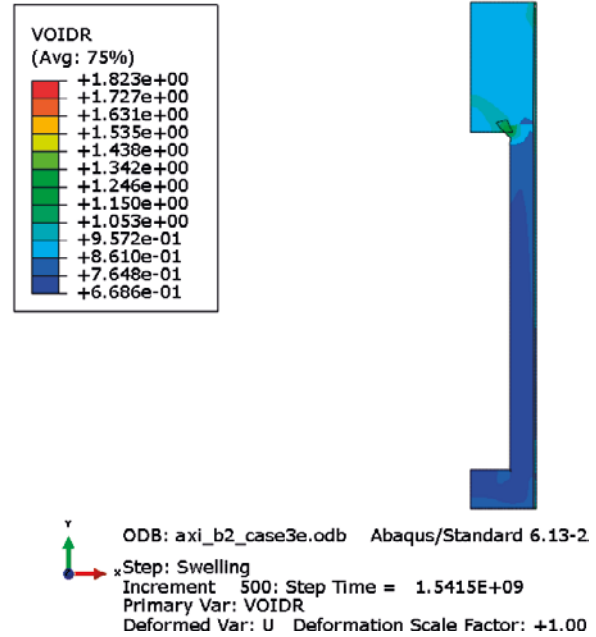
**Case 3e ( $\sigma=10$  MPa,  $t_p=50$  cm)**

Total displacement (buffer top): 27 cm

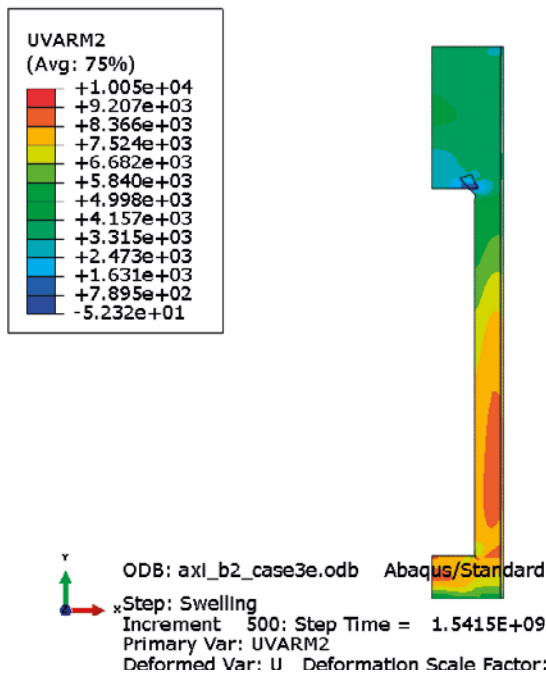
**Dry density (kg/m<sup>3</sup>)**



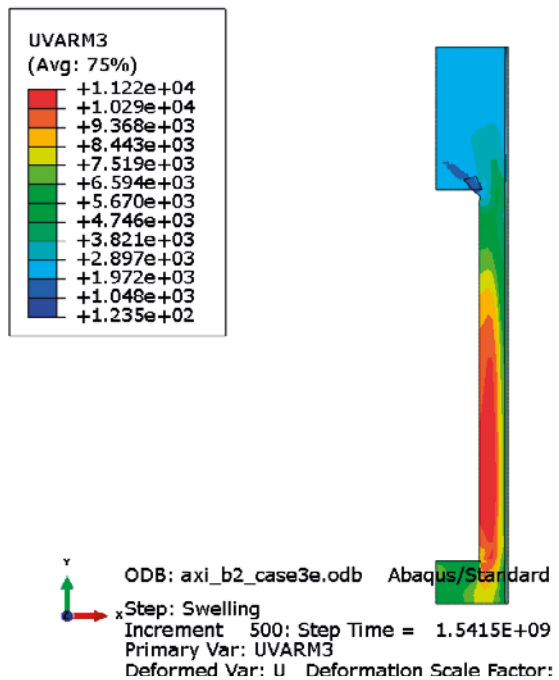
**Void ratio**



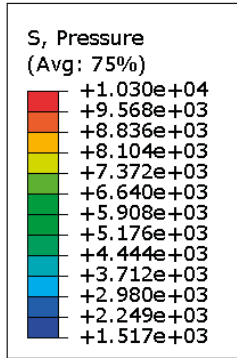
**Radial stress (kPa)**



**Axial stress (kPa)**

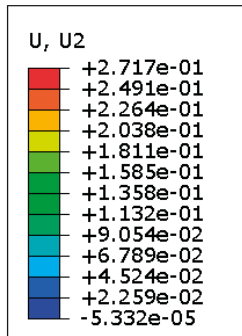


**Average stress (kPa)**



y  
x ODB: axi\_b2\_case3e.odb Abaqus/Standard 6.13-2 Thu Oct 29 04:53:01 GMT+01:00  
 Step: Swelling  
 Increment 248: Step Time = 1.0000E+12  
 Primary Var: S, Pressure  
 Deformed Var: U Deformation Scale Factor: +1.000e+00

**Axial displacements (m)**

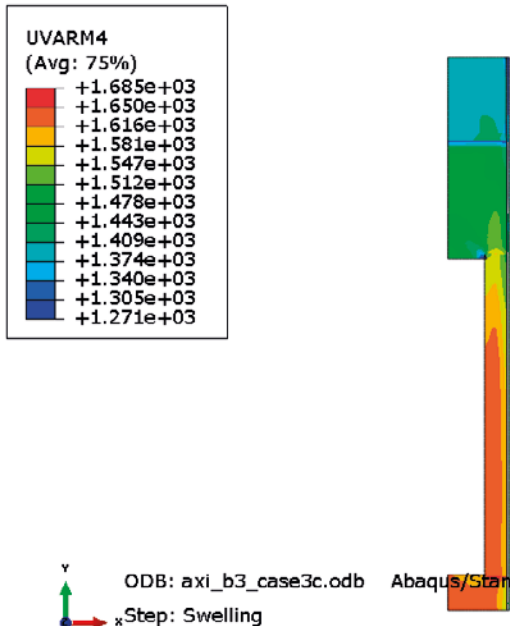


y  
x ODB: axi\_b2\_case3e.odb Abaqus/Standard 6.13-2 Thu Oct 29 04:53:01 GMT+01:00  
 Step: Swelling  
 Increment 248: Step Time = 1.0000E+12  
 Primary Var: U, U2  
 Deformed Var: U Deformation Scale Factor: +1.000e+00

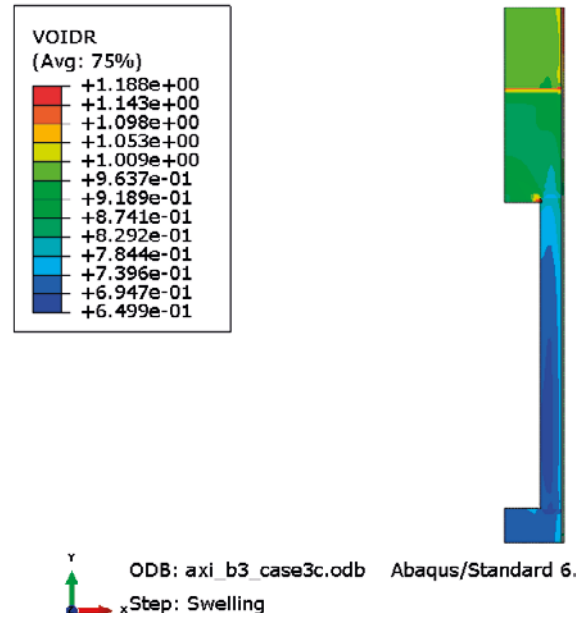
**Case 3c ( $\sigma=10$  MPa,  $t_p=10$  cm + bevel)**

**Total displacement (buffer top): 19 cm**

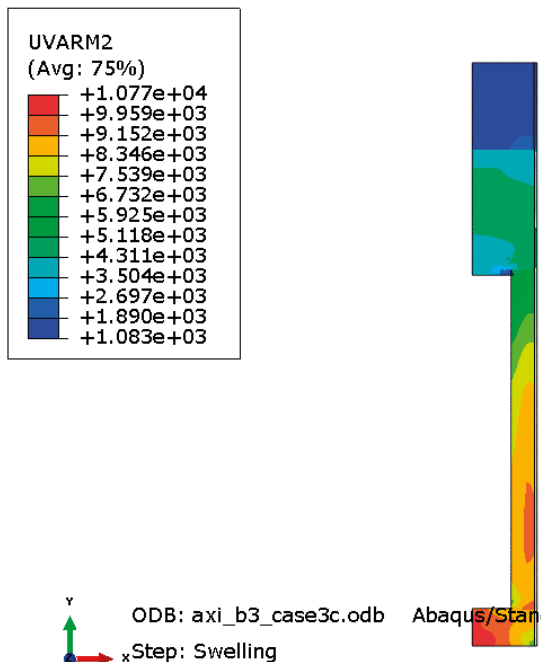
**Dry density (kg/m<sup>3</sup>)**



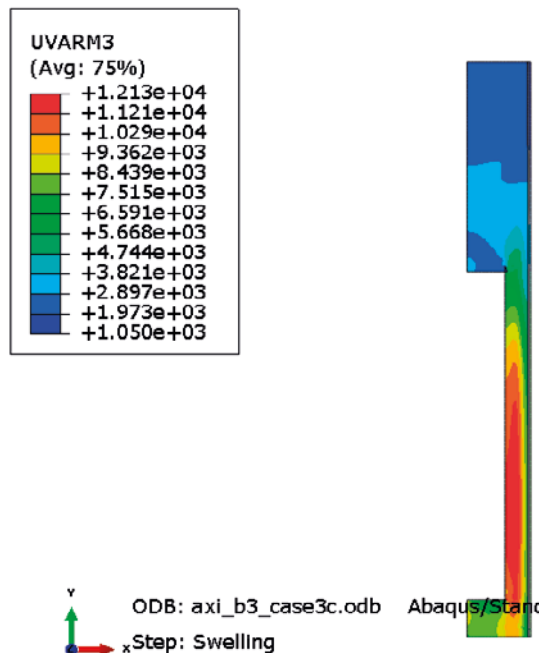
**Void ratio**



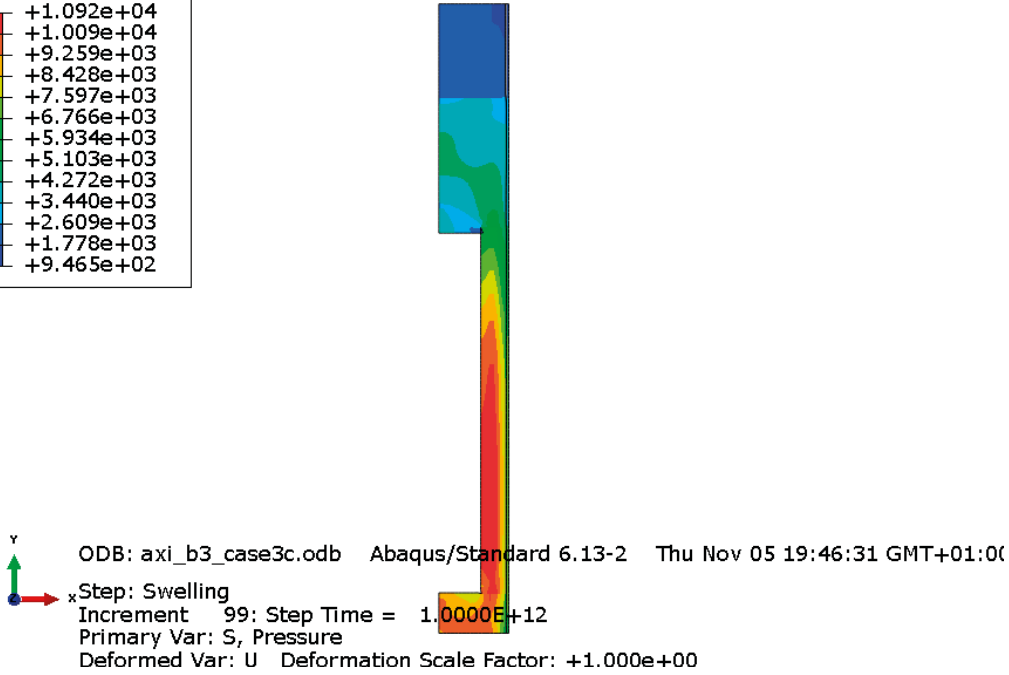
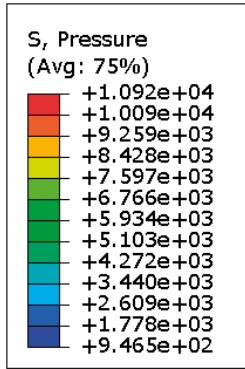
**Radial stress (kPa)**



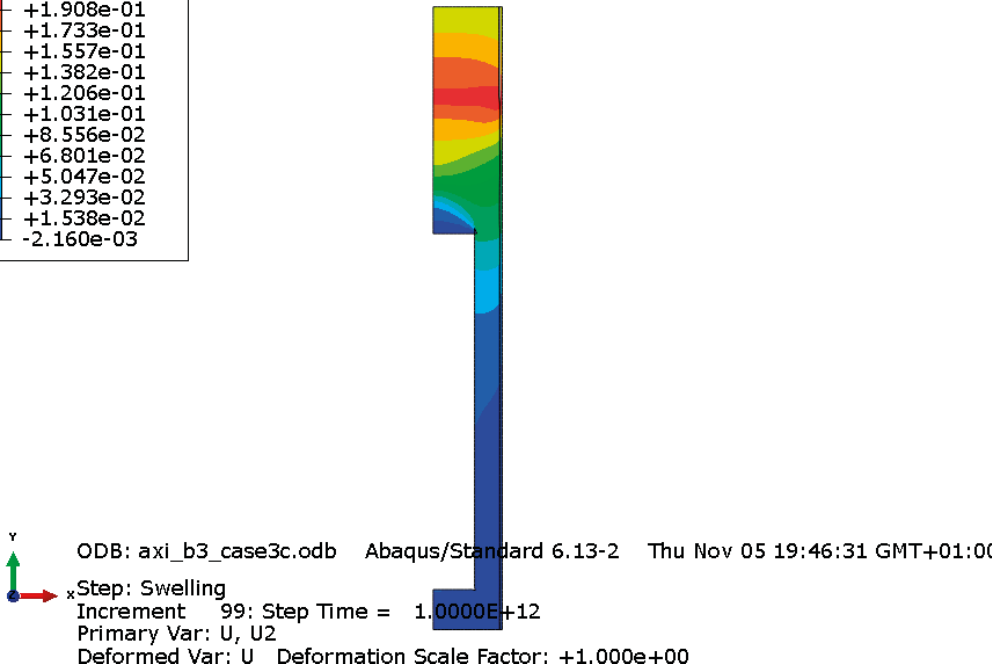
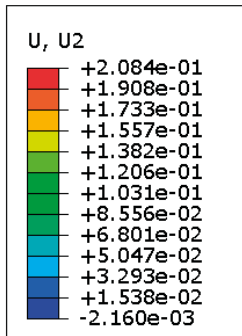
**Axial stress (kPa)**



**Average stress (kPa)**



**Axial displacements (m)**

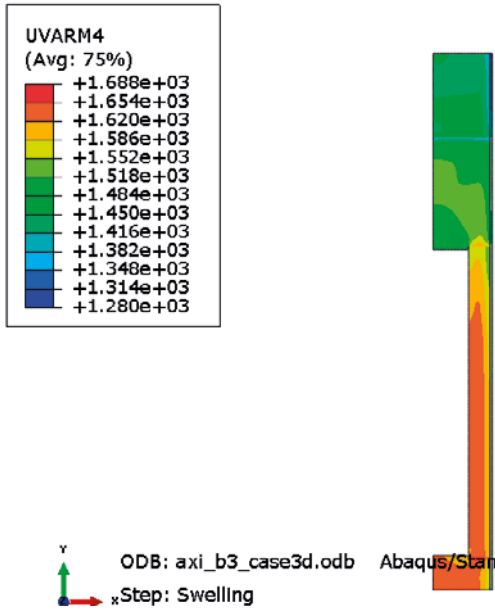




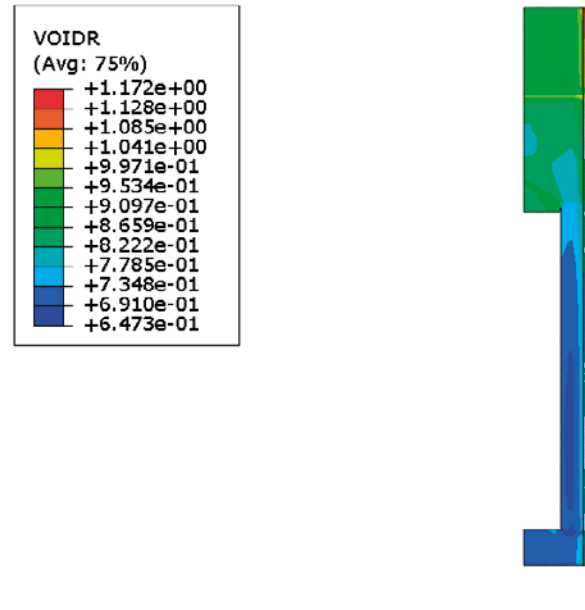
**Case 3d ( $\sigma=10$  MPa,  $t_p=10$  cm + bevel + blocks)**

**Total displacement (deposition hole top): 16 cm**

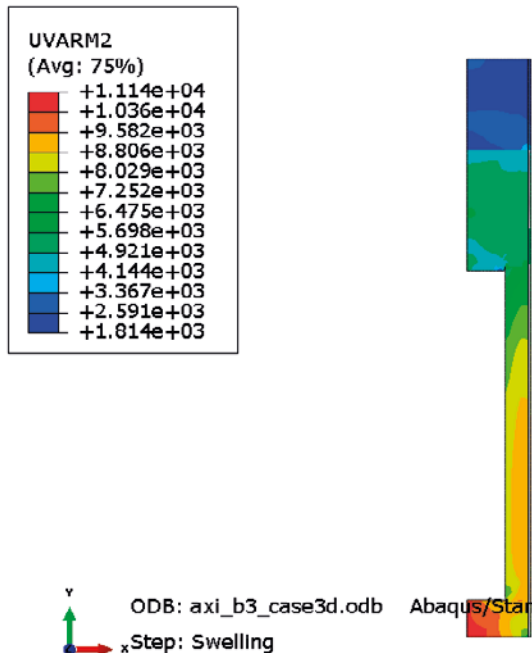
**Dry density (kg/m<sup>3</sup>)**



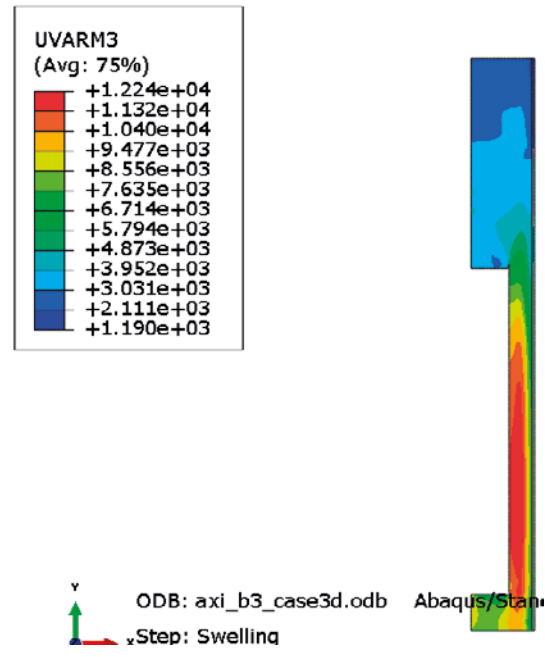
**Void ratio**



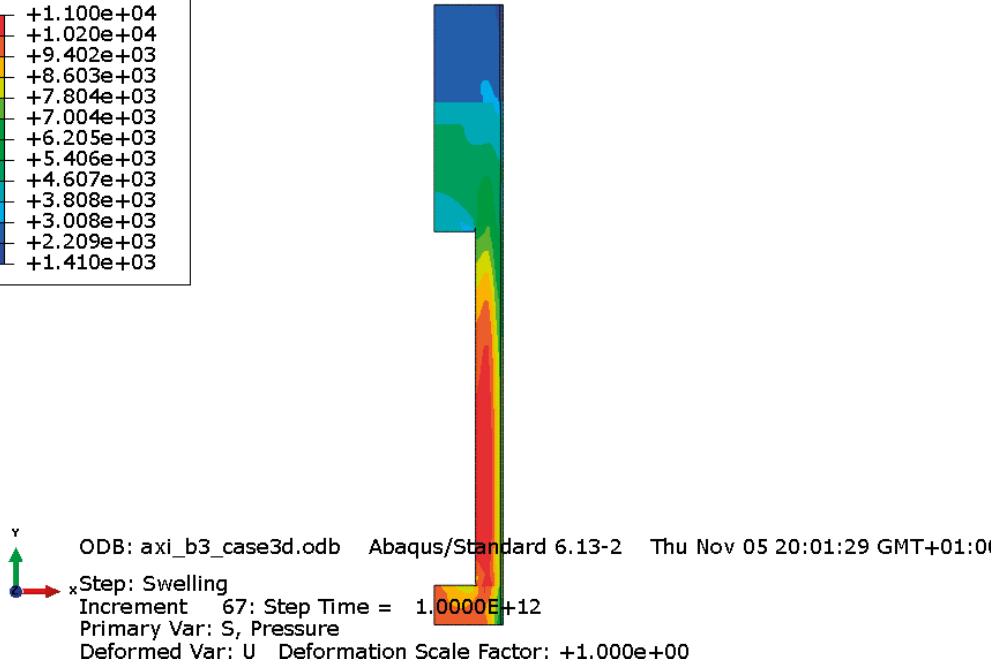
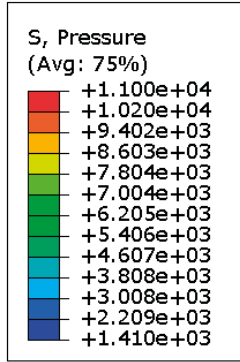
**Radial stress (kPa)**



**Axial stress (kPa)**



**Average stress (kPa)**



**Axial displacements (m)**

